OPTIMAL OPERATION OF INTEGRATED PROCESSES

Studies on Heat Recovery Systems

by
Bjørn Glemmestad

Telemark Institute of Technology
Department of Process Technology
Porsgrunn, Norway

A thesis submitted to
Norwegian University of Science and Technology, Trondheim,
for the degree of Dr. Ing.

Submitted October 1997

ABSTRACT

Three important parts of an integrated plant are reactors, separators and a heat exchanger network (HEN) for heat recovery. Within the process engineering community, much attention has been paid to design of reactors, separators and HENs. This thesis, however, is devoted to *operation* and in particular to optimal operation of HENs.

The purpose of heat integration is to save energy, but the HEN also introduces new interactions and feedback in the overall plant. A good strategy for operation of HENs should, in addition to controlling the outlet temperatures to target values (setpoints), minimize the external energy consumption when disturbances and setpoint variations are encountered.

A prerequisite for optimization is that there are extra degrees of freedom left after regulatory control is implemented. It is shown that extra degrees of freedom may not always be utilized for energy optimization, and a quantitative expression for the degrees of freedom that can be utilized for optimization is presented. A simplified expression that is often valid is also deduced.

How to operate a HEN close to optimal may often be found from structural information alone. The thesis presents some improvements and generalizations of a structure based method that has been proposed earlier. Structural information is used to divide possible manipulations into three categories depending on how each manipulation affect the utility consumption. Using these three categories and two heuristic rules for operability, the possible manipulations are ordered in a priority table. This table is used to determine which manipulation should be preferred, and which manipulation should be selected if an active manipulation is saturated. It is shown that the implementation of the method may correspond to split-range control.

A method that in addition to structural information, also utilizes parametric information is proposed. This method is heavily inspired by the structural method, however, the optimal control structure is found through solving an integer programming problem. The control structure is found periodically during operation, and as for the structure based method, this can lead to a varying control structure. The basic model does not incorporate any controllability considerations. Two methods to include controllability are proposed. Both methods are based on extending the basic model with logical inference using additional constraints. In both cases, the result is a hierarchical strategy for operation that has been embedded into the model.

A third method that combines the use of steady state optimization and optimal selection of measurements is proposed. Steady state optimization is carried out periodically during operation to compute optimal setpoints for the secondary measurements. The setpoints for the primary measurements (outlet temperatures with target values) are not subject to optimization. However, extra manipulations may be used for energy optimization and this may be done by controlling some internal temperatures (secondary measurements). When unknown disturbances and model errors are present, the selection of which secondary measurements that are controlled affects how close to optimum the process can be operated. A procedure for selection of secondary measurements for processes where optimum is located at the intersection of constraints (which is typical for HENs) is presented.

ACKNOWLEDGMENTS

This work has been carried out at Telemark Institute of Technology. Financial support from the Norwegian Research Council (NFR) through the program for computer aided chemical engineering is gratefully acknowledged.

Professor Truls Gundersen has been the main supervisor for this work, and his guidance and support have been excellent in all respects. Truls Gundersen's ability to share from his large knowledge within process integration has been of great value for me and the high standards he set for his own work have been inspiring. My co-supervisor, professor Sigurd Skogestad at Department of Chemical Engineering at the Norwegian University of Science and Technology has also played an active role in large parts of the research work. His supervision has had the same high standard as Truls Gundersen's, and his knowledge within process control has contributed significantly to this thesis.

I would also like to thank Dr.Ing. Knut Wiig Mathisen. His doctoral research forms an important basis for this work, and he also introduced me to Simulink for simulation of heat exchanger networks.

During the fall 1994 I stayed at Department of Chemical Engineering at the Norwegian University of Science and Technology in Trondheim. This was important for me in order to get to know some important research groups in Norway within process systems engineering. I would like to thank the graduate students in the Process Modeling and Simulation Group and the Process Control Group for making my stay in Trondheim pleasant. Here at Telemark Institute of Technology, I would particularly like to thank my friend and colleague Abdulreza Hashemi-Ahmady (Abdy), for many interesting discussions during our breakfast coffee breaks.

Finally, I would like to thank my significant other, Lene Månsson, for being supportive and patient during these last three years.

CONTENTS

ABBREVIATIONS

These abbreviations are used throughout the thesis. The list is in alphabetical order.

AMTD	Arithmetic Mean Temperature Difference
DCS	Distributed Control System
DIC	Decentralized Integral Controllable/Controllability
DOF(s)	Degree(s) Of Freedom
HEN	Heat Exchanger Network
ILP	Integer Linear Programming
LMTD	Logarithmic Mean Temperature Difference
LP	Linear Programming
MILP	Mixed Integer Linear Programming
MIMO	Multiple Input - Multiple Output (multivariable system)
MINLP	Mixed Integer Non-Linear Programming
MPC	Model Predictive Control
NLP	Non-Linear Programming
ODE	Ordinary Differential Equations
PDE	Partial Differential Equations
PI	Proportional-Integral (controller)
PID	Proportional-Integral-Derivative (controller)
RGA	Relative Gain Array
RHP	Right Half Plane (right half of the complex plane)
SISO	Single Input - Single Output (monovariable system)

Chapter 1

INTRODUCTION

1.1 Motivation

Increased energy cost, increased focus on environmental aspects and generally harder competition have all contributed to increasing demands regarding efficiency within the process industry during the last decades. Higher efficiency is often obtained through designs with increased process integration. Simple examples of process integration are separation and recycling of unreacted feed in the outlet stream from a reactor (material recycle), or utilizing the excess heat in a hot outlet stream from an exothermic reactor to preheat the feed using a heat exchanger (energy recycle). An efficient overall solution can usually not be achieved from one single recirculation, and tight and plantwide process integration is often required. For instance, all hot process streams may be integrated with all cold process streams in a heat exchanger network. In addition to this heat integration, there may be a number of material recycles together with integration of turbines, heat pumps etc.

Process integration is motivated from economic benefits, but it also changes the characteristics of the plant: Instead of addressing each process unit independently, the total plant has to be investigated as a whole (a systems approach). This issue should be particularly emphasized when considering *operation* and *control* of the plant, mainly due to the two following points:

1. Process integration increases interactions in the plant. That is, a change in a disturbance or manipulated input may not only give local effects, but can spread to a larger part of the plant.
2. Process integration may dramatically change the plant dynamics. As a severe example, integration of units that are all stable may result in an unstable plant.

In addition, process integration often introduces extra degrees of freedom that may be utilized for optimization during operation. This may be thought of as a possibility for further savings, but usually the situation is exactly the opposite: A process design is based on the assumption that the process is operated optimally without disturbances, and therefore the extra degrees of freedom may have to be used for optimization during operation in order not to deteriorate the benefits that process integration can give.

For the reasons pointed out above, it is clear that operation of integrated processes can be both difficult and important for the total economy of the plant. This gives motivation for further research within these two areas:

1. Design of integrated processes which also are easy to operate/control.
2. Design of operation/control systems for integrated processes.

Both of these areas are challenging and they are somewhat related to each other. Despite that the first point in some cases may be a prerequisite for obtaining good results in the second point, this thesis focuses on design of systems for operation and control of integrated processes.

In many plants, energy costs constitute a significant fraction of the total operating costs, and methods for optimal operation of heat exchanger networks (HENs) are particularly emphasized in this thesis.

1.2 Scope and overview of thesis

The main goal of this work is to contribute within the field of optimal operation of HENs. Mathisen (1994) formulated this problem as follows:

"For a HEN with given structure, heat exchanger areas and bypasses, and a given steady-state operating point (supply temperatures, heat capacity flowrates, heat transfer coefficients and target temperatures), find the set of manipulated inputs (bypass fractions and possible split fractions) that minimizes energy cost."

In addition to minimization of energy cost, it is also important to have a strategy for operation and control that results in reasonable dynamic performance of the plant. In general, we want a control system that yields a stable plant that rejects disturbances and follows setpoint commands fast and smoothly. Methods that minimize energy cost during operation together with reasonable plant dynamics are proposed in the thesis. Where it is possible, it has been attempted to generalize the methods to be applicable for other parts of processes than HENs.

The thesis consists of a total of eight chapters which are written to form one entirety. Despite this, some of the chapters can be read independently of the others as long as chapter 2 has been read. In order to succeed in proposing good methods for optimal operation of HENs, it is required with some basic knowledge both from the field of process synthesis and from the field of process control. This knowledge, together with some basic ideas on how to approach the optimal operation problem is given in chapter 2. In order to verify that the proposed

methods work, dynamic simulations are made and chapter 3 presents how this is done for HENs.

In order to perform optimization during operation, it is required that there are extra degrees of freedom after regulatory control is implemented. This is discussed in chapter 4, and it is shown that degrees of freedom may not always be utilized for energy optimization. A quantitive expression for the degrees of freedom that can be used for optimization is presented together with some simplified rules.

Chapter 5 discusses a method for optimal operation that is based only on the structure of the HEN. This method is presented earlier, but in this chapter parallels are drawn to split-range control. A way to deal with multiple controlled temperatures is also proposed. A method which is heavily inspired by this socalled sign method is presented in chapter 6. Here, quantitative information in terms of linear steady state transfer functions is utilized, and a control configuration that minimizes energy cost is found by solving an integer programming problem.

A different approach for optimal operation of HENs is proposed in chapter 7. This chapter actually contains two methods that are combined to form one powerful strategy for on-line optimization. A general steady state HEN model is formulated which is used periodically during operation to find optimal setpoints for a set of variables. In addition, a method for selection of *which* variables that are kept at setpoints between the optimizations is proposed. Special attention is paid to processes where optimum lies at the intersection of constraints, which is typical for HENs.

The last chapter provides a short discussion in addition to conclusions and suggestions for future work.

Each chapter has a separate nomenclature and reference list at the end. Earlier and more "stand-alone" versions of chapters 5 and 7 have been presented at ESCAPE-6 on Rhodes, Greece in May 1996 and at PSE-ESCAPE'97 in Trondheim, Norway in May 1997, respectively. These chapters have been partly rewritten; some topics have been more emphasized and some new parts have been included. Also, some introductory issues have been removed as these now are presented more thoroughly in chapter 2.

1.3 Related work

Synthesis of HENs is a mature research field and Gundersen and Næss (1988) cite almost 200 papers in their review article. The two dominating synthesis methods have been the pinch design method and mathematical programming. Gundersen *et al*. (1991) show that both of these methods may fail to find the global optimal solution. Further development still takes place within HEN synthesis, including methods that combine elements from different approaches.

Compared to the large literature on HEN synthesis, the number of publications concerning operation of HENs is much less. A prerequisite for optimal operation is that the HEN is sufficiently flexible (i.e. feasible operation for variations/disturbances that may be

encountered). Kotjabasakis and Linnhoff (1986) introduced sensitivity tables in order to make a base case design flexible, and a later contribution by Papalexandri and Pistikopoulos (1994a) introduces a model that includes flexibility requirements in the synthesis stage using a mathematical programming approach.

Control of single heat exchangers is considered several places in the literature, see e.g. Shinskey (1988). For regulatory control of complete HENs, Nisenfeld (1973) used the steady state RGA to find the pairing between measurements and manipulations. Mathisen *et al*. (1992) discusses controllability and control structure selection for HENs, however, energy consumption is not considered. An important contribution to controllability and control structure design in HENs is given by Mathisen (1994, chapters 3 and 4). That contribution also comprises aspects related to energy consumption, and it constitutes an important basis for a large part of this thesis.

Design of operable HENs is discussed by Marselle *et al*. (1982) and heuristic rules are proposed in order to guide the designer to find a base case HEN structure with the most promising properties concerning operability (flexibility and controllability). Mathisen (1994, chapter 7) proposes rules for use together with the pinch design method to achieve HENs with good operability properties. Operability considerations in HEN synthesis using mathematical programming is discussed by Mathisen (1994, chapter 8) and linear constraints that include operability aspects are added to Yee's stagewise model for HEN synthesis (Yee and Grossmann, 1990). A different approach for incorporation of controllability into HEN synthesis is proposed by Huang and Fan (1992) where a knowledge based strategy is proposed. Papalexandri and Pistikopoulos (1994b) include dynamics and control structure considerations in the synthesis stage using a mathematical programming approach.

Even if there is a growing literature that aims to incorporate operability aspects in the synthesis stage (research area 1 on page 2), few publications have been devoted to methods for operation of HENs (research area 2 on page 2). Marselle *et al*. (1982) and Calandranis and Stephanopoulos (1988) suggest to manipulate the duty of the last heat exchanger on a stream, however, this may not be preferred from an energy consumption point of view. Methods for operation of HENs should not only include regulatory control (keep outlet temperatures at targets), optimization should be regarded as well. That is, the method should automatically find the *optimal* operating state when the are variations in disturbances, target temperatures or in the process itself. Mathisen (1994, chapter 5) suggests a method for optimal operation of HENs that utilizes structural information. The method comprises energy optimization in addition to regulatory control, and chapter 5 in this thesis is based on that method. Bojaci *et al*. (1996) proposes a method for operation of HENs that is based on repeated steady state optimization, but their focus is not on the closed loop control system.

Recent work on control structure design by Skogestad and coworkers involves selection of controlled outputs for optimizing control, see Skogestad (1996, chapter 10) and Morud (1995, chapter 8). This may be utilized for optimal operation of HENs and it is incorporated in the method proposed in chapter 7 of this thesis.

References

Calandranis, J. and G. Stephanopoulos (1988). A structural Approach to the Design of Control Systems in Heat Exchanger Networks. *Comput. Chem. Eng.*, **12**.

Gundersen, T. and L. Næss (1988). The Synthesis of Cost Optimal Heat Exchanger Networks. An Industrial Review of The State of the Art. *Comput. Chem. Engng.* **12**, 503-530.

Gundersen, T., B. Sagli and K. Kiste (1991). Problems in Sequential and Simultaneous Strategies for Heat Exchanger Network Synthesis. In *Computer-Oriented Process Engineering*, Elsevier Science Publishers B.V, Amsterdam.

Huang, Y.L. and L.T. Fan (1992). Distributed Strategy for Integration of Process Design and Control - A Knowledge Engineering Approach to the Incorporation of Controllability into Heat Exchanger Network Synthesis. *Comput. Chem. Eng.*, **16**, 497-522.

Kotjabasakis, E. and B. Linnhoff (1986). Sensitivity Tables for the Design of Flexible Processes. How much Contingency in Heat Exchanger Networks is Cost-Effective. *Chem. Eng. Res.*, **64**, 199-211.

Linnhoff, B. and E. Kotjabasakis (1986). Downstream paths for Operable Process Design. *Chem. Eng. Prog.*, **82**, 23-28.

Marselle, D.F., M. Morari and D.F. Rudd (1982). Design of Resilient Processing Plants - II. Design and Control of Energy Management Systems. *Chem. Eng. Sci*., **37**, 259-270.

Mathisen, K.W., S. Skogestad and E.A., Wolff (1992). Bypass Selection for Control of Heat Exchanger Networks. *Paper presented at ECAPE*-1, Elsinore, Denmark.

Mathisen, K.W. (1994). Integrated design and control of heat exchanger networks. *Ph.D. Thesis.* University of Trondheim - NTH, Norway.

Morud, J. (1995). Studies on the Dynamics and Operation of Integrated Plants. *Ph.D. Thesis.* University of Trondheim - NTH, Norway.

Nisenfeld, A.E. (1973). Applying Control Computers to an Integrated Plant. *Chem. Eng. Prog.*, **69**, 45-48.

Papalexandri, K.P. and E.N. Pistikopoulos (1994a). Synthesis and Retrofit Design of Operable Heat Exchangers. 1. Flexibility and Structural Controllability Aspects. *Ind. Eng. Chem. Res.*, **33**, 1718-1737.

Papalexandri, K.P. and E.N. Pistikopoulos (1994b). Synthesis and Retrofit Design of Operable Heat Exchangers. 2. Dynamics and Control Structure Considerations. *Ind. Eng. Chem. Res.*, **33**, 1738-1755.

Shinskey, F.G. (1988). *Process Control Systems. Application, Design and Tuning*. 3rd. edn. McGraw-Hill Inc., New York.

Skogestad, S. and I. Postlethwaite (1996). *Multivariable Feedback Control, Analysis and Design*. John Wiley & Sons, London, UK.

Yee, T.F. and I.E. Grossmann (1990). Simultaneous Optimization Models for Heat Integration - II. Heat Exchanger Network Synthesis. *Comput. Chem. Eng.*, **14**, 1165-1184.

Chapter 2

BASIC IDEAS AND CONCEPTS

This chapter includes the common basis required for the subsequent chapters, particularly for those chapters that concern operation of HENs. It will also give some further motivation why good operation and control of HENs is important for the overall process. Terms like flexibility, controllability and operability will be described, and the influence of the process structure will be discussed. The chapter starts with a quick summary of the design of the overall process and a brief overview of HEN synthesis, before the topics more related to operation are presented.

2.1 Decomposing the HEN from the rest of the process

A plant transfers raw materials into products by means of chemical reactions, separation steps etc. Often a plant comprises several feed streams being converted into a main product together with wanted or unwanted byproducts in a complex process structure. In addition, utility systems for thermal energy, mechanical and electrical energy, pneumatics and so on are required. In the subsequent, the term *utility* refers to thermal energy, i.e. addition and removal of heat.

The purpose of a plant is to manufacture the desired products as economically as possible. However, government regulations (e.g. regarding environmental pollution), safety and health demands also have to be fulfilled. Three tasks that have a major impact on the overall properties of a plant are the selection of:

1. Reaction path and reactor(s).
2. Recycle and separation network.
3. Heat exchanger network and utilities.

There are two essentially different approaches to process design (Smith, 1995, chapter 1):

1. Sequential development of a process structure.
In this approach, the designer starts by making decisions about the most important part of the process and then moves to less important parts. In process design the "onion model" described by Smith and Linnhoff (1988) is usually followed, see figure 2.1.

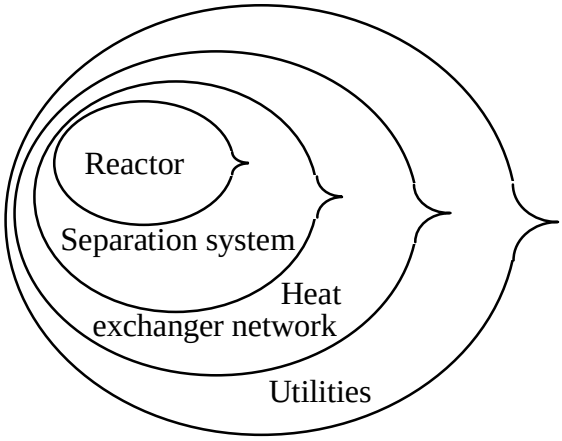

Figure 2.1 Onion diagram in process design.

The design starts with the "core" of the process which is the reactor. When reaction path and reactor have been selected, the designer can move outwards in the onion and make decisions on separation and recycle system, and so on. The flowsheet is developed sequentially and there is no guarantee that a series of optimal local decisions leads to an optimal overall process. For example, decisions made in the reactor and separation layers may give little potential for heat recovery in the outer layers. The designer may then go back to the inner layers and investigate other alternatives, hoping to find an overall solution at least close to the global optimum. Despite the danger of being trapped in local optima and the work required in investigating several alternatives, this approach also has advantages: The designer (or design team) interacts actively in the design process and can use his/her knowledge and experience. With the designer in command of the decisions taken a large variety of knowledge can be considered, but perhaps more important – the designer learns from the design process and will become a better designer in subsequent projects.

2. Simultaneous development of a process structure.
The second approach is based on a *superstructure* of the process. A superstructure (or hyperstructure) includes all process structures that will be considered. That is, the designer starts by setting up all possible reactors, all possible recycles and separators and so on. This results in a large number of candidate process structures and the design problem is formulated as a mathematical model which is solved by means of optimization. The approach usually result in an MINLP problem (see e.g. Grossmann, 1985) where the integer part represents discrete decisions such as whether a processing unit is present or not. (Note that the term "integer" in MILP or MINLP problems often actually refers to *binary* variables and not to integers). Logical propositions such as "*choose exactly one reactor*" *or* "*if reactor A is chosen, then separator D can not be chosen*" are formulated as mathematical constraints and included in the model.

This second approach will not be trapped in local optima due to sequential decisions as in the first approach. However, the second approach also have disadvantages: The optimal process structure may not be embedded in the superstructure given initially by the designer. Provided that the optimal structure *is* embedded within the superstructure, the numerical solution algorithm may fail to find the global optimum. In general such problems are non-convex and there is no guarantee that the global optimum will be found. Thus, this approach may also result in a local optimum. In addition, the combinatorial nature of such problems may impose severe limitations for the simultaneous approach when applied to medium or large size problems. The most serious disadvantage, however, is probably that the designer does not play an active role in the decision making. This means that topics like safety and health considerations or e.g. costs related to adaptation to existing infrastructure hardly will be considered in the conceptual design stage. Such considerations may be done by an experienced designer in early decisions of the sequential approach, but will be more difficult to implement in a optimization model required for the simultaneous approach. Also, the learning of the designer will be less prominent in the second approach.

Despite the fundamental differences between the sequential and simultaneous approaches, most practical designs will have elements of both. The difference between sequential and simultaneous methods may not only be applied to flowsheeting of a complete plant, it may be equally relevant for each subtask. In the next section, it will be clear that the main difference in synthesis of HENs is also between sequential and simultaneous methods. The rest of this section is devoted to decomposition of the HEN from the remaining parts of the plant and to explain why good operation and control of the HEN is important for the overall process. These issues are illustrated by an example. The example has been made as simple as possible while retaining the essential properties of a typical integrated plant.

Consider the plant in figure 2.2 where decisions regarding reaction path, reactors and separation have been made. The process does not have any material recycles.

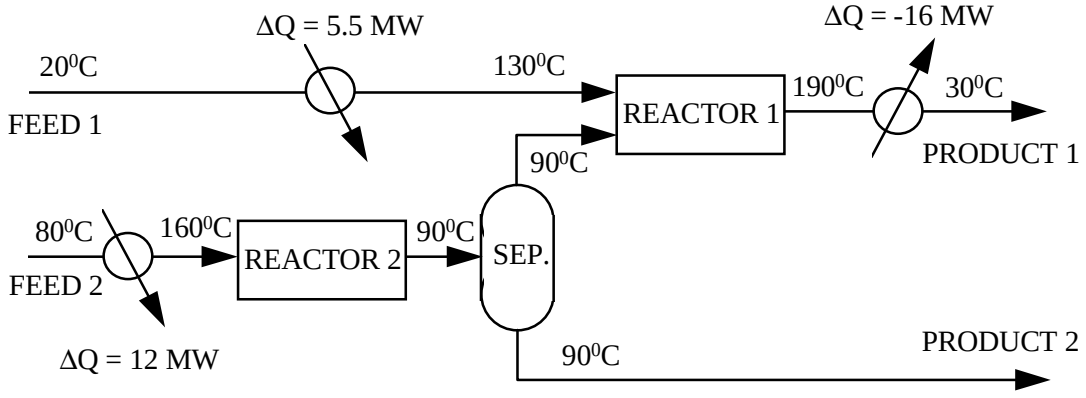

Figure 2.2 Simple process with two reactors and a separator.

The two feed streams requires heating and PRODUCT 1 requires cooling. Table 2.1 gives the data necessary for considering heat recovery between these three streams. Note that the

classification of hot and cold streams is based on whether a stream requires cooling or heating, it does not depend on temperature.

Stream name	Stream no.	T_s [°C]	T_t [°C]	CP [MW/°C]	ΔQ [MW]
PRODUCT 1	Hot 1 (H1)	190	30	0.10	16.0
FEED 2	Cold 1 (C1)	80	160	0.15	12.0
FEED 1	Cold 2 (C2)	20	130	0.05	5.5

Table 2.1 Thermal stream data for the simple heat recovery problem.

Using the data in Table 2.1, focus here is on the heat recovery problem only. The heat recovery problem has been decomposed from the rest of the process. An obvious way to satisfy the heating and cooling demands for this problem is to install two heaters and one cooler as shown in figure 2.3. The total heating and cooling duties are satisfied using external utilities (steam and cooling water) and the requirements are $Q_H = 17.5$ MW and $Q_C = 16.0$ MW for heating and cooling, respectively. This solution does not involve any heat recovery.

Figure 2.3 Trivial solution using external utilities only.

Figure 2.4 shows one possible HEN for the simple process. The countercurrent arrangement with hot streams on top from left to right and cold streams below from right to left (grid diagram) was introduced by Linnhoff and Flower (1978) and will be used throughout the thesis. In this simple HEN, two process-to-process heat exchangers (I and II) have been introduced and stream C2 does not need external heating. Compared to figure 2.3, the utility duties have been reduced to $Q_H = 8.0$ MW and $Q_C = 6.5$ MW while the number of heat transfer units has increased from three to four. Note that the reduction of *both* hot *and* cold utilities is equal to the total process-to-process heat transfer ($Q_I + Q_{II} = 9.5$ MW). This significant reduction in external energy consumption due to process integration is of course important. Linnhoff and Turner (1981) reports results from industrial applications where savings in both energy and capital costs have been achieved through heat integration.

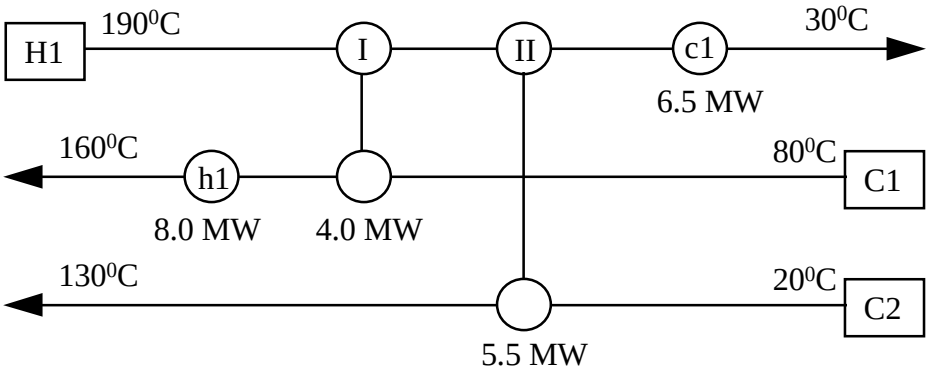

Figure 2.4 HEN for the simple process.

The HEN in figure 2.4 reduces utility consumption, however, it also introduces *interactions*. As an example, a disturbance in the supply temperature of stream H1 will not only affect the outlet temperature of the same stream but it will also affect the outlet temperatures of the two cold streams as this disturbance also will travel from hot to cold side of process-to-process heat exchangers. To see how these interactions in the HEN may influence the dynamics of the overall plant, the complete process including the HEN is drawn in figure 2.5.

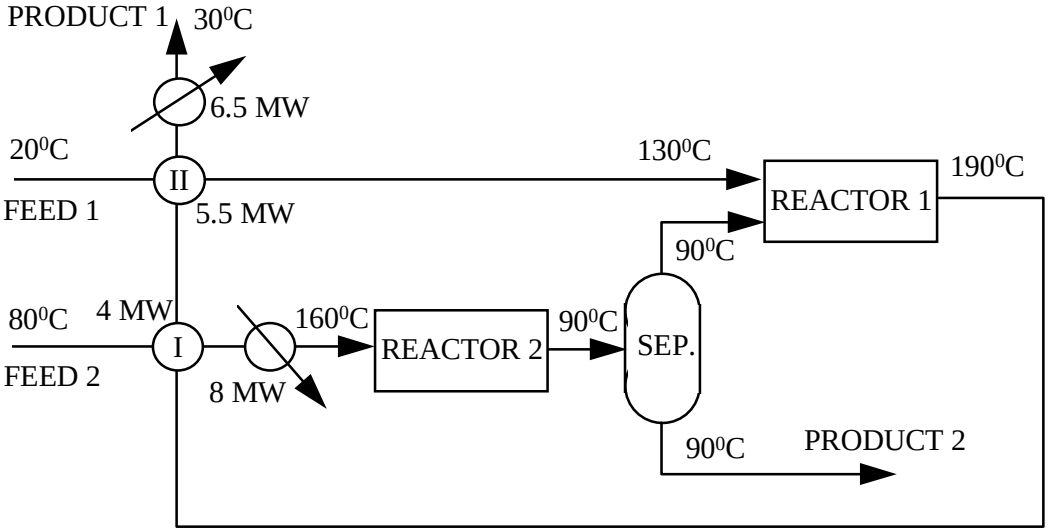

Figure 2.5 Complete plant with heat integration.

We see that the interactions in the HEN causes *feedback* in the plant, e.g. the exit temperature from REACTOR 1 will affect the inlet temperature of the same reactor through the heat exchangers. This may significantly change the overall plant dynamics, and may lead to slower response, increased sensitivity to disturbances and even instability. Of course, feedback may also give desired effects (e.g. feedback control). However, feedback introduced by heat integration makes it more difficult to deduce the plant dynamics from the dynamics of the individual plant units.

As illustrated by figure 2.4 and figure 2.5, a HEN can be considered from two different points of view:

Viewpoint 1. A HEN is a part of the process with its own properties such as heat recovery level and dynamic behavior, and it can be considered separately from the rest of the process.

Viewpoint 2. A HEN affects the overall plant properties as it connects the plant thermally. Consideration of the HEN as a separate unit has little interest.

The first point of view which focuses on the HEN as a separate unit is often employed in the synthesis of HENs. That is, the stream data is first selected from reactor, separation system and possibly recycle considerations (sequential approach). Then, the HEN is designed as a separate task even if it is clear that the optimal supply and target temperatures may change somewhat for the overall process.

Regarding the dynamics and control of an integrated plant, it could be easy to draw the conclusion that the second point of view has to be applied since it is the overall plant dynamics that is important. This conclusion is not quite true despite the fact that the dynamic behavior of the HEN itself may not be important. Consider an integrated plant where a separate control system has been designed for the HEN. Assume that the control system yields perfect control meaning that the outlet temperatures from the HEN are kept exactly at their target values (setpoints) also when disturbances are present. Now, the controlled HEN will *not* introduce any interactions or feedback in the overall plant. That is, if perfect control of the HEN is obtained, the overall plant dynamics will be as if heat integration was not present. However, the steady state benefit of heat integration in terms of reduced energy costs will be preserved. In practice, perfect control can not be achieved but we can conclude that "good" control of the HEN is desired as this will give "small" interactions and "small" effects of unwanted feedback in the overall plant. Good control of the HEN has a decoupling effect on the dynamics of the overall plant and will simplify control system design for the rest of the process. Of course, controlling the outlet temperatures from the HEN is also important since deviations from the target temperatures may affect for example reactor conversion or quality of separation in downstream units. In conclusion, dynamics and control of the HEN are important for the overall plant behavior.

2.2 HEN synthesis, a quick overview

The total design effort (on a systems level) required for a HEN typically involves the following three stages:

1. Nominal design. Synthesize one or more networks with good properties (regarding heat recovery and capital cost) for nominal stream data.
2. Flexibility and controllability. Investigate the networks with regard to flexibility and controllability, and possibly introduce some modifications (e.g. increased area) such that at least one HEN shows satisfactory results.
3. Operation. Design a control system to operate the HEN properly. This involves control structure selection and possibly some method for on-line optimization.

This section will briefly explain a few aspects related to the first of these points; synthesis of HENs for nominal stream data. HEN synthesis is often regarded as the most mature research field within process design, and progress during the last decades has been made in parallel by the two main “schools”; pinch technology and mathematical programming. A comprehensive and thorough review of HEN synthesis until the late 1980’s is given by Gundersen and Næss (1988).

Despite being thoroughly investigated, the combinatorial aspects together with the non-convex nature of the HEN synthesis problem, make the search for the cost optimal HEN a challenging task, see e.g. Gundersen *et al*. (1991). The simple concepts described in this section is part of pinch analysis.

An important concept within pinch technology is the merge of all hot process streams and all cold process streams into one temperature/heat diagram, known as the composite curves. The stream data required to draw the composite curves for the simple problem used in the previous section is given in table 2.1, and the data will be used as a simple example. The composite curves for this example are shown in figure 2.6.

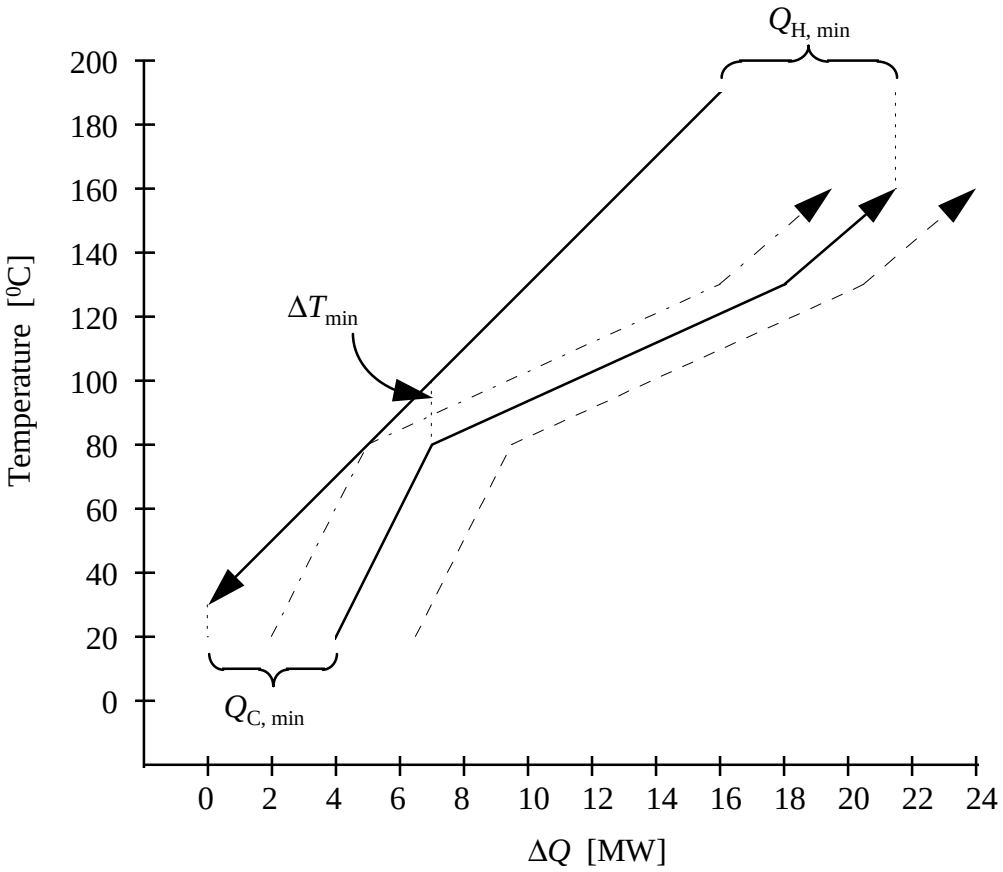

Figure 2.6 Composite curves for the simple heat recovery problem.

In this simple example, there is only one hot stream and the hot composite curve (upper line) is trivial. Both of the cold streams are present in the temperature range from 80°C to 130°C, and the slope of the cold composite curve is 1/(0.15+0.05) = 5.0 [°C/MW] in this temperature

interval. The horizontal axis is *change* of heat, thus the horizontal positions of the curves are not unique. The vertical difference between the composite curves denote the driving forces for heat transfer. For the solid composite curves in figure 2.6, the smallest temperature difference between the curves, ΔT_{min}, is selected to 20°C. At the highest temperature, the process needs addition of hot utility Q_H (e.g. steam) and at lowest temperature the process needs removal of heat to cold utility Q_C (e.g. to cooling water). In the region along the horizontal axis where both curves are present, heat may be recovered between hot and cold process streams. The point where the composite curves are closest to each other is known as *the pinch*. With the smallest driving forces, the pinch represents the bottleneck for heat transfer. The pinch also decomposes the heat recovery problem into two subproblems; (1) above pinch where only hot utility is needed, and (2) below pinch where only cold utility is needed. Transferring heat across the pinch using process exchangers will increase *both* hot and cold utility accordingly ("double penalty") and should be avoided.

Before the pinch design method can be applied, a value of ΔT_{min} has to be selected. This specification actually trades off utility consumption (operating cost) against capital cost (e.g. heat exchanger area). It is thermodynamically feasible to let the composite curves touch at the pinch (dash-dotted cold curve in figure 2.6), yielding the lowest external utility consumption possible. With no driving forces at the pinch, however, infinite heat exchanger area is required and the resulting HEN is definitely not cost optimal. A reasonable value of ΔT_{min} can be found from optimizing the trade-off between utility consumption and capital cost. This is known as supertargeting, see Ahmad *et al*. (1990).

The pinch design method consists of three stages:

1. Targeting
2. Synthesis
3. Optimization.

These will now be described very briefly using the simple example.

Targeting

An important feature related to HEN synthesis is that it is possible to quantify *targets* for minimum utility consumption, minimum number of units and minimum area *ahead* of the actual synthesis stage. Minimum utility consumption ($Q_{H,min}$ and $Q_{C,min}$) can be found using e.g. the problem table algorithm or the heat cascade, or it may be found graphically from the composite curves (when they are aligned according to the specified value of ΔT_{min}). From figure 2.6, the targets for utility consumption are identified to $Q_{H,min} = 5.5$ MW and $Q_{C,min} = 4.0$ MW. The targets for utility consumption are constrained by the value of ΔT_{min}.

The target for number of units normally arises from the "*N*–1" rule: Minimum number of units (including utility exchangers) is equal to the number of streams (including utilities) minus one. This rule is based on graph theory – no thermodynamic considerations are made, and there are cases where the rule does not give a correct target value. A rigorous target value for minimum number of units may be found using mathematical programming. For the simple example, the target for number of units (for the complete HEN) is 3+2–1 = 4. Applying the *N*–1 rule below and above the pinch separately, the target for minimum number of units for the decomposed HEN is (3+1–1) + (2+1–1) = 5.

A target value for total area may be found assuming vertical heat transfer. This target, however, is not compatible with the target for minimum number of units. Cost optimal HENs often have close to minimum number of units, and the area will often deviate from the target.

Synthesis

In this step, a HEN that satisfies the target for utility consumption (maximum energy recovery) is designed. The design starts where the process is most constrained, at the pinch, and is carried out separately above and below pinch. ΔT_{min} is the agreed minimum approach temperature for each heat exchanger, and exchangers are placed between streams such that this requirement is fulfilled. To achieve this, stream splitting may be necessary. The duty of each heat exchanger is made as large as possible, constrained by the stream with the smallest heat demand. This "tick-off" rule minimizes the number of units in the design. Utility exchangers are placed on streams that do not meet the target temperatures when using only process exchangers. Figure 2.7 shows the maximum energy recovery HEN for the example and the pinch is shown by the dashed vertical line. The utility targets are met and the number of 5 units corresponds to the target for the decomposed HEN.

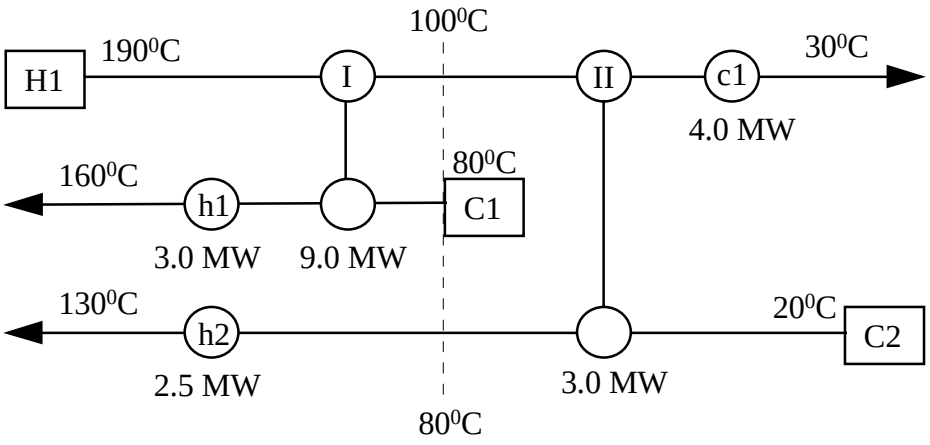

Figure 2.7 Maximum energy recovery network (ΔT_{min} = 20°C).

Optimization

In this stage, the maximum energy recovery HEN from the synthesis stage is improved in order to achieve a more cost optimal HEN. All pinch designs from the synthesis will have at least one unit more than the minimum number when the complete HEN is considered. Removing units may reduce the total HEN costs. The network in figure 2.7 has one unit above the target for the complete HEN, and excess units form *loops*. For this example, there is only one loop:

Units:	II h2 h1 I
Streams:	H1 — C2 — ST — C1 — H1

The units are physically connected by the streams as indicated above. To form a loop, the first and last stream must be identical. A loop always consist of an even number of units, and every second unit may increase and decrease its duty by the same amount of heat while maintaining the heat balance in the HEN. Manipulating a loop this way represents a degree

of freedom in the design stage, and it may be utilized to remove a unit. A heuristic rule in pinch design is to remove the unit with the smallest duty. Applied to the example, heater h2 is removed by reducing the duty to zero. This results in *increased* duties of 2.5 MW for heater h1 and exchanger II and the same *reduction* in exchanger I. Examining the resulting HEN, one will find that the constraint on ΔT_{min} is violated (hot side of exchanger I). ΔT_{min} is restored by exploiting *paths* in the HEN. In the example, there is a path from hot utility stream (ST) to the cold utility stream (CW, cooling water).

$$\begin{array}{ccccccc} & & \text{h1} & & \text{I} & & \text{c1} \\ \text{ST} & — & \text{C1} & — & \text{H1} & — & \text{CW} \end{array}$$

A path is manipulated similarly as a loop; every second unit is manipulated by opposite duties of equal magnitude. A path always comprises an odd number of units, meaning that the first and last unit (utility exchangers) are changed in the same direction. In the example, the hot outlet temperature of exchanger I is increased by reducing the duty of that exchanger. Hence, ΔT_{min} can be restored by reducing the duty of exchanger I which implies increased duties of the heater and cooler. In general, restoring a violation of ΔT_{min} implies that the duty of both utility exchangers in a path are *increased*. The completed HEN after ΔT_{min} is restored is shown is shown in figure 2.4. The composite curves for the finished HEN is shown in figure 2.6 (dashed cold line). Note that the smallest temperature difference between the composite curves are larger than the $\Delta T_{min} = 20°C$ at the hot end of exchanger I. The reason for this is that the completed HEN includes non-vertical heat transfer and heat is transferred across the pinch. This increases utility consumption but saves one unit.

In general when using pinch analysis, the designer is faced with a number of choices in the synthesis stage and particularly in the optimization stage. In practice, a number of alternative designs should be carefully investigated with respect to utility consumption, capital cost (e.g. area), operability aspects etc. before the final HEN design is settled.

The very brief and incomplete introduction to the pinch design method presented here was done without references to other works. It has mainly been included for readers without any prior knowledge about HEN synthesis More thorough introductions can be found elsewhere, see e.g. Linnhoff *et al*. (1982) or textbooks such as Douglas (1988) or Smith (1995). This thesis focuses on *operation* of HENs, and design is not emphasized. Some differences/similarities between design and operation can, however, already be pointed out with regard to the important terms presented above (composite curves, loops and paths). In operation of a given HEN, we want the utility consumption to be as small as possible. Control and operation of HENs are the main topics in the remaining sections of this chapter. The following relations between synthesis and operation can be given at this point:

Loops. Loops may be removed in the design stage, but the completed HEN design may still include one or a few loops. As it was clear from above, manipulating loops do not change the total utility consumption, hence we may expect that loops do not play any important role in operation. Loops (particularly those involving only process exchangers) introduces feedback internally in the HEN and this may change the dynamic properties of the HEN.

Paths. Manipulating a path changes the utility consumption, and manipulating paths for varying disturbances etc. to minimize utility consumption is important during operation.

Composite curves. While composite curves are fixed during design (when the heat recovery level is specified), they may change during operation due to variations in supply temperatures, heat capacity flowrates etc. In addition, the specification on ΔT_{min} (for trade-off between capital and operating costs) has no relevance during operation. The purpose during operation is to vary the manipulations in order to keep the composite curves as close to each other as possible when disturbances are present and change the shape of the composite curves.

In the remaining part of this section, the most important methods for HEN synthesis will be mentioned. A major difference of existing methods for HEN synthesis is between sequential and simultaneous approaches, as it was for the design of the overall plant. Methods for synthesis of HENs can be divided into four main categories.

1. Pinch design. Thermodynamic based sequential method.
2. Sequential approach based on mathematical programming.
3. Simultaneous approach based on mathematical programming.
4. Merge of approaches 1, 2 and 3.

In the pinch design method, the designer participates very interactively in the HEN design. Not only are the three stages (targeting, synthesis and optimization) carried out sequentially, but the synthesis stage itself is indeed sequential. The designer places the heat exchangers, one by one, starting at the pinch and moving away until the maximum energy recovery HEN is completed.

In the second category, the target for utility consumption is found using and an LP formulation. Using mathematical programming, constrained heat exchange such as forbidden matches (e.g. due to safety aspects or geographical distances) may be considered. With the target value from this first stage, rigorous targets for minimum number of units as well as the corresponding heat load distribution are found by solving an MILP problem, see Papoulias and Grossmann (1983). The actual network generation is formulated as an NLP problem (Floudas *et al*. 1986). The MILP problem may result in multiple solutions and networks may be generated for the most promising heat load distributions. The network generation (synthesis) is simultaneous in this approach. The approach is here denoted sequential since the HEN design is divided into three subtasks carried out in sequence. Each subtask is, however, performed simultaneously using mathematical programming. The introduction of the vertical MILP model for HEN synthesis (Gundersen and Grossmann, 1990) and the extended vertical MILP problem (Gundersen *et al.*, 1996) aims at improving this strategy so the MILP stage results in heat load distributions in the correct order. That is, the most promising heat load distribution should result in the HEN giving minimum total annual cost etc.

The third category includes truly simultaneous approaches using MINLP formulations. Available numerical algorithms may, however, fail to find the globally optimal HEN due to non-convexity. Further, combinatorial aspects may put severe limitations on the size of HEN synthesis problems that can be solved. In the model proposed by Yee and Grossmann (1990), only the objective function contains non-linearities and all constraints are linear. This model,

however, only allows for iso-thermal mixing, hence the globally cost optimal HEN may not be embedded in the superstructure. Examples of more recent research to overcome problems related to simultaneous HEN synthesis are convex under-estimators (Quesada and Grossmann, 1995) to overcome non-convexity problems, and reduction of the combinatorics problem using logic, see e.g. Floudas and Grossmann (1994). In addition, stochastic optimization methods such as simulated annealing and genetic algorithms are proposed in order to reduce the problem of being trapped in local optima. Despite the efforts to overcome the problems connected to simultaneous synthesis of HENs, the solution of the MINLP models still represents an obstacle that may be prohibitive at least to industrial sized problems.

At present, no existing method for HEN synthesis can guarantee to find the globally optimal solution. A new trend within HEN synthesis is to merge the best properties from the three approaches mentioned above. This forth approach involves use of pinch principles for screening of alternatives prior to the simultaneous method. Reducing the search space for the MINLP formulation in this way is described by Grossmann and Daichendt (1996). Another branch of this approach includes decomposing the composite curves into blocks and then applying simultaneous techniques for each block, see Zhu *et al*. (1995).

2.3 Introduction to operation and control of HENs

The control objective in a HEN is usually to control outlet temperatures to specified target values (setpoints, references). Target temperatures are denoted with subscript *t* and the actual (measured) outlet temperatures have subscript *o* (e.g. T_t^{H1} and T_o^{H1} are target and outlet temperatures for stream H1). The letters *r* for reference and *y* for measurement which are conventional notation in control literature will also be used. In some cases, there may be other control objectives as well. For instance, the reboiler or condenser in a distillation column may be integrated in the HEN, and the target in such case may be the heat duty of the unit. Another example is when some internal temperature has a maximum value e.g. to prevent decomposition. There may also be outlet temperatures without any specified target value (free outlet temperatures). If nothing else is specified, “targets” denote the setpoints for the outlet temperatures.

In addition to the regulatory control objective it is important that the utility cost is as small as possible. In order to have a concise understanding of what we want to achieve during operation of a HEN, the following definition is introduced.

Definition 2.1 *Optimal operation of HEN.*
For a HEN with given structure, heat exchanger areas, heat transfer coefficients and supply and target temperatures, the operation is optimal if the following three requirements are fulfilled:

- Primary goal: Target temperatures are satisfied at steady state.
- Secondary goal: Utility cost is minimized at steady state.
- Third goal: Dynamic behavior is satisfactory.

■

The secondary goal requires that there are extra degrees of freedom when manipulations have been dedicated for achieving the primary goal. As it will be clear from the next section, most HENs have degrees of freedom that can be used for utility cost minimization. The third goal is deliberately a bit more vague than the two first. It is certainly possible to define rigorous specifications on the dynamic behavior, but in many cases we will simply use hand rules and common sense to satisfy this third requirement. Of course, we want the controlled HEN to be stable and that the dynamics are not unnecessary slow or oscillatory. With this definition of optimal operation, where the two first goals apply at steady state, it is clear that it is assumed that the process is operated close to steady state most of the time and that the total operating costs are dominated by steady state performance rather than by transient responses.

To manipulate the outputs to meet the targets we differ between the following four categories of inputs:

1. Bypass fraction across one single heat exchanger
2. Bypass fraction across multiple heat exchangers
3. Duty of utility exchangers
4. Split fractions

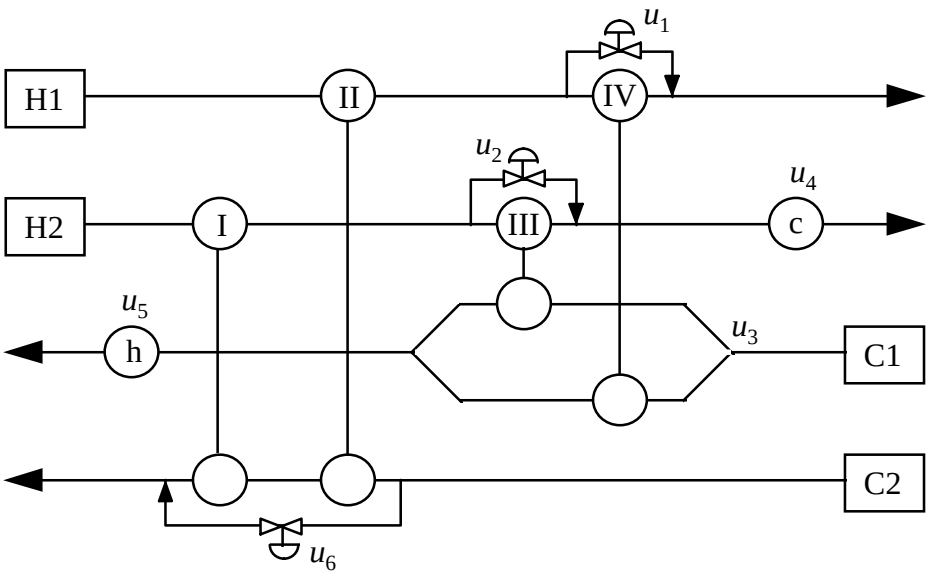

Figure 2.8 Different types of manipulations in a HEN. u_1 and u_2 are single bypasses, u_3 is a variable split fraction, u_4 and u_5 are utility duties and u_6 is a multi-bypass.

The network in figure 2.8 shows these four types of manipulations. For single bypasses (type 1) the input signal is assumed to be the bypass fraction directly. In practice, this may be implemented with a three-way control valve as the splitter, one flow transmitter in each of the two parallel streams and a flow ratio controller. Alternatively, one may install a regular control valve in the bypass stream (as indicated in figure 2.8) and perhaps a throttle in series with the heat exchanger combined with the low-level flow ratio control. (This alternative

solution will reduce the operating range and/or introduce additional pressure drop). In this thesis, the HEN will be viewed from a systems level, and the different practical realizations including the low-level flow control will not be considered in detail. We assume that the control signal is the split fraction directly (flow in bypass line divided by total flow in the stream). In practice, this signal may be the setpoint to the (fast) flow control.

Multi-bypasses may be considered in order to have a manipulation with a fast response in cases where single bypasses cannot affect all outputs directly (e.g. when both hot and cold outlet temperatures from a heat exchanger are controlled). Mathisen (1994, p.63) shows that a multi-bypass (type 2) may limit the operating range considerably compared to single bypasses, thus multi-bypasses may give serious problems with input constraints. In addition, a multi-bypass will reduce the driving forces on several heat exchangers. For these reasons, this category of manipulations will generally not be considered any further in this thesis.

Utility heat exchangers (type 3) are manufactured in various types and many different control strategies are being used. Again, since the HEN is considered from a systems level, we will not consider the implementation details and simply assume that the duty of the utility exchangers are manipulated directly. A utility exchanger is usually located as the final unit in a stream and therefore affects only the outlet temperature of this stream and no other temperatures in the network.

For networks with stream splits, the split fractions may be fixed or variable. A variable split fraction can be used as the manipulated input to control a target temperature. Often, however, a variable split fraction will be used for optimization purposes rather than for regulatory control.

As a general rule in this thesis, it is assumed that a single bypass is (or can be) placed across any heat exchanger and that utility exchangers (if present) always control the outlet temperature of that particular stream. Whether a split fraction is used as a manipulated input or not will be explained in each case. To summarize, the two most important types of manipulations are single bypasses and utility exchanger duties and this gives origin for dividing the targets into the following categories:

- **Bypass controlled targets.** Target temperatures controlled by a bypass across a process-to-process heat exchanger.
- **Utility controlled targets.** Target temperatures normally controlled by the duty of a final utility exchanger.

For problems with multiple hot or cold utilities there may be cases where a utility exchanger is located *internally* in the HEN. While internal utility exchangers may occur for industrial HEN problems, they are not considered very frequently in the academic literature. Utility controlled targets refers to outputs controlled by a *final* utility exchanger. Internal utility exchangers are not considered any further in this thesis. Thus, the term “utility exchanger”, actually refers to a final utility exchanger.

Since a utility exchanger only affects one outlet temperature, all exit temperatures from utility exchangers normally are utility controlled while the other target temperatures usually are bypass controlled. Using the HEN in figure 2.4 as a simple example, T_o^{H1} and T_o^{C1} are utility

controlled while T_o^{C2} is bypass controlled. This division into bypass controlled and utility controlled targets will be utilized in the methods presented in later chapters. The two categories of outputs can also be used to decompose HENs into a certain general structure. To do this, first split the targets (outputs) into y_U and y_{BP} for utility and bypass controlled targets as above. Then split the manipulated inputs into utility duties u_U and bypass fractions u_{BP}. Now the transfer function G from the inputs to the outputs can be divided into the following block structure:

$$\begin{bmatrix} y_U \\ y_{BP} \end{bmatrix} = \begin{bmatrix} G_{11}^{diag} & G_{12} \\ 0 & G_{22} \end{bmatrix} \begin{bmatrix} u_U \\ u_{BP} \end{bmatrix} \tag{2.1}$$

G_{11}^{diag} will always be diagonal since each final utility exchanger only affects the exit temperature of the corresponding stream, and therefore we also have $G_{21} = 0$. The first set of outputs is given by

$$y_U = G_{11}^{diag} u_U + G_{12} u_{BP} \tag{2.2}$$

Assuming that y_U are controlled by SISO feedback controllers from u_U, the last term in equation (2.2) can be considered as a disturbance. If the control of some utility controlled targets are critical, the diagonal feedback control may be combined with feedforward control from u_{BP}. Note that it *may* be possible to use bypass fractions for control of utility controlled outputs, but one must ensure that there are enough bypasses left for control of the bypass controlled outputs y_{BP} (since $G_{21} = 0$, meaning that u_U can not control y_{BP}). It is important to note that while y_U may be affected by u_{BP}, y_{BP} is *not* affected by u_U since we simply have

$$y_{BP} = G_{22} u_{BP} \tag{2.3}$$

Now, if we assume that y_U is *perfectly* controlled by u_U the following rule for decomposition of HENs can be stated.

Rule 2.1 *Decomposition of HENs.*
Assume that utility controlled targets are perfectly controlled using duties of utility exchangers, and that the utility exchangers are not saturated. Then, studying the utility consumption for the complete HEN and the dynamics of the bypass controlled targets are equivalent to study G_{22} together with a steady state expression for the duty of each utility exchanger. That is, G_{11} and G_{12} in equation (2.1) do not need to be addressed. ■

The expression for the steady state utility duty Q_U for each utility exchanger is

$$Q_U = \Delta T_U \, CP \tag{2.4}$$

where CP is the heat capacity flowrate of the process stream and ΔT_U is the positive temperature difference between the target temperature and the temperature at the inlet of the utility exchanger. The fact that dynamic models for utility exchangers may not be needed can be exploited to greatly simplify dynamic simulations of HENs as it will be done in chapter 3. An important point concerning optimization of a HEN during operation, is that there are no degrees of freedom associated with G_{11} since it is diagonal. The degree(s) of freedom (which

is a prerequisite for optimization) is associated with G_{22} (which usually has more columns than rows). Therefore, methods for optimal operation often focus on this transfer function together with simple expressions for utility consumption as in equation (2.4).

The pairing between inputs (manipulations) and outputs for regulatory control is usually rather straightforward. This is partly due to the structure in equation (2.1) which makes the pairing of u_U and y_U trivial since G_{11} is diagonal and partly because the "main rule" for pairing in HENs often can be used for the other outputs. The main rule for pairing can be stated as

Rule 2.2 *Main rule for input/output pairing in a HEN.*
For each outlet temperature that have a target value, prefer a manipulation which has a direct effect on this temperature. ■

This rule can be found several places in the literature and it is a frequently used hand rule for designers. See e.g. Mathisen (1994, chapter 4), where a number of other rules for bypass placement are stated as well. In cases where both hot and cold outlet temperatures from a heat exchanger have target values, the main rule for pairing cannot be applied and other pairings or a multivariable controller has to be used.

The pairing problem often assumes a quadratic plant, i.e. same number of inputs as outputs. This is usually not the case for HENs and when a manipulation has been assigned to each target temperature there are often extra manipulations left. How these extra manipulations are utilized may be important for other features than control such as for example energy consumption. It is important to keep in mind that rule 2.2 originates from the needs of regulatory control. Other pairings may be preferred if dynamic requirements are relaxed, and utility consumption is considered more important. Hence, there is a trade-off between dynamics and steady state performance. This interesting trade-off is important for the methods for optimal operation proposed in chapters 5, 6 and 7.

As it has been evident from this section, the methods for control of HENs presented in this thesis will be based on decentralized control. That is, SISO controllers will be used even if it is clear that the plant itself is multivariable. One might ask why not use a centralized controller that uses all measurements and computes all manipulations using dynamic optimization that simultaneously accounts for regulatory control as well as optimizing issues. Today, more and more plants have modern control systems that allow for such centralized control. At least the hardware conditions are fulfilled by means of data acquisition where all measurements are available for a computer which also can apply manipulations to the process. Despite this, most plants are based on decentralized control and some reasons for this are:

- Decentralized plant. Often a large part of the plant is trivially decentralized, or at least a pairing that gives relatively small interactions can be found.
- Easy to understand. The operation of SISO control loops (using PI or PID controllers) are fairly well understood by operators and others involved in the plant operation, and the control structure is often relatively easy to understand.
- Maintenance and modifications. Maintenance of a centralized control system (software) may be complex since it would have to comprise a complete model of the

plant together with optimization algorithms, equation solvers etc. In a decentralized control system, the different parts of the software can more easily be maintained or modified as long as the interactions from the plant to other control loops are taken into consideration.

- Modeling effort. A centralized controller requires a dynamic model of the complete plant and a considerable amount of work is normally required to obtain such a model. In a decentralized control system, the individual loops are usually tuned without any (mathematical) model at all. In practice, the tuning of a complete plant during start-up is often done in a hierarchical manner starting with the fast and low-level loops, inner loops of cascade structures etc. and moving on to more slow loops with the faster loops closed.

Regarding the first point, it was argued in section 2.1 that process integration increases plant interaction, but it should also be recalled that good control of the HEN has a decoupling effect on the overall plant.

There is a trend towards increased use of multivariable controllers such as MPC, and in many cases these are implemented in addition to (not instead of) conventional (SISO) controllers such that the MPC provides setpoints for the SISO control loops. The methods for optimal control that are proposed in this thesis are based on a decentralized control structure.

2.4 Degrees of freedom in design and operation

In section 2.2 it was demonstrated that a loop in a HEN represents a degree of freedom (DOF) that can be used to optimize the *design* by shifting the duties of the heat exchangers. In a loop, one exchanger may be removed by choosing the duty equal to zero and this breaks the loop. A HEN without any loops has no such degrees of freedom in the design phase. In *operation*, however, the situation is different. During operation we assume:

- Fixed network structure.
- Fixed installed heat exchanger areas where the effective area can be varied between zero and the installed area by manipulating a bypass.
- Specified supply and target temperatures and heat capacity flowrates of process streams.

The perhaps most fundamental difference between design and operation regarding degrees of freedom is that in design there has to be a mechanism that trades off energy cost against capital cost. This fact is rather obvious, since if only energy consumption is considered during design, the result would be a HEN with infinite area and thus infinite capital cost. In the pinch design method, the trade-off between energy and capital cost is taken care of by the specification of $\Delta T_{\min}$ (heat recovery level).

In operation, on the other hand, the trade-off between energy and capital cost is completely irrelevant. Since the HEN structure and installed areas are fixed, the capital costs are fixed as well. The only issue that matters is to exploit the installed heat exchanger areas as efficiently as possible (minimized energy cost) while maintaining the targets. Some earlier works prohibits violation of $\Delta T_{\min}$ for a HEN to be announced operable, see e.g. Calandranis and

Stephanopoulos (1986). This view is not adopted in this thesis. The inapprioprate problem formulation of constraining ΔT_{min} in flexibility/operability analysis is also pointed out by Mathisen (1994, chapter 9). Since the trade-off between capital and energy cost (e.g. by specifying ΔT_{min}) represents a constraint in design and not in operation, this is one example of differences in degrees of freedom in design and operation.

An important question regarding operation of HENs is whether optimization is possible or not. A prerequisite for doing any optimization is that there are degrees of freedom left when manipulations are used for regulatory control. The most crucial question is not how *many* degrees of freedom (DOFs) the HEN has, but simply *whether* we have zero DOFs (optimization is not possible), or one or more DOFs (optimization is possible).

Degrees of freedom of HENs during operation is discussed more thorougly in chapter 4. A simple rule to quickly conclude whether a HEN may be optimized or not, is presented. It will be distinguished between DOFs that may be utilized for utility optimization and DOFs that only can be used to shift duties internally in the HEN (without affecting the utility cost). In many cases, adding extra manipulations will not contribute to the number of DOFs that can be exploited for optimization. It will be shown that most HENs have DOFs that can be used for optimization, and a quantitative expression for the number of DOFs will be derived.

2.5 Flexibility and controllability

Operability of a plant includes all aspects related to the operation of it such as flexibility, safety and reliability, controllability, startup, shutdown etc. This section briefly introduces the two terms, flexibility and controllability.

Flexibility
Flexibility is the ability of a plant to maintain feasible steady state operation for the varying disturbances and operating points that may be encountered during operation. In a HEN, the targets should be met when supply temperatures and flowrates vary within specified regions, and also the targets themselves may be subject to changes during operation. In the case of fouling, the design should also take varying heat transfer coefficients into consideration. Finally, the error of the HEN *model* used for flexibility evaluation compared to the *real* HEN should be considered to ensure that not only the HEN model, but also the real HEN is flexible. Two important problems within flexibility analysis are the *flexibility test problem* and the *flexibility index problem*, see Biegler *et al*. (1997). The flexibility test problem aims to find an answer (yes or no) to whether a design is feasible for a given set of parameter variations. In the flexibility index problem, an index that quantifies the flexibility is introduced (Swaney and Grossmann, 1985). This index of flexibility is equal to one if the design just fulfills the flexibility requirements, above one if the flexibility exceeds the requirements, and below one if the design is infeasible somewhere within the specified uncertainty region.

The flexibility index only quantifies the flexibility for the worst case parameter (or worst case *direction* of parameter combinations). For instance, a flexibility index of 0.8 indicates that for the worst case parameter (or combination of parameters), the plant becomes infeasible when the parameter value is 80% of its nominal value. It does not give any information about

the other parameters (or directions), which also may yield infeasibility just above 80% of the nominal values, or they may have plenty of flexibility.

For HENs, flowrate variations may yield non-convexities as shown by Saboo and Morari (1984). This may give a design which is feasible for two different flowrate values and infeasible for some intermediate value. In flexibility analysis, this implies that the critical parameter values may *not* correspond to the extreme values (corner points) of the parameters. Variations in supply temperatures, however, cannot give any non-convexities due to linear responses, and the critical points corresponds to the corner points. Halemane and Grossmann (1983) show that the computation of the flexibility index is greatly simplified if the critical points in the analysis corresponds to the corner points. For HENs, this implies that variations in supply temperatures can be analyzed by checking the corner points, whereas flowrate variations may yield non-convexities and the critical points may be in the interior of the uncertainty region, see e.g. Floudas and Grossmann (1987). It should be noted that even the corner point check may not be trivial if there are many independent parameters.

Kotjabasakis and Linnhoff (1986) suggest a three-way trade-off between energy, capital cost and flexibility in HEN synthesis. While this may be a suitable view for many problems, it is not adopted in this thesis. Here, it will normally be required that the HEN is feasible for the specified region of disturbances and parameter variations. It is assumed that the variations stay within this region during operation, and therefore no extra money should be spent (or wasted) on making the HEN more flexible than needed.

The term *structural flexibility* in HENs refers to the flexibility of a given network structure when the approach temperature of the heat exchangers are allowed to be zero, that is, areas can be infinitely large. The actual flexibility will be limited by the installed area of some heat exchanger and therefore the achievable flexibility will be less than the structural flexibility.

While flexibility certainly is dependent on the network structure, the flexibility of a given structure can be modified by adjusting the heat exchanger areas. This problem of area optimization is considered by e.g. Mathisen (1994, chapter 9) and Papalexandri and Pistikopolous (1994). In this thesis, it will be assumed that the HENs to be operated have been designed with sufficient flexibility and that the issue is to achieve optimal operation for this given HEN. Problems such as designing for flexibility or area optimization is not considered.

It is important to be aware that the actual flexibility of a HEN during operation may be *limited by the control strategy*. Even if a HEN has capability of being sufficiently flexible, there is no guarantee that the control strategy will adjust the manipulations such that the full flexibility of the HEN is maintained. In the literature, this point seems to have been neglected, or it has been implicitly understood that the control system will not deteriorate the flexibility. While flexibility is a property of the HEN alone, we define *effective flexibility* as follows:

Definition 2.2 *Effective flexibility of HENs.*
The effective flexibility is the ability of a *controlled* HEN to maintain feasible steady state operation for the varying disturbances and operating points that may be encountered during operation. Effective flexibility is a property of the HEN and the control strategy. ■

In control structure design it is important to ensure that the control structure preserves sufficient flexibility such that the controlled HEN fulfills the requirement for effective flexibility.

Controllability

While flexibility concerns steady state properties, *controllability* is related to more short term responses and dynamic properties. In this thesis, the term controllability will usually be used in a loose sense simply meaning how easy the plant is to control. E.g. a manipulation with a "fast" and "large" effect on a controlled output may be preferred compared to a manipulation with a "slow" and "small" effect for controllability reasons. Such qualitative considerations is the basis for the main rule for input/output pairing in HENs.

Controllability is a property of the plant itself, irrespective of the controller. However, manipulations and measurements are defined to be a part of the plant, and the selection of these may strongly affect the controllability. Concerning control and operation of HENs, e.g. Marselle *et al.* (1982), it is often implicitely understood that a variable bypass is placed across each heat exchanger and that all outlet temperatures are measured. In this thesis, it is assumed that a bypass *is or may* be placed across each heat exchanger. In addition, extra measurements (internally in the HEN) may be utilized for improved controllability. The actual choice of manipulations and measurements results in different controllability properties and it is considered as different plants concerning controllability, despite it is the same HEN (same structure, areas etc.) within the synthesis terminology.

Quantitative analysis of controllability aims to find what control performance can be expected, or whether a specified closed-loop performance can be achieved. The closed-loop performance may be specified in the time domain (overshoot, settling time etc.) or in the frequency domain (e.g. bandwidth). A comprehensive description of quantitative controllability analysis (or performance targeting) in the frequency domain is given by Skogestad and Postlethwaite (1996). Control limitations in HENs, such as RHP-zeros, are thoroughly treated by Mathisen (1994, chapter 3), and will not be emphasized in this thesis. In chapter 6 of this thesis, it will be necessary to apply a quantitative measure of controllability in order to find a pairing that is acceptable also from a control point of view. This measure of controllability will be based on the *relative gain array* (RGA) of a linear model of the HEN. The RGA for a square plant (transfer matrix) G is defined as

$$\mathrm{RGA}(G) = G \times (G^T)^{-1} \tag{2.5}$$

where $\times$ denotes element-by-element multiplication. The RGA was introduced by Bristol (1966) as a measure of (two-way) steady state interactions in MIMO systems. The RGA, and particularly the frequency dependent $\mathrm{RGA}(G(j\omega))$, has a number of interesting control properties, see Skogestad and Postlethwaite (1996, chapters 3 and 10). Using the RGA is often a efficient tool since it does not have to be recomputed for different pairings of the same plant. One property of the steady state RGA is the ability to test if a plant is *decentralized integral controllable* (DIC), and this property will be utilized in chapter 6 of this thesis. The DIC was introduced by Skogestad and Morari (1988), and will be defined and explained in chapter 6.

Most HENs have more manipulations than targets and this yields a transfer function with more columns than rows. Even HENs (pinch problems) with *no* loops have one manipulation

in excess. As stated in Mathisen (1994, chapter 3), most HENs without loops only have one-way interaction and this corresponds to transfer function that is upper or lower triangular (with proper ordering of inputs and outputs). The pairing of a square plant that is triangular is trivial since RGA(G) = I. However, this is *not* the case for non-square plants and pairing is not trivial. As an example, consider the transfer function for the HEN in figure 2.4 that will have the form

$$\begin{bmatrix} T_{\mathrm{o}}^{\mathrm{H1}} \\ T_{\mathrm{o}}^{\mathrm{C1}} \\ T_{\mathrm{o}}^{\mathrm{C2}} \end{bmatrix} = \begin{bmatrix} g_{11} & 0 & g_{13} & g_{14} \\ 0 & g_{22} & g_{23} & 0 \\ 0 & 0 & g_{33} & g_{34} \end{bmatrix} \begin{bmatrix} u_{\mathrm{c1}} \\ u_{\mathrm{h1}} \\ u_{\mathrm{I}} \\ u_{\mathrm{II}} \end{bmatrix} \tag{2.6}$$

From equation (2.1), we recognize G_{11} = diag([g_{11}, g_{22}]) and using the trivial decomposition rule for HENs (rule 2.1), the remaining system becomes

$$T_{\mathrm{o}}^{\mathrm{C2}} = \begin{bmatrix} g_{33} & g_{34} \end{bmatrix} \begin{bmatrix} u_{\mathrm{I}} \\ u_{\mathrm{II}} \end{bmatrix} \tag{2.7}$$

The RGA of G_{22} = [g_{33} g_{34}] is a 1×2 matrix with row sum equal to one, and the pairing is not trivial. In chapter 6 where the RGA is used to find the pairing, the square system when one (or more) manipulations is assumed unused is considered. This requires the RGA to be recomputed for the possible selections of unused manipulations.

2.6 Process structure affects operability

It is rather evident that the structure of a process affects the operability. This section will first recall some results from linear systems theory to demonstrate this point. Then, it will be shown by a few simple examples that process structure may significantly change the operability of the HEN as well as for the overall process.

Let g denote the transfer function for a SISO system. That is, g is a frequency dependent complex rational function that can be written as

$$g(s) = k_g \frac{\prod_{i=1}^{i=N_{gz}} (s - z_{gi})}{\prod_{i=1}^{i=N_{gp}} (s - p_{gi})} \tag{2.8}$$

where z_g and p_g are the zeros and poles, and N_{gz} and N_{gp} denote the number of zeros or poles of the system g. k_g is a constant. Similarly, let h be a transfer function written in a similar way.

$$h(s) = k_h \frac{\prod_{i=1}^{i=N_{hz}} (s - z_{hi})}{\prod_{i=1}^{i=N_{hp}} (s - p_{hi})} \tag{2.9}$$

Introduce the short-hand notation n_g and d_g for the numerator and denominator of g in equation (2.8), and similarly n_h and d_h for h. Now, the zeros and poles of the total system when g and h are connected in a *series*, *parallel* or *feedback* structure can easily be found.

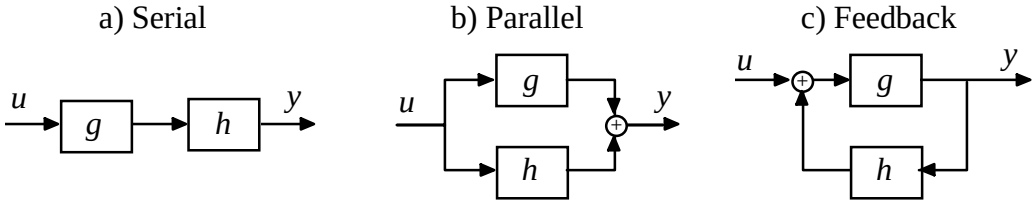

Figure 2.9 Series, parallel and feedback connection.

The transfer function for series connection is

$$\frac{y}{u}(s) = g(s)h(s) = \frac{n_g n_h}{d_g d_h} \tag{2.10}$$

which implies that the zeros and poles for the connected system simply are the zeros and poles of the individual parts (g and h). Series interconnection is typical for plants without integration and as mentioned in previous sections the dynamics of the overall plant can be predicted quite intuitively from the individual units since no new zeros or poles are introduced. Note that even if series interconnection cannot move or introduce new zeros or poles, they may be canceled. For parallel interconnection the overall transfer function becomes

$$\frac{y}{u}(s) = g(s) + h(s) = \frac{n_g d_h + n_h d_g}{d_g d_h} \tag{2.11}$$

The poles of the new system are the poles of the individual elements, meaning that connecting stable systems in parallel cannot yield an unstable overall system. The “plus” in the nominator of equation (2.11) implies that parallel interconnection gives an overall system with *new zeros*. This *may* significantly change the operability of the plant as it may introduce RHP-zeros. A RHP-zero typically occurs when a fast response with small steady state effect counteracts a slow response with large steady state effect, such that the overall step response will start moving away from the final value, yielding an inverse response. Note that while RHP-zeros often are associated with inverse response for SISO systems, an *even* number of RHP-zeros may not necessarily imply inverse response behavior. However, RHP-zeros represent a fundamental control limitation (perfect control cannot be achieved) for both SISO and MIMO systems, see Rosenbrock (1970). Effective control is only possible at low frequencies *or* at high frequencies. In process control applications, good control is usually required at low frequencies and therefore RHP-zeros imply an upper bound on the bandwidth.

If a bypassed heat exchanger has a downstream path from both hot and cold side to a controlled outlet temperature, this represents a parallel connection and the two effects will always have opposite directions. Therefore, such parallel downstream paths may result in RHP-zeros and control limitations. As the following explanation shows, such parallel paths may also give singularity at steady state. Assume that the net effect is small and that a change

in the heat transfer coefficient in one of the parallel paths (e.g. due to fowling) changes the sign of the net effect (at steady state). At some intermediate value of the heat transfer coefficient the two parallel effects will exactly cancel each other at steady state which gives a parametric singularity. For parameter values where the faster of the two opposing effects also is largest at steady state, RHP-zeros would not be expected. When the parameter passes the value that gives steady state singularity (sign changes) and the slower effect becomes dominating at steady state, a RHP-zero may occur. This illustrates that there is a connection between steady state properties (parametric singularity) and control properties (RHP-zeros). A temperature disturbance in a HEN will be dampened at steady state and it will also become slower as it traverses more heat exchangers. Therefore, the parallel path that is shortest, normally gives a response that is both fastest and largest, and this suggests that RHP-zeros may not occur very frequently in practice for HENs. Also, a manipulation that may give singularities is usually not preferred for control. In general, however, parallel paths often occur in HENs and other parts of the plant, and they may result in RHP-zeros and hence in fundamental control limitations as well as modified steady state performance.

The last of the three basic interconnection types, feedback, may perhaps give the most dramatic change of the overall plant dynamics. From figure 2.9c we may write $y = gu + ghy$ which yields the transfer function

$$\frac{y}{u}(s) = \frac{g}{1-gh} = \frac{n_g d_h}{d_g d_h - n_g n_h} \tag{2.12}$$

The zeros of g do not move, but the poles in h become additional zeros in the overall transfer function. The interconnected system will have new poles and this may dramatically affect the operability of the plant. Feedback interconnection of systems that are individually stable may yield an unstable overall system. On the other hand, an unstable plant may be stabilized by feedback control. As shown in section 2.1, feedback interconnections frequently occur in integrated processes.

In addition to these three basic interconnection types, one fourth configuration is presented where there are two sets of inputs (u_1 and u_2) and two sets of outputs (y_1 and y_2). We want to focus on the transfer function from the primary input (u_1) to the primary output (y_1) when feedback is introduced between the secondary output and input, see figure 2.10.

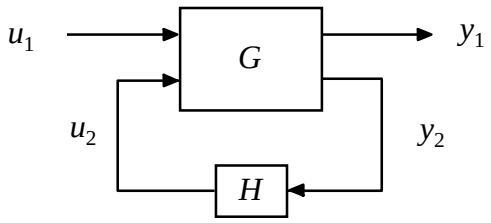

Figure 2.10 Feedback of secondary variables.

Partitioning G into four block matrices where the dimensions match the two sets of inputs and outputs, we can write:

$$\begin{bmatrix} y_1 \\ y_2 \end{bmatrix} = \begin{bmatrix} G_{1,1} & G_{1,2} \\ G_{2,1} & G_{2,2} \end{bmatrix} \begin{bmatrix} u_1 \\ u_2 \end{bmatrix} \tag{2.13a}$$

$$u_2 = H\, y_2 \tag{2.13b}$$

From equation (2.13) the transfer function from u_1 to y_1 (lower linear fractional transform of G and H) is given by

$$y_1 = \left[G_{1,1} + G_{1,2} H \left(I - G_{2,2} H \right)^{-1} G_{2,1} \right] u_1 \tag{2.14}$$

Assume a scalar transfer function, and introde the notation $n_{i,j}$ and $d_{i,j}$ for the numerator and denominator of $g_{i,j}$ and similarly n_h and d_h for the the numerator and denominator of h. Then, the zeros and poles of the resulting system are given by the zeros and poles of the individual transfer functions:

$$\frac{y_1}{u_1}(s) = \frac{n_{1,1} d_{1,2} \left(d_h d_{2,2} - n_h n_{2,2} \right) d_h d_{2,1} + d_{1,1} n_{1,2} d_h d_{2,2} n_h n_{2,1}}{d_{1,1} d_{1,2} \left(d_h d_{2,2} - n_h n_{2,2} \right) d_h d_{2,1}} \tag{2.15}$$

While this expression is more complicated than for the three previous interconnection types, it is evident that feedback in the secondary variables changes both the poles and zeros of the resulting transfer function of the primary variables. It is often stated that feedback moves the poles but not the zeros. This is true for the input and output directly involved with the feedback loop, but feedback may move the zeros for other transfer functions. As a simple example, consider a case where $g_{1,1} = \frac{1}{s+1}$, $g_{1,2} = \frac{1}{s+2}$, $g_{2,1} = \frac{2}{s+3}$, $g_{2,2} = \frac{2}{s+1}$ and $h = 1$. All elements are stable and there are no zeros, but the resulting transfer function has both one RHP-pole and a RHP-zero ($\frac{y_1}{u_1}(s) = \frac{(s-0.71)(s+1.81)(s+3.90)}{(s-1)(s+1)(s+2)(s+3)}$). This type of interconnection may indeed occur in practice, see Jacobsen (1997) where a reactor-separator system with recycle is investigated. In that paper, sufficient conditions for the existence of RPH-zeros for the connection in figure 2.10 also is given.

To conclude, series interconnection does not usually introduce any unexpected dynamic behavior, parallel interconnection moves the zeros (may introduce RHP-zeros), and feedback interconnection moves the poles (may introduce RHP-poles and hence instability). In addition to these three basic interconnection types, introducing feedback (e.g. recycle) in one part of a plant may move both poles and zeros in other parts of the plant. It should perhaps be mentioned that *real* plants have neither poles nor zeros, since these are mathematical terms that apply for rational functions. However, it is assumed that the results for the linearized transfer functions also capture the essence of the behavior of the real plants. Non-linear effects and constraints in real plants (or more rigorous models) may certainly result in much more complex behavior.

From these results for interconnection of linear systems, a few practical examples will now be shown, where the process structure affects the operability in some other ways than pointed out above. Figure 2.11 shows two heat exchangers that may be a part of a larger HEN. Assume that the annual cost from nominal steady state considerations is only marginally different for the two alternatives.

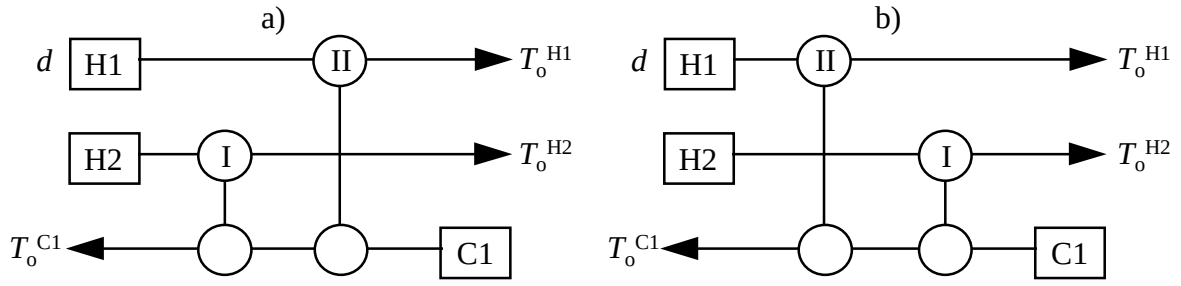

Figure 2.11 Two alternative orders for heat exchangers

We shall consider the two alternatives in the figure for two different cases.

Case 1 Disturbance rejection.
Assume that T_s^{H1} may vary considerably (indicated with *d* in the figure) and that it is critical to have accurate control of T_o^{H2}. In alternative A, the disturbance will affect the controlled output since there is a downstream path from *d* to T_o^{H2} through the two heat exchangers. There is no such downstream path in alternative B, and the disturbance will not affect the critical target at all. Alternative B is clearly preferred in this case. ■

Case 2 "Good" control.
Assume that it is critical to have good control of T_o^{H1} and T_o^{C1} when there may be various disturbances in all three supply streams. In alternative A, the main rule for input/output pairing can be used. Bypassing II on the hot side and I on the cold side yield direct (or at least fast) effect on both outputs and only one-way interaction (u_I does not affect T_o^{H1}). The main rule for input/output pairing can not be applied to alternative B (when single bypasses are used), since bypassing both side of the same heat exchanger can not control two temperatures independently at steady state. Bypassing II on the hot side and using a multi bypass across both I and II on the cold side give direct effect on both outputs, but may give problems with input constraints. With one single bypass on each heat exchanger, this structure will give two-way interactions and they may be strong, see Mathisen (1994, chapter 4). For this case, alternative A is clearly preferred. ■

The figures 2.12 and 2.13 show an example where different HEN structures give different overall plant properties. The HEN is integrated with two reactors, R1 and R2. In figure 2.12 there are thermal feedback loops from the outlet to the inlet of each reactors. The outlet temperature of reactor R1 affects the inlet temperature through only one heat exchanger (II), while the outlet temperature of reactor R2 affects the inlet through two heat transfer units (I and h).

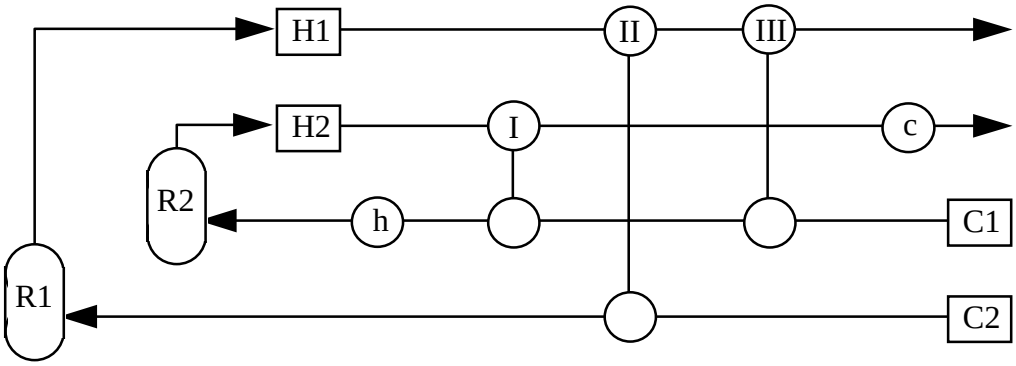

Figure 2.12 Overall plant structure.

In figure 2.13, there are also feedback loops, however, the reactor outlet temperature (from both reactors) have to traverse three heat transfer units before it reaches the inlet of the same reactor. For reactor R2, the disturbance also has to traverse R1. This *indicates* that the structure in figure 2.13 yields weaker feedback loops, and that it *may* be preferred compared with the structure in figure 2.12 due to possible improved overall plant dynamics. While no clear conclusions can be drawn for this example, it should be clear that the two structures give different properties for the total plant.

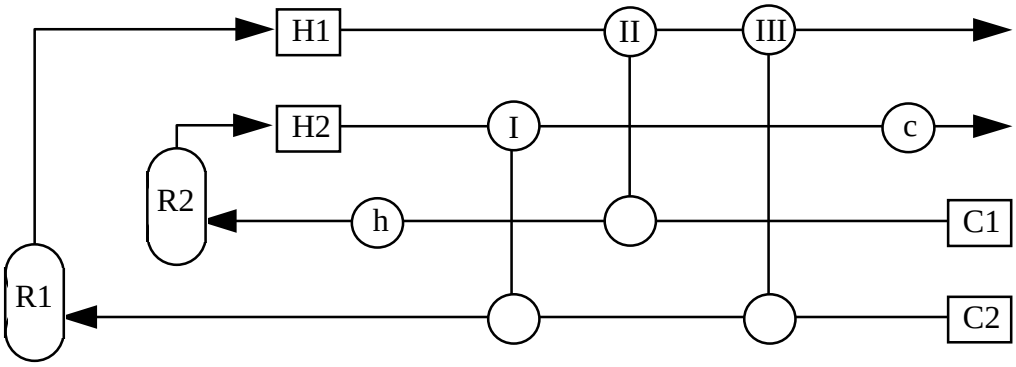

Figure 2.13 Modified overall plant structure.

Finally in this chapter, it is emphasized that the structure may *change during operation*. If a bypass should saturate it would normally be at zero (fully closed bypass pipe and full duty of heat exchanger). This makes the bypass inactive since it cannot be manipulated. This changes the *control structure* and if the bypass fraction was controlling a target temperature, a new bypass will have to be assigned for this purpose, if possible. The saturation of a bypass at zero will not change the structural properties of the HEN regarding propagation of temperature effects. As an example, consider the bypass across heat exchanger II in figure 2.4 being saturated at zero. Still, the bypass on heat exchanger I can by used for control of the bypass controlled target.

A utility exchanger may be saturated at zero duty, and this should be encouraged since utility consumption should be as low as possible. An upstream manipulation has to be assigned if the outlet temperature of the utility exchanger still needs to be controlled. Saturation of utility exchangers may also change the problem type from a pinch problem to a threshold problem. This implies that the HEN cannot be optimized (any *further*) at this operating

condition. It is already operated optimally, since a bad control strategy may turn it back to a pinch problem with an unnecessary large utility consumption.

While saturation at zero does not change the network structure (only the control structure), this is not the case when a heat exchanger is completely bypassed (saturation at one). This corresponds to removing the heat exchanger. If for instance heat exchanger I in figure 2.4 is completely bypassed, this HEN is divided into two subnetworks (and both are threshold problems). It is evident that when a bypass is fully closed, the outlet temperature of this exchanger can not be controlled by any upstream effects on the opposite side. It may be of more practical interest to note that when a bypass fraction increases, the upstream effect traversing to the opposite side decreases. This may be good for disturbance rejection, but makes control more difficult.

In this section, it has been shown that the structure of a process (or HEN) may considerably affect how easy it is to operate. Also, the operation of a process may change not only the control structure, but may also also change the process structure itself, e.g. by bypassing a heat exchanger completely.

Notation

CP	Heat capacity flowrate
d	Denominator
G	Transfer function
k_g	Constant in transfer function g
k_h	Constant in transfer function h
n	Numerator
N	Number of, e.g. N_z is number of zeros.
N_{DOF}	Number of degrees of freedom
N_{target}	Number of targets
N_{units}	Number of units
p	Poles (in a transfer function).
Q_C	Cold utility consumption
Q_H	Hot utility consumption
Q_{in}	Energy flow in
Q_{out}	Energy flow out
T	Temperature
T_o	Outlet temperature
T_s	Supply temperature
T_t	Target temperature
y	Output or measurement
y_{BP}	Bypass controlled outputs
y_U	Utility controlled outputs
u	Input/manipulation
u_{BP}	Bypass fractions
u_U	Utility duties
z	Zeros (in a transfer function)
ΔT_{min}	Minimum temperature difference

References

Ahmad, S.B., B. Linnhoff and R. Smith (1990). Cost Optimum Heat Exchanger Networks - 2. Targets and Design for Detailed Cost Models. *Comput. Chem Engng*., **14**, 751-767.

Biegler, L.T., I.E. Grossmann and A.W. Westerberg (1997*). Systematic Methods for Chemical Process Design*. Prentice-Hall Inc. Upper Saddle River, NJ.

Bristol, E.H. (1966). On a New Measure of Interactions for Multivariable Process Control. *IEEE Transactions on Automatic Control*. AC-11, 133.

Calandranis, J. and G. Stephanopoulos (1986). Structural Operability Analysis of Heat Exchanger Networks. *Chem. Eng. Res. Des.*, **64**, 347-364.

Douglas, J.M. (1988). *Conceptual Design of Chemical Processes.* McGraw-Hill, Singapore.

Floudas, C.A., A.R. Ciric and I.E. Grossmann (1986). Automatic Synthesis of Optimum Heat Exchanger Network Configurations. *AIChE Journal*., **32**, 276-290.

Floudas, C.A. and I.E. Grossmann (1987a). Synthesis of Flexible Heat Exchanger Networks with Uncertain Flowrates and Temperatures. *Comp. Chem. Eng.* **11,** 319.

Floudas, C.A. and I.E. Grossmann (1987b). Automatic Generation of Multiperiod Heat Exchanger Configurations. *Comp. Chem. Eng.* **11,** 123.

Floudas, C.A. and I.E. Grossmann (1994). Algorithmic Approaches to Process Synthesis: Logic and Global Optimization. *Proc. from FOCAPD'94*, Snowmass, Colorado, 198-221.

Grossmann, I.E. (1985). Mixed Integer Programming Approach for the Synthesis of Integrated Process Flowsheets. *Comp. Chem. Eng.*, **9,** 163.

Grossmann, I.E. and M.M. Daichendt (1996). New Trends in Optimization-based Approaches to Process Synthesis. *Comput. Chem. Engng.*, **20**, 665-683.

Gundersen, T. and L. Næss (1988). The Synthesis of Cost Optimal Heat Exchanger Networks. An Industrial Review of The State of the Art. *Comput. Chem. Engng.* **12**, 503-530.

Gundersen, T. and I.E. Grossmann (1990). Improved Optimization Strategies for Automated Heat Exchanger Network Synthesis through Physical Insights. *Comput. Chem. Engng.*, **14**, 925-944.

Gundersen, T., B. Sagli and K. Kiste (1991). Problems in Sequential and Simultaneous Strategies for Heat Exchanger Network Synthesis. In *Computer-Oriented Process Engineering*, Elsevier Science Publishers B.V, Amsterdam.

Gundersen.T, S. Duvold and A. Hashemy-Ahmady (1996). An Improved Vertical MILP Model for Heat Exchanger Network Synthesis. *Comput. Chem. Engng.*, **20**, 97-102.

Halemane, K.P. and I.E. Grossmann (1983). Optimal Process Design under Uncertainty. *AIChE Journal*, **29,** 425.

Jacobsen, E.W., (1997). Effect of Recycle on Plant Zero Dynamics. *Comput. Chem. Engng.*, **21** Suppl., 279-284.

Kotjabasakis, E. and B. Linnhoff (1986). Sensitivity Tables for the Design of Flexible Processes (1) - How Much Contingency in Heat Exchanger Networks is Cost-Effective? *Chem. Eng. Res. Des.*, **64,** 197.

Linnhoff, B. and J.R. Flower (1978). Synthesis of Heat Exchanger Networks. *AIChE Journal*, **24,** 633.

Linnhoff, B. and J.A. Turner (1981). Heat Recovery Networks: New Insights Yield Big Savings. *Chemical Engineering*, 2 November, 56.

Linnhoff, B. *et al*. (1982). *User Guide on Process Integration for the Efficient Use of Energy*. Inst. Chem. Engrs., Rugby, UK.

Mathisen, K.W. (1994). Integrated Design and Control of Heat Exchanger Networks. *Ph.D. Thesis*. University of Trondheim - NTH, Norway.

Papalexandri, K.P. and E.N. Pistikopoulos (1994). Synthesis and Retrofit Design of Operable Heat Exchangers. 1. Flexibility and Structural Controllability Aspects. *Ind. Eng. Chem. Res.*, **33**, 1718-1737.

Papoulias, S.A. and I.E. Grossmann (1983). A Structural Optimization Approach to Process Synthesis - II. Heat Recovery Networks. *Comput. Chem. Engng.*, **7**, 707-721.

Quesada, I. and I.E. Grossmann (1995). A Global Optimization Algorithm for Linear Fractional and Bilinear Programs. *Jl. Global Optim.*, **6**, 39-76.

Rosenbrock, H.H. (1970). *State-space and Multivariable Theory*, Nelson, London, UK.

Saboo, A.K. and M. Morari (1984). Design of Resilient Processing Plants - IV. Some new Results on Heat Exchanger Network Synthesis. *Chem. Eng. Sci.*, 39: 579.

Skogestad, S. and M. Morari (1988). Variable Selection for Decentralized Control. *AIChE Annual Meeting*, Washington DC. Paper 126f. Reprinted in *Modeling, Identification and Control*, 1992, **13** No. 2, 113

Skogestad, S. and I. Postlethwaite (1996*). Multivariable Feedback Control, Analysis and Design*. John Wiley & Sons, Chichester, UK.

Smith, R. and B. Linnhoff (1988). The Design of Separators in the Context of Overall Processes. *Trans. IChemE, ChERD*, **66**, 195.

Smith, R. (1995). *Chemical Process Design*. McGraw-Hill, Inc. New York, USA.

Swaney, R.E. and I.E. Grossmann (1985). An Index for Operational Flexibility in Chemical Process Design. I & II. *AIChe J.*, **31**.

Yee, T.F. and I.E. Grossmann (1990). Simultaneous Optimization Models for Heat Integration - II. Heat Exchanger Network Synthesis. *Comput. Chem. Eng.*, **14**, 1165-1184.

Zhu, X.X., B.K. O'Neill, J.R. Roach and R.M. Wood (1995). A New Method for Heat Exchanger Network Synthesis Using Area Targeting Procedures. *Comput. Chem. Engng.*, **19**, 197-222.

Chapter 3

SIMULATION OF HENs

This chapter describes how dynamic simulations of HENs can be carried out. The type and complexity of the model of each heat exchanger significantly affect the efforts required for HEN simulation, and focus is on the development of a general heat exchanger model that simplifies the simulations. Some fundamentals of heat transfer and steady state properties of ideal countercurrent heat exchangers are briefly described, and the chapter closes by explaining how dynamic simulation of controlled HENs are performed.

3.1 Governing equations for heat transfer

A quite general expression for the energy balance (e.g. Bird *et al*., 1960), using cartesian tensor notation, is

$$\underbrace{\frac{\partial}{\partial t}\left(\rho\hat{E}\right)}_{\text{Accumulation}} + \underbrace{\frac{\partial}{\partial x_i}\left(\rho u_i \hat{E}\right)}_{\text{Convection}} = \underbrace{\frac{\partial}{\partial x_i}\left(\alpha \frac{\partial \hat{E}}{\partial x_i}\right)}_{\text{Diffusion}} + S \tag{3.1}$$

where $\hat{E}$ is specific energy (mass basis) and u_i are the velocity components in the three spatial directions, x_i. It is assumed that the heat transfer due to diffusion is given by Fourier's law.

$$q_i = -k\frac{\partial T}{\partial u_i} \tag{3.2}$$

Here, k is the *thermal conductivity* of the material, and the *thermal diffusivity* α in equation (3.1) is given by $\alpha = k/c_v$. Equation (3.1) gives the specific energy at any point within arbitrary system boundaries. The source term S denotes energy flow across the system boundaries, and it may also include heat transfer not included in the other terms, such as radiation. Equation (3.1), together with similar expressions for conservation of mass and impulse, may be used for detailed studies of heat exchangers to investigate for instance different geometries inside the unit, see e.g. Sha *et al*. (1982). The governing equation (3.1) may also be used to derive simplified expressions for various cases. We shall approach modeling of heat exchangers by setting up energy balances for the idealized countercurrent configuration shown below, and see that the result conforms to a simplified version of equation (3.1).

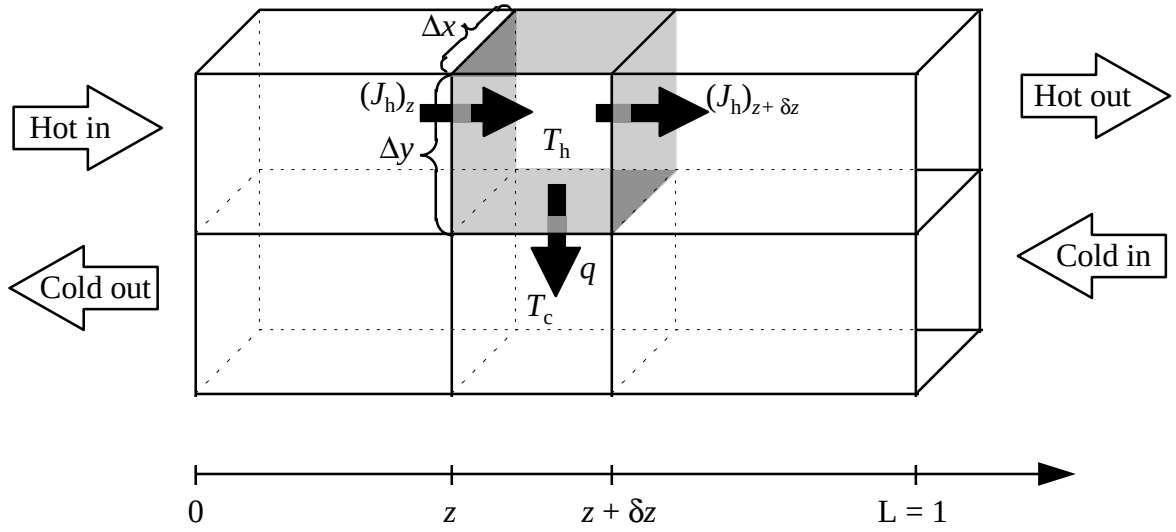

Figure 3.1 Sketch of ideal countercurrent heat exchange.

Heat q is transferred from the hot to the cold stream through the wall with an assumed constant heat transfer coefficient U. First, consider the hot side, where the density ρ_h and the mass flux J_h are assumed constant. There are no temperature gradients in the crosswise directions, and diffusion of energy is assumed negligible (compared to convection) in the streamwise direction z. Also, mechanical energy is assumed small, thus the dynamic equation for thermal energy in the hot control volume indicated in figure 3.1 becomes

$$\frac{d}{dt}\left(\rho_h \Delta x \Delta y \delta z \hat{E}_h^U\right) = \left(J_h \Delta x \Delta y \hat{E}_h^U\right)_z - \left(J_h \Delta x \Delta y \hat{E}_h^U\right)_{z+\delta z} - \underbrace{U \Delta x \delta z (T_h - T_c)}_{q} \qquad (3.3)$$

$\hat{E}_h^U$ is the specific internal energy in the hot side control volume. Rearranging somewhat and letting δz approach zero, we get

$$\underbrace{\frac{\partial}{\partial t}\left(\rho_h \hat{E}_h^U\right)}_{\text{Accumulation}} + \underbrace{J_h \frac{\partial \hat{E}_h^U}{\partial z}}_{\text{Convection}} = \underbrace{-\frac{U}{\Delta y}(T_h - T_c)}_{\text{Source}} \qquad (3.4)$$

This is identical to equation (3.1) in one dimension (z-direction). Note that for the convective term, we have $J_h = \rho_h u_z$ where both the density and the z-direction velocity u_z are constants. Also, the diffusive term is zero in equation (3.4) since this was assumed negligible compared to the convective term. The source term is the heat transferred into the system across the boundaries. For the hot side, the source term is negative since heat is transferred from the hot to the cold stream. Now, we introduce the specific heat capacity

$$c_v = \left(\frac{\partial \hat{E}^U}{\partial T} \right)_v \tag{3.5}$$

The assumption of incompressible fluids leads to $c_v = c_p$ and the heat capacity flowrate will be defined as $CP = \rho F c_v$, and terms related to pressure work are neglected. With the definition of c_v, the equation describing the temperature $T_h = T_h(t,z)$ in the hot side of the idealized heat exchanger is obtained. The corresponding equation for the cold side is derived similarly, and this yields two coupled partial differential equations

$$\frac{\partial T_h}{\partial t} + \frac{F_h L}{V_h} \frac{\partial T_h}{\partial z} = -\frac{UA}{\rho_h V_h c_{v,h}} (T_h - T_c) \tag{3.6}$$

$$\frac{\partial T_c}{\partial t} - \frac{F_c L}{V_c} \frac{\partial T_c}{\partial z} = \frac{UA}{\rho_c V_c c_{v,c}} (T_h - T_c) \tag{3.7}$$

In these equations, A is the total heat exchanging area, F_h and F_c are volumetric flowrates on hot and cold side, and V_h and V_c are total volumes of hot and cold side. The total length, L, is equal to unity in figure 3.1, and this implies that z is dimensionless. Equations (3.6) and (3.7) form *one* basis for modeling of heat exchangers. In the next section it will be shown that discretizing these equations in the spatial direction (z-direction) may lead to exactly the same set of equations as when the mixing tank concept is used as basis. The remaining part of this section will concern some basic steady state properties of ideal countercurrent heat exchange. At steady state and when introducing the number of transfer units $NTU_h = UA/CP_h$ and $NTU_c = UA/CP_c$ (where $CP_h = \rho_h F_h c_{v,h}$ and $CP_c = \rho_c F_c c_{v,c}$), equations (3.6) and (3.7) may be written as

$$\frac{d}{dz} \begin{bmatrix} T_h \\ T_c \end{bmatrix} = \begin{bmatrix} -NTU_h & NTU_h \\ -NTU_c & NTU_c \end{bmatrix} \begin{bmatrix} T_h \\ T_c \end{bmatrix} \tag{3.8}$$

Using the inlet temperatures as boundary conditions:

$$T_h(z = 0) = T_{h,in} \tag{3.9}$$

$$T_c(z = 1) = T_{c,in} \tag{3.10}$$

the solution to equation (3.8) is given by the two following equations:

$$T_{\mathrm{h}}(z) = T_{\mathrm{h,in}} - \frac{NTU_{\mathrm{h}}\left(1 - e^{(NTU_{\mathrm{c}} - NTU_{\mathrm{h}})z}\right)}{NTU_{\mathrm{h}} - NTU_{\mathrm{c}} e^{(NTU_{\mathrm{c}} - NTU_{\mathrm{h}})}}\left(T_{\mathrm{h,in}} - T_{\mathrm{c,in}}\right) \tag{3.11}$$

$$T_{\mathrm{c}}(z) = T_{\mathrm{c,in}} - \frac{NTU_{\mathrm{c}}\left(e^{(NTU_{\mathrm{c}} - NTU_{\mathrm{h}})} - e^{(NTU_{\mathrm{c}} - NTU_{\mathrm{h}})z}\right)}{NTU_{\mathrm{h}} - NTU_{\mathrm{c}} e^{(NTU_{\mathrm{c}} - NTU_{\mathrm{h}})}}\left(T_{\mathrm{h,in}} - T_{\mathrm{c,in}}\right) \tag{3.12}$$

These equations show that the temperature through an ideal heat exchanger is a nonlinear function of the position z. The outlet temperatures are given by

$$T_{\mathrm{h,out}} = T_{\mathrm{h}}(z=1) = T_{\mathrm{h,in}} - \frac{NTU_{\mathrm{h}}\left(1 - e^{(NTU_{\mathrm{c}} - NTU_{\mathrm{h}})}\right)}{\underbrace{NTU_{\mathrm{h}} - NTU_{\mathrm{c}} e^{(NTU_{\mathrm{c}} - NTU_{\mathrm{h}})}}_{P_{\mathrm{h}}}}\left(T_{\mathrm{h,in}} - T_{\mathrm{c,in}}\right) \tag{3.13}$$

$$T_{\mathrm{c,out}} = T_{\mathrm{c}}(z=0) = T_{\mathrm{c,in}} + \frac{NTU_{\mathrm{c}}\left(1 - e^{(NTU_{\mathrm{c}} - NTU_{\mathrm{h}})}\right)}{\underbrace{NTU_{\mathrm{h}} - NTU_{\mathrm{c}} e^{(NTU_{\mathrm{c}} - NTU_{\mathrm{h}})}}_{P_{\mathrm{c}}}}\left(T_{\mathrm{h,in}} - T_{\mathrm{c,in}}\right) \tag{3.14}$$

where the thermal efficiencies P_{h} and P_{c} are introduced. These are *defined* as

$$P_{\mathrm{h}} = \frac{T_{\mathrm{h,in}} - T_{\mathrm{h,out}}}{T_{\mathrm{h,in}} - T_{\mathrm{c,in}}} \tag{3.15}$$

$$P_{\mathrm{c}} = \frac{T_{\mathrm{c,out}} - T_{\mathrm{c,in}}}{T_{\mathrm{h,in}} - T_{\mathrm{c,in}}} \tag{3.16}$$

The definitions of thermal efficiencies apply for all flow configurations. One physical interpretation of thermal efficiency is that it denotes the fraction of the heat in the stream that is recovered compared to the maximum heat transfer being thermodynamically feasible. The thermal efficiencies are physically bounded between zero and one, and the ratio between them is $P_{\mathrm{h}}/P_{\mathrm{c}} = CP_{\mathrm{c}}/CP_{\mathrm{h}}$. For ideal countercurrent flow, the expressions for P_{h} and P_{c} are as indicated in equations (3.13) and (3.14). Also, note that the thermal efficiencies are functions of flow configuration and NTU_{h} and NTU_{c}, only.

Using the thermal efficiencies, the correlation between the inlet and outlet temperatures of an ideal countercurrent heat exchanger is

$$\begin{bmatrix} T_{\mathrm{h,out}} \\ T_{\mathrm{c,out}} \end{bmatrix} = \begin{bmatrix} 1 - P_{\mathrm{h}} & P_{\mathrm{h}} \\ P_{\mathrm{c}} & 1 - P_{\mathrm{c}} \end{bmatrix} \begin{bmatrix} T_{\mathrm{h,in}} \\ T_{\mathrm{c,in}} \end{bmatrix} \tag{3.17}$$

This equation show that the relationship between inlet and outlet temperatures is linear. Considering *changes* in the inlet and outlet temperatures, the thermal efficiencies can be written as

$$P_{\mathrm{h}} = \frac{\Delta T_{\mathrm{h,out}}}{\Delta T_{\mathrm{c,in}}}, \quad P_{\mathrm{c}} = \frac{\Delta T_{\mathrm{c,out}}}{\Delta T_{\mathrm{h,in}}} \tag{3.18}$$

That is, an alternative interpretation of thermal efficiency is that it denotes the *gain* when an outlet temperature is affected by a change in the inlet temperature of the opposite stream. This implies that thermal efficiency, usually used in connection with design/sizing of heat exchangers, also have implications concerning control and operation of heat exchangers and HENs. For instance, the transfer matrix in equation (3.17) looses rank when $P_{\mathrm{h}} + P_{\mathrm{c}} = 1$, meaning that the outlet temperatures cannot be controlled *independently* using the inlet temperatures, see Mathisen (1994, chapter 3).

The temperature driving force in an ideal countercurrent heat exchanger is given by

$$\Delta T_{\mathrm{m}} = \begin{cases} \dfrac{(T_{\mathrm{h,in}} - T_{\mathrm{c,out}}) - (T_{\mathrm{h,out}} - T_{\mathrm{c,in}})}{\ln\left[(T_{\mathrm{h,in}} - T_{\mathrm{c,out}}) / (T_{\mathrm{h,out}} - T_{\mathrm{c,in}})\right]} & \text{when } CP_{\mathrm{h}} \neq CP_{\mathrm{c}} \\ (T_{\mathrm{h,in}} - T_{\mathrm{c,out}}) \quad \left(= (T_{\mathrm{h,out}} - T_{\mathrm{c,in}})\right) & \text{when } CP_{\mathrm{h}} = CP_{\mathrm{c}} \end{cases} \tag{3.19}$$

The upper part of this expression (when $CP_{\mathrm{h}} \neq CP_{\mathrm{c}}$) is the logarithmic mean temperature difference (LMTD), and it will be denoted ΔT_{lm}. The total heat transferred from hot to cold side of a heat exchanger can now be written in the simple form

$$Q = UA\Delta T_{\mathrm{m}} \tag{3.20}$$

The total heat transfer coefficient, U, is usually assumed to consist of three parts (the film theory); one filmcoefficient on the hot side (h_{h}), one filmcoefficient on the cold side (h_{c}) and one contribution from the heat conduction through the dividing wall given by k_{wall} and the geometry. For a flat wall with uniform thickness, l, and when neglecting geometrical effects near the edges, the total heat transfer coefficient is given by

$$\frac{1}{U} = \frac{1}{h_{\mathrm{h}}} + \frac{1}{h_{\mathrm{c}}} + \frac{l}{k_{\mathrm{wall}}} \tag{3.21}$$

The film coefficients are flow dependent, and estimates can be found using the Dittus-Boelter equation. This equation gives the Nusselt number ($Nu = hD/k$) as function of the Reynolds number and the Prandtl number. In the subsequent, the simulations are based on a specified total heat transfer coefficient, U, which is assumed to be independent of flow.

This section has given some basis for heat transfer, and the following section will utilize this for practical modeling of heat exchangers.

3.2 Dynamic model of a single heat exchanger

The type and complexity of the heat exchanger model greatly influences the time required and quality of the results from HEN simulations. The idea is to develop a general heat exchanger model consisting of a set of ordinary differential equations (ODE). Then, some standard simulation tool including an ODE-solver can be utilized for simulation. When heat exchangers are modeled, the basis is normally the mixing tank concept (lumped models/concentrated parameter models), *or* the distributed parameter models (partial differential equations) presented in the previous section. The presentation in this section aims at having elements from both these approaches. The three most important requirements for the general heat exchanger model are

1. The model should be simple.
2. Good agreement with steady state behavior of ideal countercurrent heat exchangers.
3. Fair agreement with the dynamic behavior of heat exchangers.

It will be necessary to simulate HENs with several units that may have heat load loops and controllers. Therefore, requirement 1 is crucial in order to simulate the complete HEN efficiently. It may be surprising that requirement 2 concern good agreement with *ideal* countercurrent heat exchangers instead of *real* heat exchangers. This is due to the importancy of comparing the results (at steady state) with the properties of the HEN from the early synthesis stage. At this stage, simple steady state models based on ideal countercurrent heat exchange (using LMTD) is normally used. The comparison with such models is considered most important when a method for operation is verified at a systems level. In practice, one should encourage that the simulations reflects the *real* HEN for the particular case, however, this requires decisions regarding heat exchanger types etc. to be taken in advance.

The following assumptions are made for the heat exchanger model:

- Constant densities of the two fluids.
- Constant specific heat capacities of the two fluids.
- Constant and flow independent heat transfer coefficient.
- No phase changes.

A countercurrent heat exchanger can be modeled from the assumption that each side consists of a series of ideal mixing tanks as shown in figure 3.2.

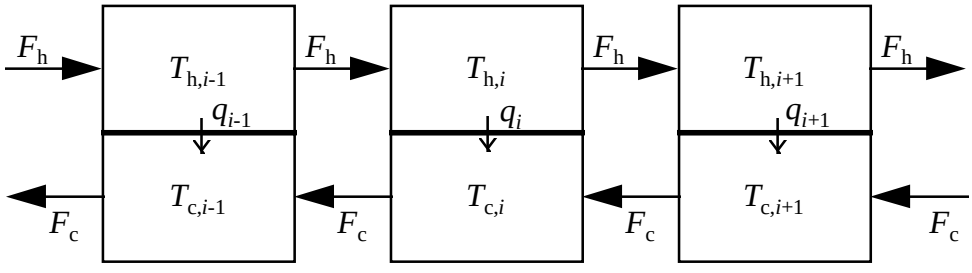

Figure 3.2 Sketch of mixing tank model.

The model for each stage becomes

$$\frac{\partial T_{\mathrm{h},i}}{\partial t} = \frac{F_{\mathrm{h}}}{V_{\mathrm{h},i}}\left(T_{\mathrm{h},i-1} - T_{\mathrm{h},i}\right) - \frac{UA_i}{\rho_{\mathrm{h}} V_{\mathrm{h},i} c_{\mathrm{v,h}}}\Delta T_{\mathrm{m},i} \tag{3.22}$$

$$\frac{\partial T_{\mathrm{c},i}}{\partial t} = \frac{F_{\mathrm{c}}}{V_{\mathrm{c},i}}\left(T_{\mathrm{c},i+1} - T_{\mathrm{c},i}\right) + \frac{UA_i}{\rho_{\mathrm{c}} V_{\mathrm{c},i} c_{\mathrm{v,c}}}\Delta T_{\mathrm{m},i} \tag{3.23}$$

where A_i is the heat exchanging area at stage i and $V_{\mathrm{h},i}$ and $V_{\mathrm{c},i}$ are the volumes of each compartment at hot and cold side. Numbering each stage from 1 to N, the heat exchanger model consists of $2N$ ordinary differential equations. At the inlet the boundary conditions are $T_{\mathrm{h},0} = T_{\mathrm{h,in}}$ and $T_{\mathrm{c},N+1} = T_{\mathrm{c,in}}$, and at the outlet we have $T_{\mathrm{h},N} = T_{\mathrm{h,out}}$ and $T_{\mathrm{h},1} = T_{\mathrm{c,out}}$.

The mixing tank concept can easily be modified to fit other configurations than countercurrent flow. Letting index i denote the hot side tank number and j the cold side tank number, the connection of hot and cold mixing tanks can be done by introducing a function $j = L(i)$. E.g. $j = L(i) = N + 1 - i$ results in a countercurrent configuration. This notation was introduced by Correa and Marchetti (1987), and the function L for some other configurations such as 1-2 shell-and-tube heat exchangers are given by Mathisen (1994, chapter 2, appendix 3). We will, however, assume countercurrent heat exchangers since this is normally assumed in the synthesis stage.

In equations (3.22) and (3.23), $\Delta T_{\mathrm{m},i}$ is the temperature driving force at stage i. Three alternatives (a, b and c) for this expression are:

a) Pure mixing tank model: $$\Delta T_{\mathrm{m},i} = T_{\mathrm{h},i} - T_{\mathrm{c},i} \tag{3.24a}$$

b) AMTD: $$\Delta T_{\mathrm{m},i} = 0.5\left[\left(T_{\mathrm{h},i-1} - T_{\mathrm{c},i}\right) + \left(T_{\mathrm{h},i} - T_{\mathrm{c},i+1}\right)\right] \tag{3.24b}$$

c) LMTD: $$\Delta T_{\mathrm{m},i} = \frac{\left(T_{\mathrm{h},i-1} - T_{\mathrm{c},i}\right) - \left(T_{\mathrm{h},i} - T_{\mathrm{c},i+1}\right)}{\ln\left[\left(T_{\mathrm{h},i-1} - T_{\mathrm{c},i}\right) / \left(T_{\mathrm{h},i} - T_{\mathrm{c},i+1}\right)\right]} \tag{3.24c}$$

The first alternative is the only option consistent with the *pure* mixing tank concept. The assumption of ideal mixing will underestimate the transferred heat at steady state since the driving forces are less than for ideal countercurrent flow. Using few stages, this may result in a considerable steady state error. In alternative *b*, the inlet temperatures at each stage are taken into consideration and the driving force is assumed to be the arithmetic mean of the temperature differences at each side of the stage. This compensates for the underestimation at steady state from the first alternative. Alternative *c* simply uses the LMTD which of course give perfect accordance with ideal countercurrent heat exchange at *steady state*. This option, however, may give serious problems in a dynamic simulation not only because it is undefined when the two temperature differences ($T_{\mathrm{h},i\text{-}1} - T_{\mathrm{c},i}$) and ($T_{\mathrm{h},i} - T_{\mathrm{c},i+1}$) are equal: In a dynamic simulation, it may for instance be a step in an inlet temperature resulting in crossover in the heat exchanger until steady state is reached. LMTD is derived for steady state, and with opposing temperature differences, it does not give any meaningful answer (since complex numbers have no physical interpretation in this case). Using LMTD in dynamic simulation

may easily abrupt an ongoing simulation and it is disregarded due to these problems. The Paterson approximation (Paterson, 1984) and the Chen approximation (Chen, 1987) are good approximations of the LMTD, developed to cope with the discontinuity of the LMTD for equal temperature differences. However, both of these approximations give the same problems as LMTD when crossover occurs (since they both involve the geometric mean), thus they are not suited for dynamic simulations.

Before proceeding, it will be shown that discretizing the partial differential equations (3.6) and (3.7) in the *z*-direction may result in *exactly* the same equations as in (3.22) and (3.23). Figure 3.3 shows control volumes and nodes on the hot and cold side along the *z*-axis.

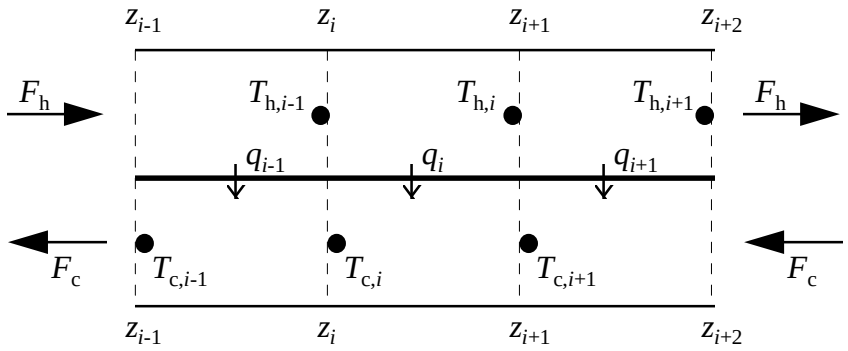

Figure 3.3 Illustration for discretization of equations (3.6) and (3.7).

As discretization method we will use a control volume approach to ensure that the energy balance is preserved for each control volume and not only within the total system boundaries, see Patankar (1980). Note that the nodes (marked with circular dots) are not located at the center of the control volumes, but are moved downstream to the "wall" of the each control volume. From equation (3.6) (the hot side) we obtain for control volume *i*:

$$\frac{\partial T_h}{\partial t}\int_{z_i}^{z_{i+1}}\partial z + \frac{F_h L}{V_h}\int_{T_{h,i-1}}^{T_{h,i}}\partial T_h = -\frac{UA}{\rho_h V_h c_{v,h}}\int_{z_i}^{z_{i+1}}(T_h - T_c)\partial z \tag{3.25}$$

According to figure 3.3, control volume *i* includes the region $i < z < i+1$. When *z* varies from *i* to *i*+1, T_h varies from $i-1$ to *i* due to the downstream shifting of the nodes. Hence, T_h is integrated from $i-1$ to *i* in equation (3.25). Performing the two first integrations, the equation can be written as

$$\frac{\partial T_h}{\partial t} + \frac{F_h}{V_h \frac{\Delta z}{L}}\left(T_{h,i} - T_{h,i-1}\right) = -\frac{UA}{\rho_h V_h c_{v,h}}\underbrace{\frac{1}{\Delta z}\int_{z_i}^{z_{i+1}}(T_h - T_c)\partial z}_{\Delta T_{m,i}} \tag{3.26}$$

Now, recognizing that $V_{h,i} = V_h \Delta z/L$ (similarly for cold side) and $A_{h,i} = A_h \Delta z/L$, and doing similar for the cold side (integrating T_c from *i* to $i + 1$) we obtain

$$\frac{\partial T_{\mathrm{h},i}}{\partial t} = \frac{F_{\mathrm{h}}}{V_{\mathrm{h},i}}\left(T_{\mathrm{h},i-1} - T_{\mathrm{h},i}\right) - \frac{UA_i}{\rho_{\mathrm{h}} V_{\mathrm{h},i} c_{\mathrm{v,h}}}\Delta T_{\mathrm{m},i} \tag{3.27}$$

$$\frac{\partial T_{\mathrm{c},i}}{\partial t} = \frac{F_{\mathrm{c}}}{V_{\mathrm{c},i}}\left(T_{\mathrm{c},i+1} - T_{\mathrm{c},i}\right) + \frac{UA_i}{\rho_{\mathrm{c}} V_{\mathrm{c},i} c_{\mathrm{v,c}}}\Delta T_{\mathrm{m},i} \tag{3.28}$$

which are identical to equations (3.22) and (3.23) found from the mixing tank concept. Assuming that the temperature in control volume *i* is constant and equal to $T_{\mathrm{h},i}$ on the hot side and $T_{\mathrm{c},i}$ on the cold side, $\Delta T_{\mathrm{m},i}$ from equation (3.26) becomes identical to alternative *a* in equation (3.24) (pure mixing tank). This assumption leads to discrete jumps in temperature from one control volume to the next. To be more realistic, one may assume the temperature to vary *linearly* between the nodes. Then, integrating $\Delta T_{\mathrm{m},i}$ in equation (3.26) results in AMTD as in alternative *b* in equation (3.24). Finally, one may assume the temperature variations between the nodes to follow the expressions in equations (3.13) and (3.14) which results in using LMTD (which we have decided to disregard).

To conclude so far, the modeling of a heat exchanger using the mixing tank concept, or discretizing the governing partial differential equations may result in identical sets of ordinary differential equations (provided the number of mixing tanks is equal to the number of control volumes, and the total volume and total area is divided into parts of equal size). It remains to (1) select a typical number of mixing tanks/control volumes, (2) select which of the alternatives *a* or *b* (from equation 3.24) should be used as mean temperature difference, and (3) select how bypass manipulations should be implemented. In the following, the mixing tanks and control volumes will be denoted "cells" as a common term. The number of cells is the number of tanks/volumes at each side.

Mathisen (1994, chapter 2) recommends a minimum of two cells in the pure mixing tank concept and minimum three cells when LMTD is used for dynamic purposes. Steady state considerations may give a higher bound on the minimum number of cells, particularly for the *pure* mixing tank concept. One way to compensate for the underestimation of the transferred heat is to increase the heat transfer coefficient. For *equal heat capacity flowrates* and *N* number of cells, the heat transfer coefficient has to be increased by the following ratio (Domingos, 1969).

$$\frac{U}{U_{\mathrm{lm}}} = \frac{N}{N - NTU_{\mathrm{lm}}} \tag{3.29}$$

where $NTU_{\mathrm{lm}} = U_{\mathrm{lm}}\mathrm{A}/CP$. Mathisen (1994, chapter 2) recommends a minimum number of cells for steady state considerations to be at least equal to NTU_{lm}. This is a rather loose bound since *U* approaches infinity when *N* approaches NTU_{lm}. If one requires the error in the pure lumped model to be less than 10%, this implies $N \geq 11NTU_{\mathrm{lm}}$. Also, the increase of *U* is dependent on the operating point when the heat capacity flowrates are different from each other. As a practical example, consider heat exchanger II in figure 2.4. Using a pure mixing tank model with four cells, *U* has to be increased by 94% in order to transfer the same heat as the steady state model in the nominal case. If $T_{\mathrm{s}}^{\mathrm{H1}}$ is decreased by 20°C, the increase in *U* should be almost four times. If only three cells are used, the increase is more than 180% in

the nominal case, and when T_s^{H1} is decreased by 20°C the duty will be too small even if U is infinite.

Using AMTD instead, the steady state error is much smaller. The relative error in transferred heat caused by AMTD (compared to LMTD) is given by

$$\frac{\text{AMTD} - \text{LMTD}}{\text{LMTD}} = \frac{0.5(\Delta T_2 / \Delta T_1 + 1)}{\Delta T_2 / \Delta T_1 - 1} \ln\left(\frac{\Delta T_2}{\Delta T_1}\right) - 1 \tag{3.30}$$

where ΔT_1 and ΔT_2 are the temperature differences between the hot and cold fluid at each side of the heat exchanger. The error is a function of the variable ($\Delta T_2/\Delta T_1$) only, and figure 3.4 shows the error.

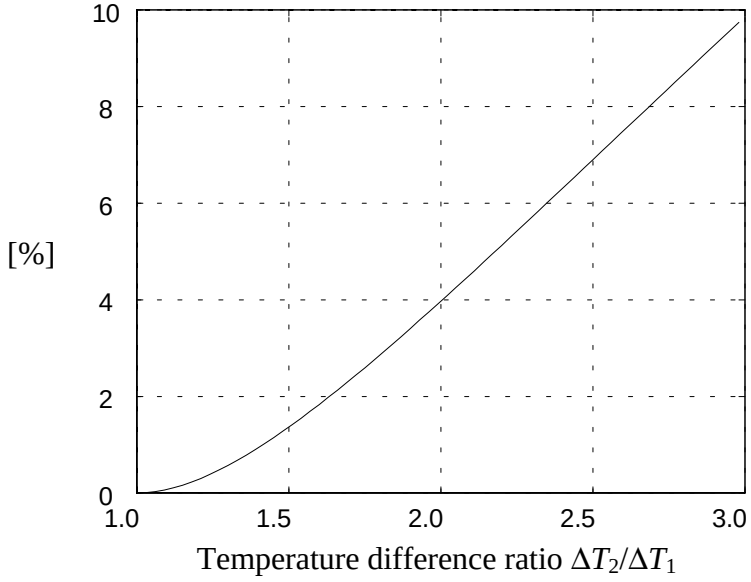

Figure 3.4 Relative error (in %) using AMTD compared to LMTD.

The error in a complete heat exchanger will be reduced as the number of cells increases since the parameter $\Delta T_2/\Delta T_1$ will approach 1 for each cell. This is the case also for the pure mixing tank model, but for AMTD the steady state error is much smaller for the same number of cells. To compare, U in heat exchanger II in figure 2.4 should be modified (reduced) by only 3.5% using AMTD and four cells (compared to 94% increase for the pure mixing tank model). Without any modifications, T_o^{C2} is only 0.5°C above correct value (i.e. using LMTD), and this is acceptable.

To achieve good agreement with the LMTD based models used in HEN synthesis, most simulations in this thesis have been carried out using AMTD and four cells (on each side) in the model. Heat transfer coefficients have not been modified. There is, however, a risk using AMTD as pointed out by Sangro (1996): While the pure mixing tank model underestimates the duty, the use of AMTD *overestimates* the duty compared to LMTD. Since LMTD origins from ideal countercurrent heat exchange, and since this is known to be the most effective configuration, AMTD will give a steady state duty slightly above the maximum possible theoretically. In most cases, this will not have any practical implications when comparing the simulations results with the models used during design. In some cases, however, the use of

AMTD may lead to crossover at steady state. This can occur when there are large differences in the heat capacity flowrates of the two fluids, and this very unphysical behavior of the models may give severe error in the simulation of a HEN. When simulating HENs using AMTD based models, it is important to verify that the error from equation (3.30) is acceptable for each heat exchanger and for all variations (in disturbances, parameters etc.) that may be encountered during the complete simulation.

Mathisen (1994, chapter 2) points out that wall dynamics should be included in many cases also for liquid heat exchangers. This may be important in order to have a correct response in outlet temperature due to changes in the inlet temperature of the opposite fluid. Despite this, wall dynamics is not included in the models used for simulation in this thesis. The reasons for this are (1) to have simple models (this was the first requirement stated at the beginning of this section) and (2) it is assumed that the dynamics of a *complete* HEN usually will not change significantly if dynamics of the dividing wall is neglected.

In order to simulate controlled HENs it is required to somehow incorporate variable bypass fractions. This is implemented directly into the heat exchanger model. The variable u denotes the fraction of the inlet stream being bypassed the heat exchanger on hot or cold side, and the stream actually flowing through the unit is $CP = (1-u)CP_{\text{in}}$. The outlet temperature after mixing is

$$T_{\text{out}} = uT_{\text{in}} + (1-u)\hat{T}_{\text{out}} \tag{3.31}$$

where $\hat{T}_{\text{out}}$ is the outlet temperature of the heat exchanger prior to mixing with the bypass stream.

In order to simplify the simulations and to reduce the risk of errors, it is important to specify few parameters for each heat exchanger in a HEN. This is achieved by specifying a nominal heat transfer coefficient (of 400W/°Km^2) and a nominal specific area (of 80m^2/m^3). Further, it is assumed that the volumes on hot and cold side are equal (nominally). Now, specifying *UA*, the area and volumes are easily calculated and hence a reasonable heat exchanger model is found by specifying only one parameter. *UA* for each heat exchanger is available from the early phase synthesis stage, and dynamic simulations can be carried out without the need for any more detailed decisions.

To summarize, the general heat exchanger model assumes incompressible flow (liquids), flow independant heat transfer coefficient, and it consists of four cells in a countercurrent configuration. The heat transfer from hot to cold side of each cell is found using arithmetic mean temperature difference and this corresponds to assuming linear temperature variations (streamwise) within each cell. A variable bypass is included in the general model.

3.3 Dynamic simulation of HENs

This section will show how the general heat exchanger model is used for simulation of HENs. The simulations are carried out using SIMULINK which is an extension of the MATLAB programming language. SIMULINK has a graphical user interface and it includes various solvers for sets of ordinary differential equations. The reasons for choosing SIMULINK were

mainly the graphical interface making it simple to generate new network structures and the additional ODE-solvers supplied with SIMULINK which turned out to be sufficient for HEN simulation

The heat exchanger model described in the last section is implemented as an S-function (see SIMULINK User's guide) which simply is an MATLAB function written in a format that SIMULINK can use as a *block*. A HEN is created simply by using the mouse to "drag-and-drop" blocks and lines between blocks. The SIMULINK representation of the HEN in figure 2.4 may take the form as shown in figure 3.5.

The HEN structure is easily recognized in figure 3.5 with the process streams represented by the wide lines. Stream H1 is defined with an inlet temperature of 190°C and *CP* equal to 100kW/°K. The Mux ("multiplexer") block H1 simply stacks the two input signals into one vector signal. The heat exchanger block "hxl_I" (which contains the general heat exchanger model) has four inputs where the two in the middle are the hot and cold inlet stream. The upper input of the heat exchanger blocks is the hot side bypass fraction and the lower input is the cold side bypass fraction. Thus, the actual heat exchanger implementation has bypasses on both hot and cold side making it more general. An unconnected input automatically takes the value of zero, meaning that the bypass is not used. The step blocks in figure 3.5 are for investigation of the responses due to steps in the bypass fraction of the hot side of heat exchanger I and the cold side of heat exchanger II. The two outputs in the middle from the heat exchanger blocks are the hot and cold outlet streams. These include one signal for the outlet temperature computed by the model and one signal for the *CP*-value. The *CP*-value is fed directly from the input to the output of the heat exchanger block, providing information to the next downstream heat exchanger. The upper and lower outputs from the heat exchanger blocks are dummies. The ability to rotate and flip blocks in SIMULINK makes it possible to draw the cold streams from right to left as shown in figure 3.5. This allows the HENs to be drawn in the countercurrent configuration quite similar to the grid diagrams, and this is important to easily verify that the simulated HEN structure is correct.

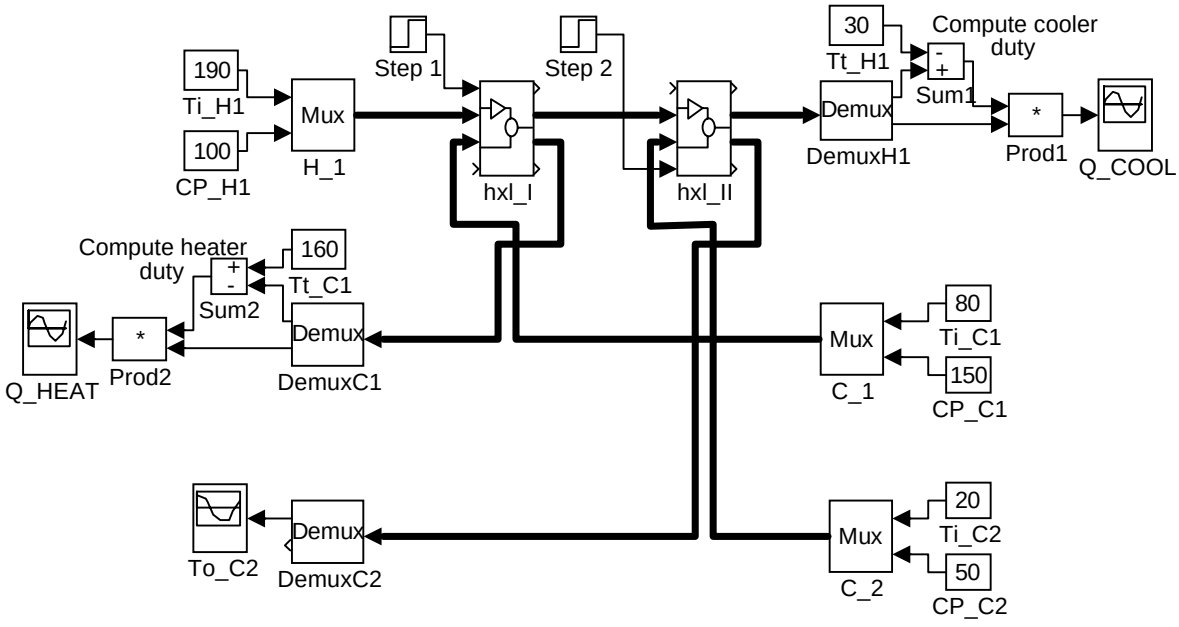

Figure 3.5 SIMULINK representation of a simple HEN.

One conspicuous feature of the HEN figure 3.5 compared to the grid diagram in figure 2.4 is the absence of the cooler and the heater. Recalling the decomposition rule for HENs from section 2.3 (Rule 2.1), the most important features of a HEN can be found from studying the responses in the bypass controlled outlet temperatures in addition to the utility consumption (assuming perfect control of the utility controlled outputs). This is exactly what is done in the upper right part of figure 3.5: The hot outlet temperature of heat exchanger II (upper output signal from the demultiplexer, "DemuxH1") is subtracted from the target temperature (30°C) and multiplied by CP_{H1} (lower output from "DemuxH1"). This is actually equation (2.4) shown graphically, and the result (cooler duty), is displayed during simulation by means of the "Auto-Scale Graph" block "Q_COOL". Similar calculations are done for stream C1 and "Q_HEAT" displays the heater duty. In this way, the bypass controlled outlet temperature together with the utility duties of the HEN can be investigated dynamically involving only two heat transferring units as opposed to the four units of the complete HEN. As a consequence, using the decomposition principle for simulation of HENs, modeling of final utility exchangers are completely avoided and the complexity of the simulations is significantly reduced.

SIMULINK (version 1.3) includes ODE-solvers (integrators) using methods such as an fifth order Runge-Kutta, Gear's method (for stiff systems) and an Adam's method. All of the algorithms uses variable step-lengths. A switch can be set to automatically choose Gear's method or Adam's method, depending on the stiffness, however, the manual advises against using these methods on discontinuous systems. A method denoted *linsim* is recommended by the manual for systems being relatively linear. The manual is economical on information about this method, except that it extracts the linear dynamics of a system, leaving only the nonlinear part to be simulated. Tests on all algorithms supplied with SIMULINK (version 1.3) have shown that the *linsim* algorithm performed best on simulation of HENs modeled as described in the previous section. Therefore, this algorithm is used for obtaining the results shown in this thesis.

3.4 Dynamic simulation of controlled HENs

As it was clear from chapter 2, most methods in this thesis will be based on decentralized control, and only simple controllers will be used (PI). A controller can be implemented as an S-function (as for the heat exchanger model) and a temperature can be "measured" simply by dragging a line from the process stream to the controller. Figure 3.6 shows the SIMULINK representation of the HEN in figure 5.5 when the control strategy proposed in chapter 5 is implemented.

In this case, the utility duties are not computed by SIMULINK during the simulation, but the inlet temperatures to the final utility exchangers are stored, and the utility duties are computed off-line using a simple MATLAB code. In figure 3.6, the outlet temperature of stream C1 is controlled by the bypass fractions across heat exchangers I, III and IV. The controller block actually contains three SISO-controllers where only one is active at a time. (The control strategy is explained in chapter 5).

Simulation of controlled HENs (using SIMULINK) will often introduce a problem usually not encountered by passive HENs. When the bypass of a manipulated bypass directly affects the outlet temperature (no dynamics) and the proportional part of the controller directly effects the bypass fraction when the measured temperature changes, an *algebraic loop* is introduced in the system. That is, the system is no longer a set of ordinary differential equations, but it is a set of *differential-algebraic* equations (DAE). SIMULINK does not include any efficient algorithms for solving DAE-systems, and iteration is performed at each time step to find a feasible solution. A possible way to change the DAE-system into a set of ODE, is to include some dynamics in the algebraic loops. For HENs, this may be done by introducing a small volume to represent energy hold-up in the bypass line. If this volume is selected too small, the system will become unnecessary stiff, and if the volume is selected too large, it may significantly affect the overall dynamics of the controlled HEN. For simulation results presented in this thesis, the volume of the bypass line is selected to be 20% of the total heat exchanger volume. Now, using equation (3.31) for mixing the bypass stream with the exit stream of the heat exchanger, the variable T_{in} has to be replaced by the temperature in the bypass mixing tank.

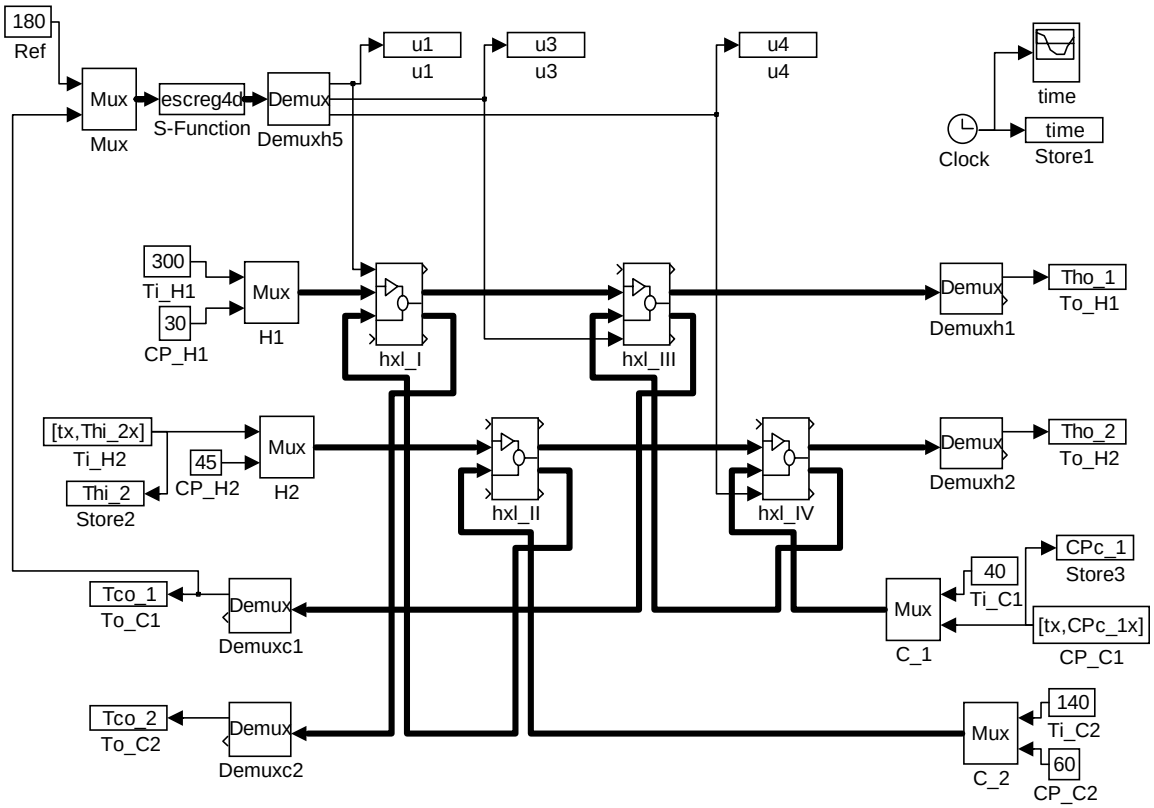

Figure 3.6 SIMULINK representation of a controlled HEN.

The method proposed in chapter 7 involves a steady state optimization to be carried out at periodic time intervals. This is also easily incorporated since all MATLAB functions are available in SIMULINK. The method is implemented by creating a SIMULINK block that utilizes the optimization functions in the MATLAB Optimization Toolbox.

3.5 Conclusions

The aim of this chapter has been to explain how the dynamic simulation results shown in this thesis are obtained. The main goal has been to develop models and use a simulation tool that make the simulations as easy to perform as possible, while retaining the essential properties of the HENs. In addition, some basic steady state properties of ideal countercurrent heat exchange has been shown.

The simulation of HENs is based on a simple heat exchanger model consisting of a set of ordinary differential equations. It has been shown that the particular model can be derived from the mixing tank concept, or from simplifying and discretizing the governing equation for heat transfer. Using arithmetic mean temperature difference in the mixing tank concept corresponds to assuming linear temperature variations between the nodes in the second approach.

In the literature on dynamic modeling of heat exchangers and HENs, the mixing tank concept (lumped models) and the distributed parameter models (based on partial differential equations) are often considered as two completely different approaches. In the description in this chapter, it has been tried to include both these approaches. It has been demonstrated that the two different approaches may result in exactly the same mathematical model.

Notation

A	Heat transfer area [m^2]
CP	Heat capacity flowrate [W/°K]
c_v	Specific heat capacity [J/(°Kkg)]
D	Diameter [m]
$\hat{E}$	Energy [J/kg]
$\hat{E}^U$	Internal energy [J/kg]
F	Volumetric flowrate [m^3/s]
h	Film coefficient for heat transfer [W/(°Km^2)]
k	Thermal conductivity. Dimensions may vary, but are often [W/(°Km)]
NTU	Number of transfer units [–]
q	Heat transferred from hot to cold side of each mixing tank/control volume [J]
Q	Total heat transferred from hot to cold side [J]
T	Temperature [°C]
U	Heat transfer coefficient [W/(°Km^2)]
UA	Heat transfer coefficient times area [W/°K]
V	Volume [m^3]

Subscripts

c	Cold
h	Hot
i	Index for mixing tank / control volume / temperature node, and index for velocities and positions using tensor notation (eq. 3.1).
lm	Logarithmic mean

m Mean (does not imply any specific averaging method)
o Outlet
s Supply

Greek

α Thermal diffusivity [m^2/s]
ΔT Temperature difference [°K]
ρ Density [kg/m^3]

References

Bird, R.B., W.E. Stewart and E.N. Lightfoot (1960). *Transport Phenomena*. John Wiley & Sons, Singapore.

Chen, J.J.J. (1987). Letter to editors. Comments on a Replacement for the Log-arithemic Mean. *Chem. Eng. Sci.*, **42**, 2488.

Correa, D.J. and J.L. Marchetti (1987). Dynamic Simulation of Shell-and-Tube Heat Exchangers. *Heat Transfer Eng.*, **8**, 50.

Domingos, J.D. (1969). Analysis of Complex Assemblies of Heat Exchangers. *Int. Journal of Heat Mass Transfer.*, **12**, 537.

Mathisen, K.W. (1994). Integrated Design and Control of Heat Exchanger Networks. *Ph.D. Thesis*. University of Trondheim - NTH, Norway.

Patankar, S.V. (1980). *Numerical Heat Transfer and Fluid Flow*. Hemisphere Publishing Corp., USA.

Paterson, W.R. (1984). A Replacement for the Logarithmic Mean. *Chem. Eng. Sci.*, **39**, 1635.

Sangro, K.I. (1996). Models for Dynamic Simulation of Heat Exchanger Networks. *Diploma Thesis* (in Norwegian). Telemark Institute of Technology, Porsgrunn, Norway.

Sha, W.T., C.I. Yang, T.T. Kao and S.M. Cho (1982). Multidimensional Numerical Modeling of Heat Exchangers. *Journal of Heat Transfer*, **104**, 417.

SIMULINK User's Guide (1992). The MathWorks Inc., Massachusetts, USA.

Chapter 4

DEGREES OF FREEDOM IN OPERATION OF HENs

In order to perform optimization during operation, there has to be at least one extra degree of freedom (DOF) after regulatory control is implemented. This chapter gives a thorough discussion of DOFs in the operation of HENs, and it will be shown that extra manipulations often cannot be utilized for optimization of utility cost. A rule to quickly verify whether a HEN problem may be optimized during operation is presented, and an equation for the number of DOFs that can be utilized for optimization ($N_{DOF,\,U}$) is derived.

4.1 Introduction

In section 2.4 it was briefly demonstrated that the number of DOFs (N_{DOF}) during operation is different from the synthesis stage. During operation we assume:

- Fixed network structure.
- Fixed installed heat exchanger areas where the effective area can be varied between zero and the installed area by manipulating a bypass. Process exchangers without bypass will also be considered in section 4.4.
- Specified supply and target temperatures and heat capacity flowrates of process streams.

An important question regarding operation of HENs is whether optimization is possible or not. A prerequisite for doing any optimization is that there are degrees of freedom left when manipulations are used for regulatory control. The most crucial question is not how *many* DOFs the HEN has, but simply *whether* we have zero DOF (optimization is not possible), or

one or more DOFs (optimization is possible). To answer this question quickly for a given network, the simple rule being derived in section 4.3 is helpful.

The chapter is organized as follows: The remaining part of this introduction discusses the number of manipulations required for regulatory control of target temperatures, to see if there may be extra manipulations. Section 4.2 shows that extra manipulations (more than needed for regulatory control) often may not be utilized for optimization and the number of DOFs that can be utilized for utility optimization ($N_{DOF,\,U}$) is defined. Section 4.3 presents the rule to find whether optimization should be considered or not. A quantitative expression for $N_{DOF,\,U}$ is derived in section 4.4, and some examples are given in section 4.5.

The primary goal of optimal operation requires that the targets are met at steady state and this implies that it has to be possible to control the target temperatures independently. To achieve this, the HEN must be *functionally* controllable (Rosenbrock, 1970, p.170) which for a linear system requires that the rank of the transfer matrix (at steady state) is equal to or greater than the number of outputs. If we assume that manipulations are selected such that independent control of the target temperatures is possible, i.e. the system is non-singular, it is clear that *the number of manipulations for regulatory control is equal to the number of targets*. In practice, it is often straightforward to choose manipulations that yield a regulatory control system without singularities in HENs simply using the main rule for input/output pairing (rule 2.2 in section 2.3). Control of utility controlled targets is trivially non-singular due to the diagonal structure. Potential singularities in control of the bypass controlled targets *may* occur and it is usually a structural property of the HEN. In Mathisen (1994, chapter 3) a number of singular network structures are presented.

A necessity for optimal operation is of course that regulatory control is possible (primary goal in definition 2.1). As shown above this requires at least as many manipulations as targets. Euler's rule from graph theory states that the number of edges in a graph is given by

$$N_{edges} = N_{nodes} + N_{loops} - N_{subnetworks} \tag{4.1}$$

Applied to HENs, edges represent units (process or utility exchangers) and nodes represent streams (process or utility streams). The discussion starts by considering HENs with minimum number of units (no loops). For a connected network ($N_{subnetworks} = 1$) with no loops ($N_{loops} = 0$), the (minimum) number of units is given by

$$N_{units,\,min} = N_P + N_U - 1 \tag{4.2}$$

where N_P is the number of process streams and N_U is the number of different utility types. A pinch problem has at least two utility streams (one hot and one cold) and hence the number of units is at least one more than the number of process streams. Each unit (process or utility exchanger) can be manipulated and represents a DOF that can be used for regulatory control. The maximum number of targets is equal to the number of process streams (all outlet temperatures are controlled). Thus, it can be concluded that all pinch problems have at least one extra manipulation after regulatory control is implemented.

Threshold problems may have only one utility stream and therefore the minimum number of units may be equal to the number of process streams. In such cases there are no extra manipulations for optimization. If, however, one or more outlet temperatures do not have any

target values, the number of manipulations required for regulatory control is less than the minimum number of units and there will be extra manipulations. Also, for threshold problems with loops (more than minimum number of units) and problems with multiple hot and/or cold utilities (e.g. different steam levels) there will be extra manipulations. To conclude this section, it has been found that pinch problems *always* have extra manipulations whereas threshold problems *may* have extra manipulations. This is, however, only an intermediate result, based on the assumption that all heat exchanger duties can be manipulated. More useful results will be deduced in the following sections.

4.2 DOF with respect to utility consumption

In this section, it will be shown that introducing loops (more than minimum number of units/more manipulations) may *not* always increase the number of DOFs that can be used for optimization. Let N_t be the number of targets and assume that each target has one manipulation assigned for regulatory control. Marselle *et al.* (1982) and Mathisen (1994, chapter 1) states that N_{DOF} is given by

$$N_{DOF} = N_{units} - N_t \tag{4.3}$$

N_{units} is the total number of manipulations since each unit is regarded as a manipulation (and variable split fractions are disregarded in this discussion). N_{DOF} from equation (4.3) may be thought of as the extra degrees of freedom with respect to bypass fractions. However, it is not always possible to exploit these DOF to anything useful, and the network in figure 4.1 illustrates this.

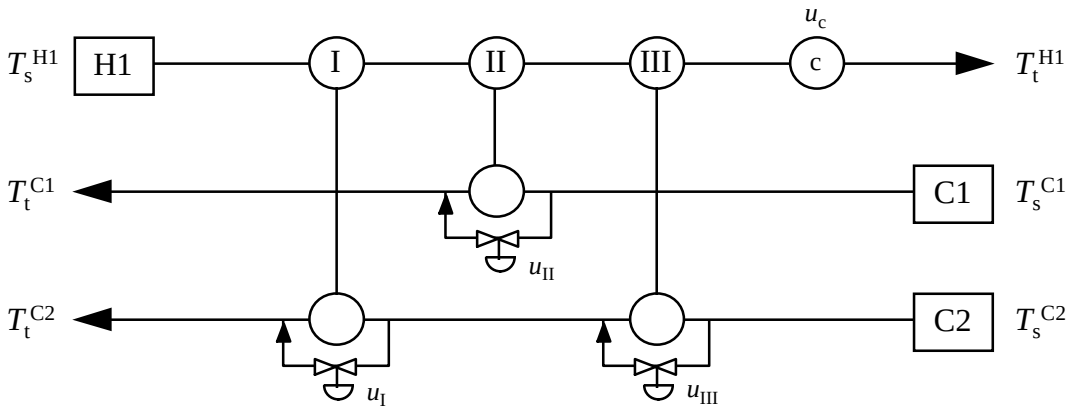

Figure 4.1 Network where DOF cannot affect utility consumption.

In this HEN the three outlet temperatures should be controlled, and with four manipulations we would expect N_{DOF} to be one. Examining the network we see that the duty of heat exchanger II, Q_{II}, (and hence u_{II}) is dictated by the deficit heat of stream C1 and the sum $Q_I + Q_{III}$ is dictated by the deficit heat of stream C2. Now, with the duties fixed for all three process exchangers, it is clear that these duties together with the excess heat in stream H1 dictate the utility consumption Q_c and hence u_c. The DOF in this example can only be used to shift duties between the heat exchangers I and III. It does *not* affect the utility consumption and it can *not* be utilized for any meaningful optimization during operation.

The result for this example is rather obvious since it is a threshold problem with only one utility stream. Thus, the utility consumption can not be manipulated when the target temperatures are fixed. While this case may not be used as a counter example to equation (4.3), it shows that using this equation may give misleading results regarding optimization during operation. While (4.3) gives $N_{DOF} = 1$ (hence one would expect optimization to be possible), the correct statement is that the utility consumption is fixed and optimization should not be considered.

The discussion above motivates the need for a definition of degrees of freedom that is suited for optimal operation of HENs.

Definition 4.1 *Degrees of freedom with respect to utility consumption* $N_{DOF,\,U}$.
The number of DOFs with respect to utility consumption $N_{DOF,\,U}$ is the number of DOFs that can be utilized for optimization of utility consumption when targets are satisfied. ■

Note that with degrees of freedom in the subsequent, we usually mean the *extra* degrees of freedom left when regulatory control is implemented

4.3 A simple rule to check scope for optimization

At the end of section 4.1, we concluded that pinch problems always have extra manipulations while threshold problems may have extra manipulations. In this section, a few simple rules to determine whether extra manipulations can be used for utility optimization will be derived.

From the arguments given previously, the most important aspect is to determine whether $N_{DOF,\,U} = 0$ or whether $N_{DOF,\,U} \geq 1$. This can be done with the total energy balance of a HEN as basis, see figure 4.2.

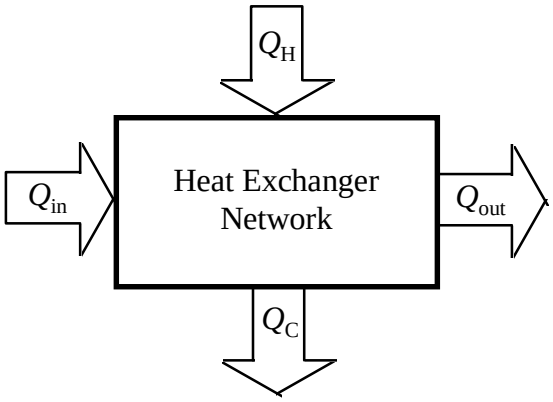

Figure 4.2 Total energy balance in a HEN.

In the figure, Q_{in} and Q_{out} are the energy flow in and out of the HEN via the process streams while Q_H and Q_C are hot and cold utilities. The steady state energy balance when only thermal energy is considered becomes

$$Q_{in} + Q_H = Q_{out} + Q_C \tag{4.4}$$

This total energy balance together with the result above (equation 4.2 and the two paragraphs after that) regarding number of manipulations for pinch and threshold problems will now be used to derive rules to find whether a HEN can be optimized during operation or not. Pinch problems and threshold problems are treated separately.

Pinch problems.
From equation (4.2) it was found that pinch problems always have at least one extra manipulation. Also, pinch problems have $Q_H > 0$ and $Q_C > 0$ and there will always be a path from hot to cold utility since we assume a connected network (disconnected networks can of course be treated as connected subnetworks, both for pinch and threshold problems). We may always increase or decrease Q_H and Q_C with the same amount of heat and still preserve the energy balance. Therefore, the extra manipulation(s) can be used to minimize utility consumption and for pinch problems we always have $N_{DOF,\,U} \geq 1$. If some outlet streams are free, i.e. have no targets, also Q_{out} may be varied and this introduces additional degrees of freedom. Note that the nominal design often is optimal in the nominal operating point. There is, however, no guarantee that a control system will find this operating condition, since it is possible to operate the HEN with unnecessary large utility consumption. Therefore, optimization should be considered in order to operate the HEN with (close to) minimum utility consumption at any operating point.

Threshold problems.
In threshold problems we have $Q_H = 0$ or $Q_C = 0$. First, consider a threshold problem with only one utility stream (e.g. one steam level) and that all outlet temperatures have targets such that Q_{out} is fixed at any operating point. From the total energy balance we see that the utility consumption is fixed (equal to $|Q_{in} - Q_{out}|$) which means that we have $N_{DOF,\,U} = 0$. Above, from equation (4.2) it was stated that threshold problems with minimum number of units and no free outlet temperatures have no extra manipulations and therefore no degrees of freedom. Now, we have found that this holds also for threshold problems independent of the number of units. That is, introducing loops (additional manipulations) in threshold problems does *not* increase $N_{DOF,\,U}$. The extra manipulations can only be used to shift duties internally in the HEN.

The situation changes if some of the outlet temperatures are free. Then, Q_{out} can be varied at any operating point and there always exists a path from the utility exchanger(s) and to the free outlet temperature(s). This means that the HEN may be optimized during operation and that we have $N_{DOF,\,U} \geq 1$. Also note that if there are more than one utility stream (e.g. cooling water and a cryogenic refrigerant), optimization is meaningful also when all outlet temperatures have targets (even if total utility consumption in terms of kW, MW etc. is fixed). In such cases one may minimize the most expensive utility stream, or more general, minimize total utility *cost*.

These results for pinch and threshold problems are summarized in rule 4.1. This rule is very simple to use but as it will be clear from the explanation below, it only serves as necessary conditions for $N_{DOF,\,U} \geq 1$.

Rule 4.1 *Degrees of freedom with respect to utility consumption of HENs.*
Based on the structural properties of a connected HEN problem, the following three rules (one rule for each problem type) states whether the HEN can be optimized or not:

a) Pinch problems (all cases) $N_{DOF,\,U} \geq 1$

b) Threshold problems with no free outlet temperatures $N_{DOF,\,U} = 0$

c) Threshold problems with at least one free outlet temperature $N_{DOF,\,U} \geq 1$

The rules a) and c) are necessary conditions for optimization ($N_{DOF,\,U} \geq 1$), whereas rule b) is sufficient to state that optimization is not possible ($N_{DOF,\,U} \leq 0$). ■

According to rule 4.1, the question whether a HEN can be optimized or not, is *independent of the internal HEN structure*, it only depends on the problem type and which outlet temperatures that should be controlled. This implies that in many cases, adding more units (introducing more loops) will not increase $N_{DOF,\,U}$. However, the only thermodynamic constraint that has been considered is the total energy balance of the HEN. It has been assumed that each unit has positive temperature driving forces such that heat transfer is possible, and it has been assumed that the duty of each unit may be manipulated. If for example the duty of a utility exchanger drops to zero for given operating conditions, this unit can no longer be used for control purposes, and an upstream exchanger has to be bypassed to reach the target temperature. In this way, the HEN will loose one degree of freedom with respect to bypass fractions and it *may* also reduce $N_{DOF,\,U}$. A reduction in $N_{DOF,\,U}$ may lead to only one feasible operating condition for a HEN that can be optimized at other operating points. It may also lead to infeasible operation, meaning that the primary goal of optimal operation (reach targets) cannot be met.

Rule 4.1 assumes that a bypass is placed across each process heat exchanger. If this is not the case, $N_{DOF,\,U}$ may be reduced. As an example consider a pinch design with minimum number of units (one unit more than the number of targets). If one unit cannot be manipulated (e.g. because bypass is not installed), all manipulations must be used for regulatory control, thus optimization is not possible.

Despite the fact that rule 4.1 (a and c) is only necessary conditions for $N_{DOF,\,U} \geq 1$, it may give valuable information regarding optimization during operation from a quick glance at the network, or simply from the problem type. If the HEN consists of more subnetworks, then rule 4.1 must be applied to each subnetwork.

4.4 A quantitative expression for the number of DOF

A quantitative equation for the number of degrees of freedom that can be utilized for utility optimization ($N_{DOF,\,U}$) of HENs is derived. The same equation is valid for HENs with loops, splits and multiple utilities, and it is not required that all process exchangers have bypasses for manipulation. Pinch and threshold problems as well as HENs where there are outlet temperatures without target values (free outlet temperatures) are covered. In the general equation for $N_{DOF,\,U}$, however, internal utility exchangers are disregarded. That is, for streams where a utility exchanger is present, it is assumed to be the last unit in that stream.

With utility optimization, we mean optimization of utility *cost*, and not only the total consumption. It is assumes that different utilities (e.g. different steam levels) have different cost. This implies that for cases where there are multiple utilities (e.g. high and low pressure steam), also the distribution (e.g. HP/LP-ratio) between the different utilities is considered. The expression for $N_{DOF,\,U}$ will be developed starting with a trivial example.

Example 4.1 *Trivial example for* $N_{DOF,\,U}$
The HEN in figure 4.3 has 4 manipulations and 2 targets, thus equation (4.3) gives $N_{DOF} = 2$. For this example one may argue that the two process exchangers are placed side by side, and they may be treated as one unit. Since the heat removed from the hot stream equals the heat received by the cold stream, the two bypasses only contributes with one free variable and therefore the number of DOFs that can be used for optimization is only 1 (identified as the path from the heater *h* to the cooler *c*).

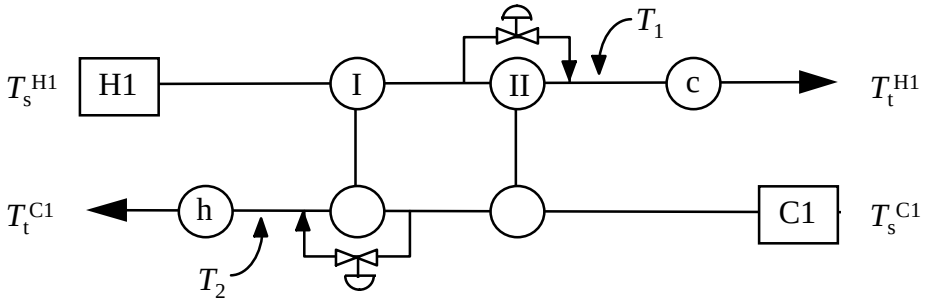

Figure 4.3 Trivial HEN.

An alternative explanation being better suited for generalization to other HENs is the following: Specifying the temperature T_1 freely, T_2 is given by an energy balance around the two process exchangers, and vice versa. Hence, the two variable duties Q_I and Q_{II} only spans a one-dimensional space in T_1 and T_2. Utility consumption takes place in the utility exchangers, and with one free variable (T_1/T_2) together with varying the duties of the utility exchangers, there are totally 3 free variables that affect the utility consumption. With 2 constraints (specifications on the target temperatures) there is one DOF left for utility optimization, thus $N_{DOF,\,U} = 1$. So for a total of 2 degrees of freedom ($N_{DOF} = 2$), only 1 can be used for utility optimization ($N_{DOF,\,U} = 1$). Note, however, that one temperature between the process exchangers may be specified or one bypass may saturated *without reducing* $N_{DOF,\,U}$ (since the process exchangers still spans a one-dimensional space in T_1 and T_2). In other words: Even though the extra unit (loop) in figure 4.3 does not increase $N_{DOF,\,U}$, it serves as a "spare" degree of freedom. ■

To generalize, we divide a HEN into two parts – the "inner" HEN and the "outer" HEN, as shown in figure 4.4. For this general HEN, all outlet temperatures have target values. We will come back to free outlet temperatures at the end of the section.

The inner HEN consists of all process exchangers, splitters and mixers etc. The utility consumption takes place in the outer HEN which consists of the utility exchangers and target values. Streams with target values enter the outer HEN even if they do not have a utility exchanger. It is important to notice that all information from the inner to the outer HEN

passes through the streams entering the outer HEN. Thus, the number of streams put limitations on the number of free variables passed from the inner to the outer HEN. In figure 4.3, the two temperatures T_1 and T_2 constitute the interface between the inner and the outer HEN. The next example demonstrates how the concept of inner and outer HEN can be used to find $N_{\mathrm{DOF,\,U}}$.

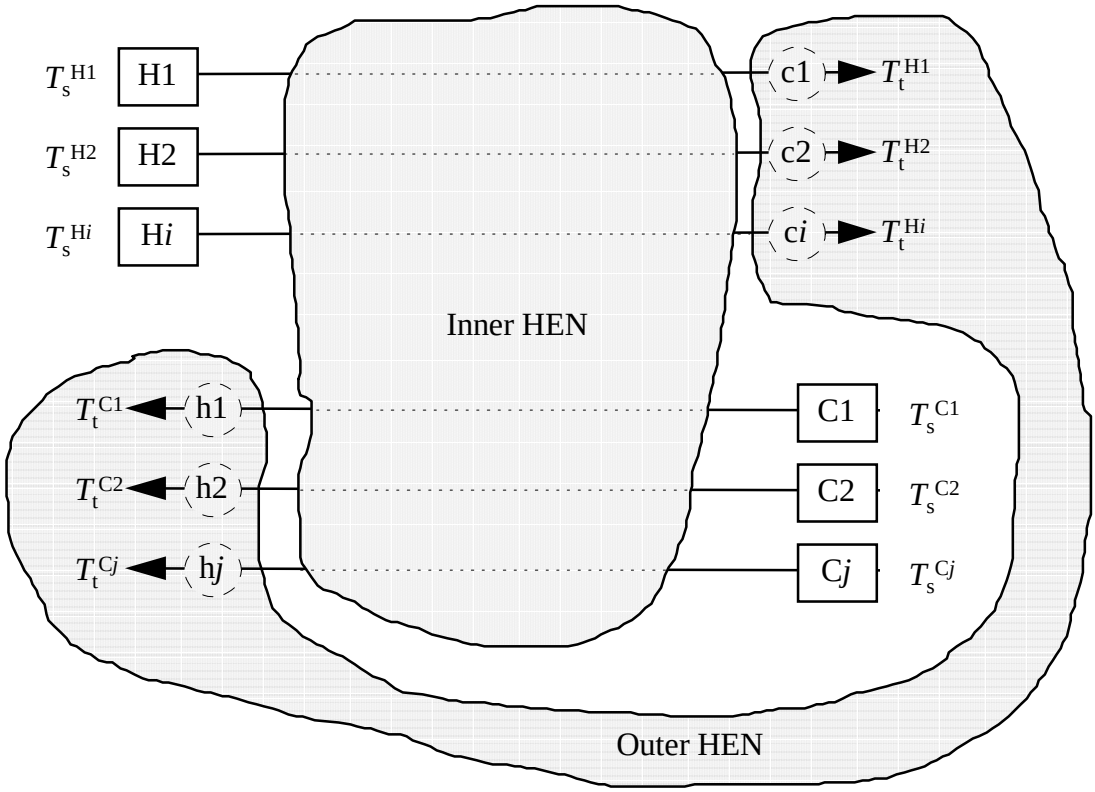

Figure 4.4 Inner and outer HEN.

Example 4.2 *Simple example for $N_{\mathrm{DOF,\,U}}$ using inner and outer HEN*.
The HEN in figure 4.5 has at total of 6 manipulations and 4 targets. The interface between the inner and outer HEN is the four temperatures T_1 to T_4.

Each process exchanger has a bypass and the duties are denoted Q_{I}, Q_{II}, Q_{III} and Q_{IV}. For the 4 streams the following equations for the inner HEN can be written:

$$\left.\begin{aligned} CP_{\mathrm{H1}}\left(T_1 - T_{\mathrm{s}}^{\mathrm{H1}}\right) &= -Q_{\mathrm{I}} - Q_{\mathrm{IV}} \\ CP_{\mathrm{H2}}\left(T_2 - T_{\mathrm{s}}^{\mathrm{H2}}\right) &= -Q_{\mathrm{II}} - Q_{\mathrm{III}} \\ CP_{\mathrm{C1}}\left(T_3 - T_{\mathrm{s}}^{\mathrm{C1}}\right) &= Q_{\mathrm{I}} + Q_{\mathrm{III}} \\ CP_{\mathrm{C2}}\left(T_4 - T_{\mathrm{s}}^{\mathrm{C2}}\right) &= Q_{\mathrm{II}} + Q_{\mathrm{IV}} \end{aligned}\right\} \Rightarrow \underbrace{\begin{bmatrix} -1 & 0 & 0 & -1 \\ 0 & -1 & -1 & 0 \\ 1 & 0 & 1 & 0 \\ 0 & 1 & 0 & 1 \end{bmatrix}}_{\text{Rank = 3}} \begin{bmatrix} Q_{\mathrm{I}} \\ Q_{\mathrm{II}} \\ Q_{\mathrm{III}} \\ Q_{\mathrm{IV}} \end{bmatrix} = \begin{bmatrix} b_1 \\ b_2 \\ b_3 \\ b_4 \end{bmatrix} \qquad (4.5)$$

where $b_1 = CP_{\mathrm{H1}}(T_1 - T_{\mathrm{s}}^{\mathrm{H1}})$ etc.

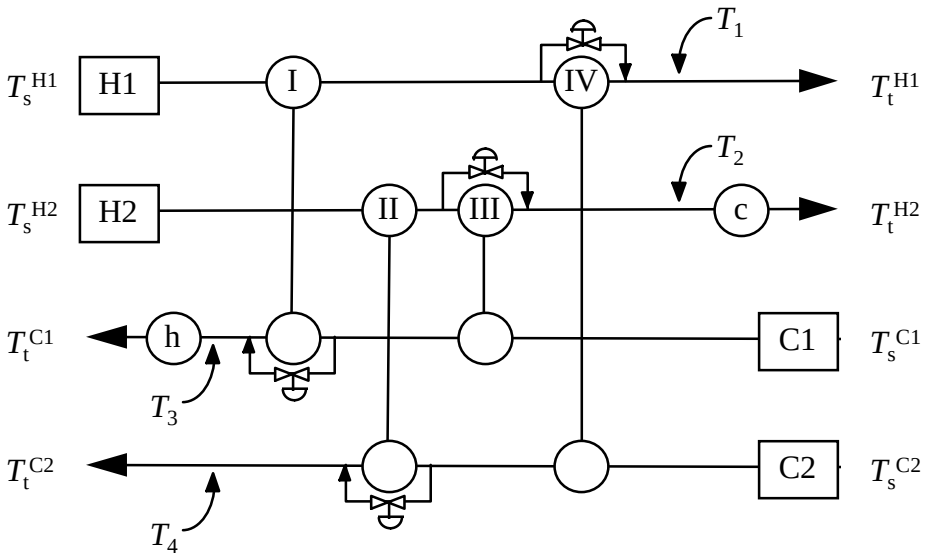

Figure 4.5 Simple HEN for demonstrating $N_{DOF,\,U}$.

The rank of the 4×4 matrix is 3 as indicated in equation (4.5). This implies that the 4 bypasses only spans a 3-dimensional space in the temperatures T_1, T_2, T_3 and T_4. We could actually conclude that the 4 bypasses could not span more than 3 dimensions without putting up equation (4.5), since if three of the temperatures T_1 to T_4 are specified, the fourth is given by an energy balance for the inner HEN. By looking at the set of equations and the corresponding rank, however, we can guarantee that the bypasses span a space with dimension equal to 3. The 3-dimensional space spanned by the bypasses implies that the inner HEN contributes with 3 free variables that may be utilized for utility optimization. The 2 utility exchangers give 2 more free variables, and with the 4 constraints (targets) we have:

$$N_{DOF,\,U} = \underbrace{3+2}_{\text{Free variables}} - \underbrace{4}_{\text{Constraints}} = 1 \tag{4.6}$$

Also in this example, there is one "additional" DOF that cannot be used for utility optimization; one temperature in the inner HEN may be specified or one bypass on the process exchangers may become inactive (e.g. saturated) without reducing $N_{DOF,\,U}$, since the inner HEN still spans a 3-dimensional space. ■

So far, we have assumed that each utility exchanger contributes with one free variable in the optimization of utility cost. This may seem to be an obvious assumption due to the structure of HENs given by equation 2.1. The diagonal structure from the utility exchangers to the utility controlled target temperatures suggests that no singularities can occur here. However, before we can put up the equation for $N_{DOF,\,U}$, it is required to consider the case where utility exchangers are parts of a loop, see figure 4.6.

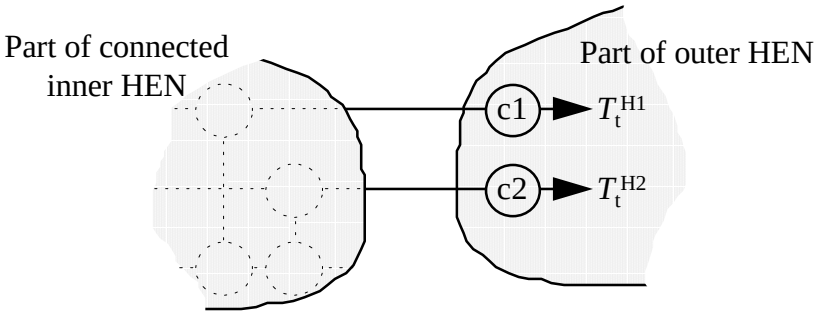

Figure 4.6 Utility exchangers forming a loop.

Assuming that the two coolers use the same type of utility, e.g. cooling water, they form a loop together with the connection in the inner HEN. Manipulating the loop, every second unit may increase or decrease its duty by the same amount while maintaining the energy balance (satisfy targets). When the two coolers use the same type of utility, the distribution of heat between these two units is indifferent for the total utility cost. The two units may be considered to represent two independent variables, while the loop may be considered as an additional constraint. Hence the net contribution of two utility units forming a loop is one free variable. More in general, $N_{\text{utility units}}$ utility exchangers using the same utility stream form $N_{\text{utility units}} - 1$ independent loops, thus contributing with only 1 free variable for utility optimization.

If the two coolers in figure 4.6 use different utility streams (e.g. c1 uses cooling water and c2 uses a cryogenic refrigerant), then they would not form a loop but instead they would form a path from the cooling water to the refrigerant. Manipulating this path will change the distribution of these two utility streams and with different cost, this may be used for optimization. Thus the two coolers contribute with two free variables for utility optimization.

The net contribution of free variables from the outer HEN is equal to $N_{\text{utility units}} - N_{\text{utility loops}}$ (number of utility units minus number of independent loops involving utilities). Above, it was argued that several utility exchangers on the same utility stream only give 1 free variable for optimization due to the formations of loops. This applies for each utility stream and we have

$$N_{\text{utility units}} - N_{\text{utility loops}} = N_{\text{U}} \tag{4.7}$$

As before, N_{U} is the number of different utility types. That is, 2 steam levels and cooling water gives $N_{\text{U}} = 3$, no matter how many utility units that are installed. From equation (4.7), the net contribution of free variables from the outer HEN simply is N_{U}. That is, the number of utility units is not directly involved in $N_{\text{DOF, U}}$, and we do not have to find the number of independent loops involving utility exchangers. Now, the equation for $N_{\text{DOF, U}}$ is given in theorem 4.1.

Theorem 4.1 *Degrees of freedom that can be used for utility optimization*, $N_{DOF,\,U}$
For a HEN with no utility exchangers and no target specifications in the inner HEN, the number of degrees of freedom that can be used for utility optimization in a HEN is given by:

$$N_{DOF,\,U} = R + N_U - N_t \tag{4.8}$$

where R is the dimension of the space spanned by the temperatures of the streams entering the outer HEN, due to all possible manipulations in the inner HEN. N_U is the number of utility streams and N_t is the number of target temperatures.

Proof: R is the number of free variables from the inner HEN. In the outer HEN, utility exchangers represent variables, but more than one unit on the same utility stream (same utility type) form loops. Manipulating such loops where the utility cost is the same do not affect the utility cost, thus each utility stream represent one free variable for utility optimization (equation 4.7). No singularities can occur in the outer HEN due to the diagonal structure, hence the total number of free variables is $R + N_U$. With a total number of N_t constraints, this proves the theorem. ■

In the rest of this section, the role of loops in the inner HEN, split fraction and process exchangers without bypasses will be discussed. Then, HENs that have free outlet temperatures are discussed, and it is shown that theorem 4.1 holds also for such cases. Finally, equation (4.8) will be simplified such that R do not have to be computed as shown in example 4.2.

Loops in inner HEN
Adding more than minimum number of units to a HEN design introduces loops. In most cases, this will not increase $N_{DOF,\,U}$. The reason to this is that the number of process streams between the inner and outer HEN is an upper bound on R. Usually (process exchangers without bypasses may result in exceptions), R is one less than the number of process streams since if all temperatures except one is specified, the last temperature is given by an energy balance. A typical case is the HEN in figure 4.5 which has one loop (one excess unit). However, the extra unit does not increase $N_{DOF,\,U}$ since R is limited by the four process streams and the energy balance of the inner HEN. In fact, one can add as many units and manipulations in the inner HEN as one like without increasing $N_{DOF,\,U}$, since R cannot exceed 3 for this case.

Split fractions
The same argument as for loops in the inner HEN applies for variable split fractions: Usually, $N_{DOF,\,U}$ is not increased since R is limited by the number of process streams and the energy balance. Figure 4.7 shows a configuration that may be part of a larger HEN.

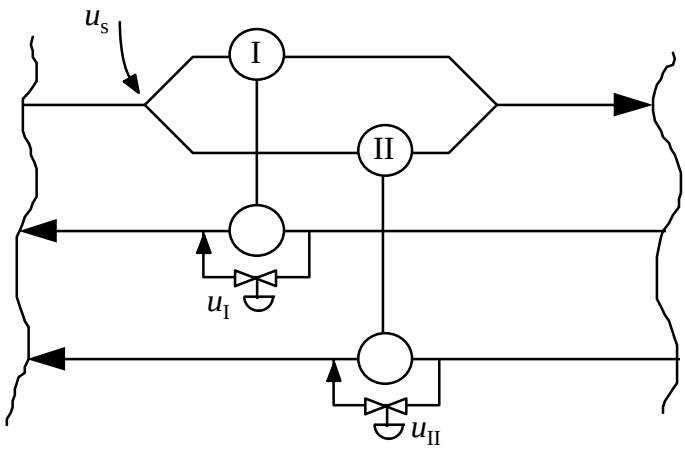

Figure 4.7 Part of HEN with variable stream split (u_s).

Even if there are 3 manipulations (u_I, u_{II} and u_s), only 2 free variables can be transferred to the surroundings. Again, the energy balance for the shown part of the HEN fixes the third of the stream exit temperatures. Addition of the split fraction will not contribute to increasing $N_{DOF,\,U.}$ However, the presence of the split fraction allows one of the bypasses to be saturated without reducing the number of free variables to the surroundings. Also, if one of the process exchangers do not have any bypass installed, then the addition of the split fraction will increase the number of free variables from 1 to 2. This leads to the next topic:

Process exchangers without bypasses

It has been argued above, that R is normally bounded by the number of process streams (N_P) minus one. However, R can of course not exceed the number of manipulations in the inner HEN. In cases where there are process exchangers without bypasses and the total number of manipulations is less than $N_P - 1$, then the number of manipulations will limit R and $N_{DOF,\,U}$ is limited by the process exchangers without bypasses. If there are excess units (loops) in the inner HEN, then removing bypasses will not reduce $N_{DOF,\,U}$ unless R is reduced.

Free outlet temperatures

When considering free outlet temperatures, it is important to recall that only those streams with targets enter the outer HEN. That is, the number of streams entering the outer HEN is always (per definition of outer HEN) equal to N_t. For HENs with free outlet temperatures, we have $N_t = N_P - N_F$, where N_F is the number of free outlet temperatures. For all HENs, an upper bound on R is N_t. This follows trivially since N_t is the number of "information channels" transferred to the outer HEN. Here, we assume that there are enough manipulations to span the whole space with dimension N_t. For a HEN with no free outlet temperatures, however, R is restricted to $N_t - 1$ ($= N_P - 1$) since the energy balance around the inner HEN represents one constraint. Now, adding a process stream with a free outlet temperature (and connecting it to the HEN with one or more units), the free outlet serve as a sink/source for the inner HEN. That is, the streams entering the outer HEN span the full space with dimension N_t, thus R and also $N_{DOF,\,U}$ are increased by one. Going one step further, we may add another process stream with a free outlet temperature and connect it to the HEN. R already spans the full space, and it is now constrained by N_t. That is, R and $N_{DOF,\,U}$ are *not increased any further*. To conclude so far we have found that for HENs where

R is not limited by the manipulations in the inner HEN, *adding one or more process streams with free outlet temperatures increases $N_{DOF,\,U}$ by 1.*

Another approach is to consider the case where a target is relaxed (a target temperature is turned into a free outlet temperature) without introducing any new streams. The result is the same, but the arguments are slightly different: The starting point is a HEN with no free outlet temperatures and we have $R = N_t - 1$. Relaxing one target specification, N_t is reduced by one and one less stream is entering the outer HEN. However, the free outlet temperature serves as a sink/source and *R* now spans the full space of the new set of streams/temperatures entering the outer HEN. That is, *R* is unchanged and with N_t reduced by 1, $N_{DOF,\,U}$ is increased by 1. Proceeding by relaxing another target, N_t is reduced again, but now also *R* is reduced since it is bounded by N_t. With both *R* and N_t reduced by one, $N_{DOF,\,U}$ is unchanged. Similar to above, we have found that for HENs where *R* is not limited by the manipulations in the inner HEN, *relaxing one or more target specifications increases $N_{DOF,\,U}$ by 1.* This result is demonstrated by example 4.4 in the next section. Note that the result does not hold when *R* is limited by the number of manipulations in the inner HEN. In such cases, $N_{DOF,\,U}$ may be increased by more than 1 (until $R = N_t$).

Simplification of equation (4.8)

Equation (4.8) covers all situations discussed above such as loops, splits, units that cannot be manipulated and free outlet temperatures, however, it requires computation of the rank *R*. Now, this equation will be simplified, yet still it will be valid for most HENs. Focus will be on the term $R - N_t$ which is part of equation (4.8). First, the case where there are no free outlet temperatures is considered.

As pointed out above, an *upper* bound on *R* for cases with no free outlet temperatures is equal to $N_t - 1$. On the other hand, the smallest number of process exchangers to form a connected inner HEN is $N_P - 1$ ($= N_t - 1$). Assuming that these process exchangers have bypasses and that there are no singularities, a *lower* bound on *R* is $N_t - 1$. With upper bound equal to lower bound, we can conclude that $R = N_t - 1$, hence the term $R - N_t$ in equation (4.8) equals –1.

For HENs with free outlet temperatures, an upper bound on *R* is N_t since the free outlet temperature(s) can be considered as a sink/source for the energy balance of the inner HEN. The smallest number of process exchangers to form a connected inner HEN is $N_P - 1$ and with $N_t = N_P - N_F$, we have $N_P - 1 = N_t + N_F - 1$. Assuming that the duties of the process exchangers can be manipulated and that no singularities are present a *lower* bound on *R* is N_t. Again, the upper bound equals the lower bound and we have $R - N_t = 0$.

Inserting these results in equation (4.8), we have found that $N_{DOF,\,U}$ for HENs where all process exchangers have bypasses and there are no singularities, is

HENs with no free outlet temperatures:	$N_{DOF,\,U} = N_U - 1$	(4.9a)
HENs with (one or more) free outlet temperatures:	$N_{DOF,\,U} = N_U$	(4.9b)

For HENs with more than minimum number of units, this result also hold if some process exchangers do not have bypass installed or if there are singularities, as long as *R* is not reduced below its upper bound.

4.5 Examples

In this section, the use and validity of rule 4.1, theorem 4.1 and equation (4.9) is demonstrated by 3 examples.

Example 4.3 *HEN with multiple utilities.*
The HEN in figure 4.8 has a total of 11 manipulations and 6 targets. There are 4 utilities: LP-steam, HP-steam, cooling water (CW) and a refrigerant (R1). The inner HEN has 6 units (1 loop) and all these have bypass installed.

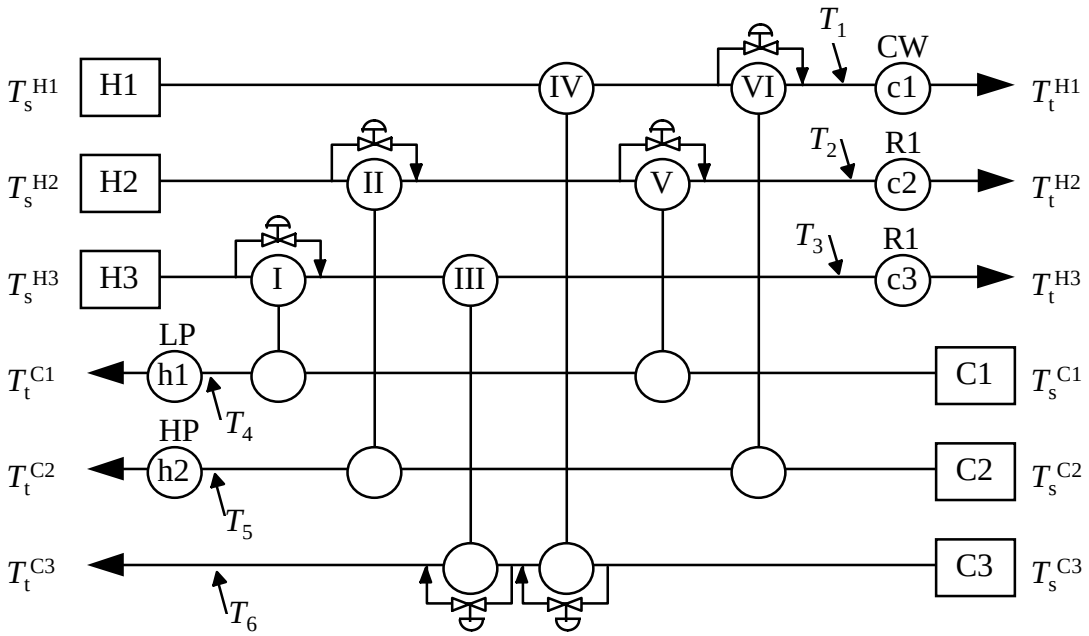

Figure 4.8 HEN with multiple utilities.

Rule 4.1 suggests that optimization is possible. Using theorem 4.1 to find $N_{\mathrm{DOF,\,U}}$, we first compute R by putting up the equations for the inner HEN as in example 4.2. In matrix form, we get

$$\begin{bmatrix} 0 & 0 & 0 & -1 & 0 & -1 \\ 0 & -1 & 0 & 0 & -1 & 0 \\ -1 & 0 & -1 & 0 & 0 & 0 \\ 1 & 0 & 0 & 0 & 1 & 0 \\ 0 & 1 & 0 & 0 & 0 & 1 \\ 0 & 0 & 1 & 1 & 0 & 0 \end{bmatrix} \begin{bmatrix} Q_{\mathrm{I}} \\ Q_{\mathrm{II}} \\ Q_{\mathrm{III}} \\ Q_{\mathrm{IV}} \\ Q_{\mathrm{V}} \\ Q_{\mathrm{VI}} \end{bmatrix} = \begin{bmatrix} b_1(T_1) \\ b_2(T_2) \\ b_3(T_3) \\ b_4(T_4) \\ b_5(T_5) \\ b_6(T_6) \end{bmatrix} \tag{4.10}$$

The rank of the matrix is 5, thus we have $R = 5$. With $N_{\mathrm{U}} = 4$ and $N_{\mathrm{t}} = 6$, equation (4.8) in theorem 4.1 gives

$$N_{\mathrm{DOF,\,U}} = R + N_{\mathrm{U}} - N_{\mathrm{t}} = 5 + 4 - 6 = 3 \tag{4.11}$$

For this example, equation (4.9a) also gives $N_{\mathrm{DOF,\,U}} = 3$ since the assumptions made in the simplifications of (4.8) are fulfilled. The 3 DOF for utility optimization can be identified as

- Heat recovery level (total utility energy consumption)
- Distribution of LP-steam and HP-steam.
- Distribution of cooling water/refrigerant.

Equation (4.3) suggests a total of 5 DOF (11 manipulations and 6 targets), thus we expect that there are 2 additional DOF that do not affect the utility cost. These are identified as

- Distribution of duties between the coolers c2 and c3 (manipulating loop formed by outer and inner HEN together).
- Distribution of duties in process exchangers (manipulating loop in inner HEN).

■

Example 4.4 *HEN with free outlet temperatures.*
This example demonstrates that more than one free outlet temperature may not increase $N_{\mathrm{DOF,\,U}}$, see figure 4.9. The HEN structure is identical as in example 4.2 where we found $N_{\mathrm{DOF,\,U}} = 1$ when all outlet temperatures had targets.

First, we consider the case where $T_{\mathrm{o}}^{\mathrm{H1}}$ is free. The interface from the inner to the outer HEN is constituted by the temperatures T_2, T_3 and T_4 and N_{t} is reduced to 3. The matrix to compute R is

$$\begin{bmatrix} 0 & -1 & -1 & 0 \\ 1 & 0 & 1 & 0 \\ 0 & 1 & 0 & 1 \end{bmatrix} \begin{bmatrix} Q_{\mathrm{I}} \\ Q_{\mathrm{II}} \\ Q_{\mathrm{III}} \\ Q_{\mathrm{IV}} \end{bmatrix} = \begin{bmatrix} b_1(T_2) \\ b_2(T_3) \\ b_3(T_4) \end{bmatrix} \tag{4.12}$$

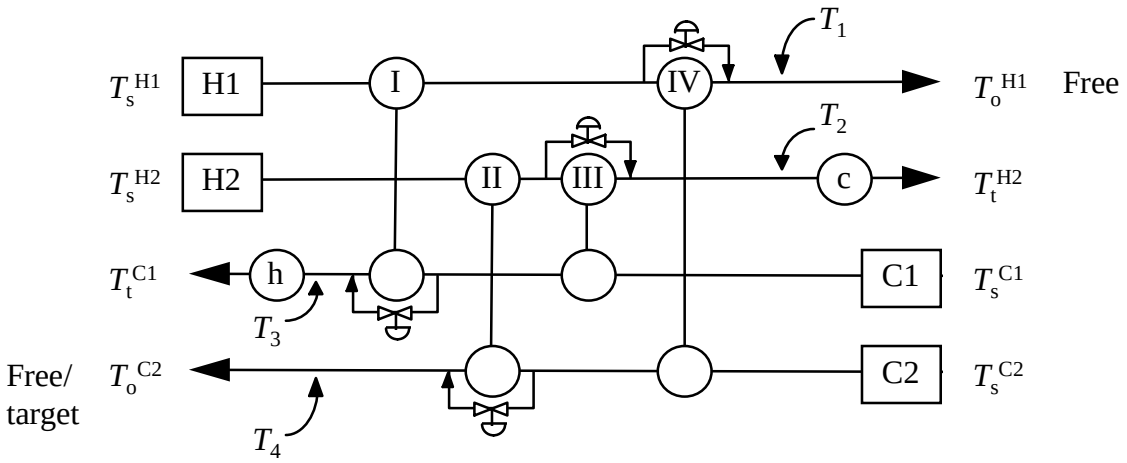

Figure 4.9 HEN with free outlet temperatures.

The rank of the matrix in equation (4.12) is $R = 3$ which is the same as in example 4.2. The matrix is identical to the matrix in equation (4.5) with the first row deleted, and stream H1 serves as a sink/source for the energy balance. The result is

$$N_{DOF,\,U} = R + N_U - N_t = 3 + 2 - 3 = 2 \tag{4.12}$$

Now, we go one step further and also let T_o^{C2} be free. The interface to the outer HEN are the 2 temperatures T_2 and T_3, and the corresponding equations for the inner HEN become equal to equation (4.12) with the last row deleted. This yields $R = 2$ and since also $N_t = 2$, the result with 2 free outlet temperatures is

$$N_{DOF,\,U} = R + N_U - N_t = 2 + 2 - 2 = 2 \tag{4.13}$$

$N_{DOF,\,U}$ do not increase when the number of free outlets is increased above 1. This only holds when the manipulations in the inner HEN spans the whole space of N_t dimensions. In other examples where $R < N_t$, relaxing target specifications may increase $N_{DOF,\,U}$ until $R = N_t$. ■

Example 4.5 *HEN with split and a process exchanger without bypass.*
The HEN in figure 4.10 has a total of 7 manipulations (including the split fraction u_s) and 6 targets. It is a pinch problem with 2 utilities, rule 4.1 suggest that optimization is possible and equation (4.9a) results in $N_{DOF,\,U} = 1$. Note that process exchanger V does not have a bypass, and we should be careful when using equation (4.9a). Below it is shown that this HEN in fact has $N_{DOF,\,U} = 0$, thus no optimization of utility cost should be considered for this design. The explanation uses only simple physical insight described in the previous section, no equations are needed.

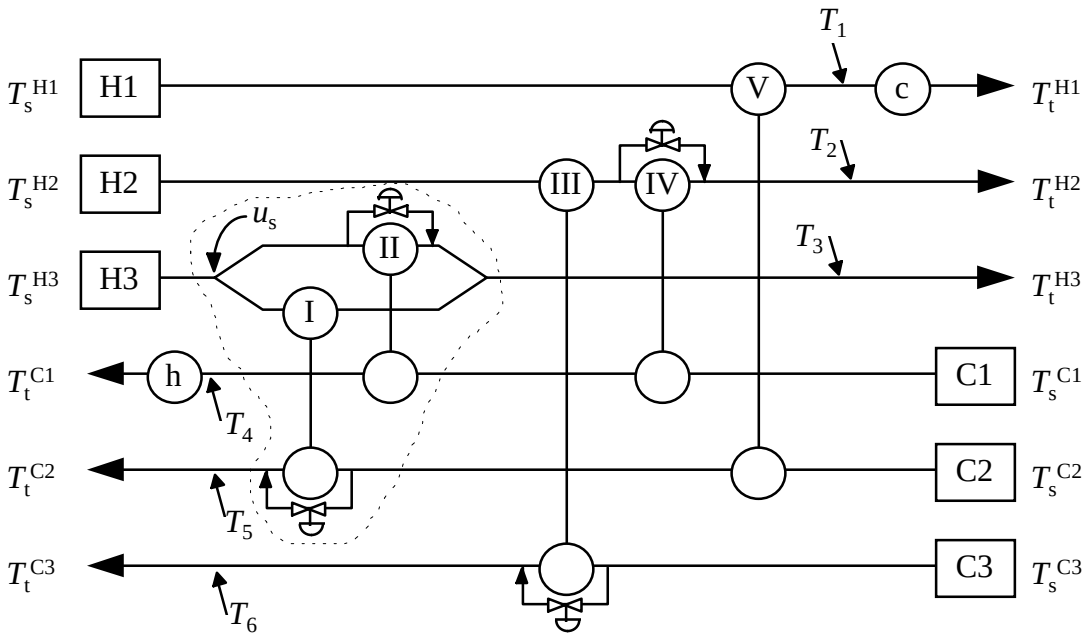

Figure 4.10 HEN with variable stream split (u_s) and a process exchanger without bypass.

The reason for $N_{DOF,\,U} = 0$ is that the 3 manipulations u_s, u_I and u_{II} only spans a 2-dimensional space in the temperatures T_3, T_4 and T_5. This is easily seen by drawing a system boundary

around the splitted part of stream H3 and the process exchangers I and II on streams C1 and C2 (see dotted line). The energy balance for this subsystem only allows for 2 temperatures to be freely specified. That is, the 3 manipulations u_s, u_I and u_{II} only contributes with 2 free variables to the surroundings. We can already conclude that these 2 free variables have to be used for control of T_3 and T_5, thus we cannot control T_4. The 2 other manipulations in the inner HEN (u_{III} and u_{IV}) gives a total number of free variables from the inner HEN of $R = 4$. From this, we obtain

$$N_{DOF,\,U} = R + N_U - N_t = 4 + 2 - 6 = 0 \tag{4.14}$$

This example has demonstrated that it may not always be possible to optimize pinch problems even if there are extra manipulations. In addition it has been shown that it is not always necessary to write down equations and compute the rank R mathematically. ■

4.6 Conclusions

It has been shown that degrees of freedom in operation of HENs may not always be utilized for utility optimization and the number of DOFs that can be used for optimization, $N_{DOF,\,U}$ is defined. Most important for operation is not how many DOFs that can be used for optimization, but whether optimization is possible ($N_{DOF,\,U} \geq 1$) or not ($N_{DOF,\,U} = 0$). If $N_{DOF,\,U} < 0$, the operation of the HEN is infeasible (targets cannot be met) and the HEN design or the target specifications have to be modified.

A rule to quickly find whether optimization is possible or not has been established. We concluded that threshold problems with free outlet temperatures and pinch problems may be optimized, whereas threshold problems with no free outlet temperatures never can be optimized. For threshold problems and pinch problems with free outlet temperatures, this rule only serve as a necessary condition for optimization.

A quantitative expression for $N_{DOF,\,U}$ is developed and as part of that the HEN was divided into the inner HEN and the outer HEN. In many cases, the number of physical streams entering the outer HEN (streams with target value) represents a bottleneck for $N_{DOF,\,U}$. The equation requires computation of the rank of the transfer matrix from manipulations in the inner HEN to the temperatures of the streams entering the outer HEN, thus the detailed HEN structure is considered. By making some assumptions about the inner HEN (bypasses on all process exchangers and no singularities), $N_{DOF,\,U}$ is simply given by the number of utility streams.

The following three chapters concern methods for optimal operation of HENs. In those chapters it is assumed that the HENs to be operated have $N_{DOF,\,U} \geq 1$. As it has been clear from this chapter, it should always be verified that the HEN has $N_{DOF,\,U} \geq 1$ before any optimizing control scheme is considered.

Notation

CP_{Cj}	Heat capacity flowrate of cold stream *j*.
CP_{Hi}	Heat capacity flowrate of hot stream *i*.
N_{DOF}	Number of degrees of freedom.
$N_{DOF,\,U}$	N_{DOF} that can be utilized for optimization of utility cost.
N_F	Number of free outlet temperatures.
N_P	Number of process streams.
N_t	Number of target specifications.
N_U	Number of different utility types (same as number of utility streams).
Q_i	Heat load (duty) of heat exchanger *i* (where *i* is a Roman numeral)
R	Rank. (Dimension of the space when the temperatures in the streams to the outer HEN are spanned by all manipulations in the inner HEN).
T_o^{Cj}	Outlet temperature of cold stream *j*.
T_o^{Hj}	Outlet temperature of hot stream *i*.
T_s^{Cj}	Supply temperature to cold stream *j*.
T_s^{Hj}	Supply temperature to hot stream *i*.
T_t^{Cj}	Target temperature of cold stream *j*.
T_t^{Hj}	Target temperature of hot stream *i*.
u	Manipulation (often bypass fraction).

References

Marselle D.F., M. Morari and D.F. Rudd (1982). Design of Resilient Processing Plants - II. Design and Control of Energy Management Systems. *Chem. Eng. Sci.*, ***37***, 259-270.

Mathisen, K.W. (1994). Integrated Design and Control of Heat Exchanger Networks. *Thesis*. (Trondheim University - NTH, Department of Chemical Engineering, Norway).

Rosenbrock, H.H. (1970). *State-space and Multivariable Theory*, Nelson, London, UK.

Chapter 5

OPTIMAL OPERATION USING STRUCTURAL INFORMATION

This is the first of three chapters concerning specific methods for optimal operation of HENs. The method being discussed in this chapter utilizes the *structural* properties of the network. A control strategy is developed that, in addition to controlling the target temperatures, minimizes the utility consumption. The method results in a decentralized control structure with variable pairing. The procedure is based on an idea suggested by Mathisen *et al.* (1994) but in that paper no applications to validate the method are presented. The method is also described by Glemmestad *et al.* (1996), and the content of this chapter is, with the exception of some extensions, taken from that paper.

5.1 Introduction

This chapter concerns operation of a HEN with given structure and heat exchanger areas. In addition to structure and areas, the stream data (heat capacity flowrates, supply temperatures and target temperatures) are specified, and finally disturbances, such as variations in supply temperatures, flowrates and possibly in heat transfer coefficients are given. The goal is to find a control strategy that yields optimal operation. Optimal operaton was defined in section 2.3, and to recall, the control system should (1) satisfy targets at steady state, (2) minimize utility consumption and (3) give reasonable dynamic behavior.

The main rule for input/output pairing of HENs (Rule 2.2), is motivated from the needs of regulatory control (dynamic behavior). The method in this chapter aims to find a pairing that minimizes utility consumption instead, and this pairing may not always result in the best possible dynamic properties.

A prerequisite for optimization is that there are at least one degree of freedom in operation. As it was shown in section 2.4, most HENs have this feature (e.g. all pinch problems). In addition, optimum is often constrained meaning that for the operating state with minimum utility consumption, one or more manipulations are saturated (e.g. fully closed bypass). The location of optimum during operation for HENs is treated more thoroughly in section 5.3. The fact that optimum often is constrained is, however, very important when structural properies are utilized for optimal operation of a HEN. The idea of the method is the following:

Assume for simplicity a HEN with only one DOF that can be used for utility optimization. If one can find one manipulation that have to be saturated in optimum, then adjusting this manipulation to the saturation limit, there will be only one feasible solution for the remaining manipulations. That is, the number of remaining manipulations are equal to the number of targets. The optimal operating state of the HEN is achieved by using decentralized feedback control involving the remaining manipulations. In general, the method uses the structural properties of the HEN to find which manipulation should be saturated, and then feedback control is applied for the remaining system (with only one feasible solution).

The structural properties of the HEN are contained in *sign matrices*. These matrices describe how the manipulations affect outlet temperatures and utility consumption. The elements of the sign matrices are simply "+" and "–" etc. to denote whether an effect is positive or negative. The sign matrices are found from the HEN structure and simple physical insight. The procedure does not result directly in a particular manipulation that should be saturated, but in a *priority table* for the manipulations. This priority table is implemented in the control scheme and the optimal operating state will be found "automatically" during operation. The set of saturated manipulations may depend on the disturbances that are present, thus the control structure may change during operation. The method is introduced by an illustrating example where the idea is explained from simple physical insight.

5.2 An illustrating example

Based on the stream data in table 5.1, a pinch design with evolution can result in the HEN shown in figure 5.1. The design is based on a minimum heat recovery approach temperature of 20°K and the nominal value of 190°C in T_s^{H1}. The nominal stream data and the HEN is identical to the simple HEN used previously in the thesis except for the heat capacity flowrates which are reduced by a factor of one hundred (has no practical implications). The only disturbance is ±20°C in T_s^{H1} and its influence on the output temperatures should be completely rejected during steady state operation. Using the decomposition principle (Rule 2.1), we assume that T_o^{H1} and T_o^{C1} are perfectly controlled by the cooler and heater duties, respectively. The focus is on how to control the only bypass controlled temperature T_o^{C2}, using the bypass fractions u_I and u_{II}. Common engineering to control T_o^{C2} would be to increase the area of exchanger 2 and equip it with a bypass and a controller. This strategy would increase the capital cost of the HEN. Alternatively, one could avoid additional area of the process exchangers by increasing the heater and cooler duties which instead would increase the operating cost. We shall develop a procedure that maintains the target

temperatures and at the same time gives minimum utility consumption at steady state together with minimum added area.

Stream	T_s [°C]	T_t [°C]	CP [kW/°C]
H1	190±20	30	1.0
C1	80	160	1.5
C2	20	130	0.5

Table 5.1 Stream data for illustrating example.

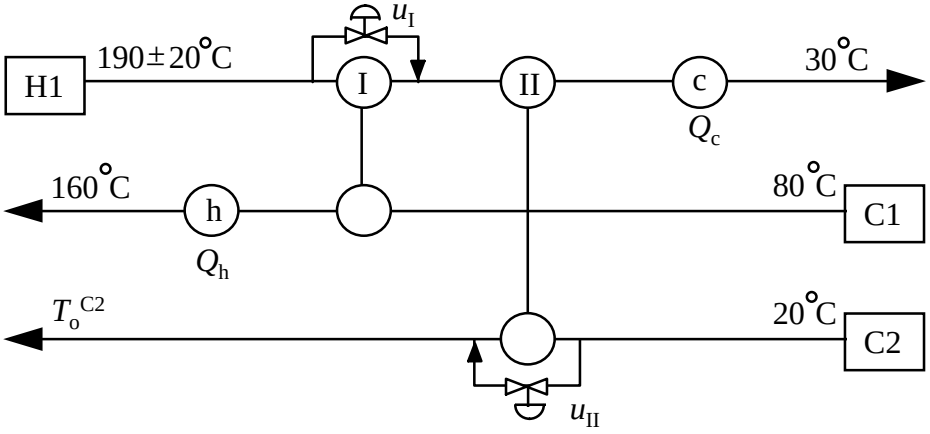

Figure 5.1 Network for illustrating example.

Assuming that bypasses (but no extra area) are placed across both heat exchangers, we have four manipulations (two bypass fractions and two utility duties) to control the three outlet temperatures. That is, there is one degree of freedom with respect to control and this degree of freedom will be used to minimize the utility consumption. T_o^{H1} and T_o^{C1} are perfectly controlled by utilities so we have two possible manipulations (u_I and u_{II}) to control the only bypass controlled target temperature T_t^{C2}.

First, assume that the outlet temperature T_o^{C2} is too low, for example due to a negative disturbance in T_s^{H1}. To increase the outlet temperature, u_I could be increased or u_{II} could be decreased. Increasing bypass u_I will increase downstream temperatures on stream H1 and decrease downstream temperatures in stream C1. To maintain the utility controlled target temperatures, the heat load has to be increased in the cooler as well as in the heater. Alternatively, decreasing u_{II} will give a desired increase in T_o^{C2} along with decreasing downstream temperatures in H1. This corresponds to a *reduction* in the utility consumption of the cooler. When the outlet temperature is too low we therefore prefer to reduce u_{II}. If this bypass is saturated at 0, we have to increase bypass u_I.

Next, assume that T_o^{C2} too high. A similar argument will imply that the preferred manipulation is to reduce u_I which at the same time will reduce utility consumption. If u_I is saturated, we must increase bypass u_{II} which also increases the utility consumption. Based on the arguments above, we will use the following control configuration for the HEN:

When T_o^{C2} is too high:
If $u_I > 0$, then pair T_o^{C2} and u_I in a SISO-controller and let $u_{II} = 0$,
else pair T_o^{C2} and u_{II} in a SISO-controller and keep $u_I = 0$.

When T_o^{C2} is too low:
If $u_{II} > 0$, then pair T_o^{C2} and u_{II} in a SISO-controller and let $u_I = 0$,
else pair T_o^{C2} and u_I in a SISO-controller and keep $u_{II} = 0$.

Figure 5.2 shows the result when this variable control structure is implemented. The controllers are simple PI-controllers with anti-windup. An important observation is that one of the manipulations u_I or u_{II} is always saturated at zero, and this implies that the optimal solution lies on the constraints of the feasible region. When u_I is used instead of u_{II}, the transient response becomes somewhat worse. We shall, however, not be too concerned about this since we assume that the process is continuos and that the setpoints and disturbances are fairly steady.

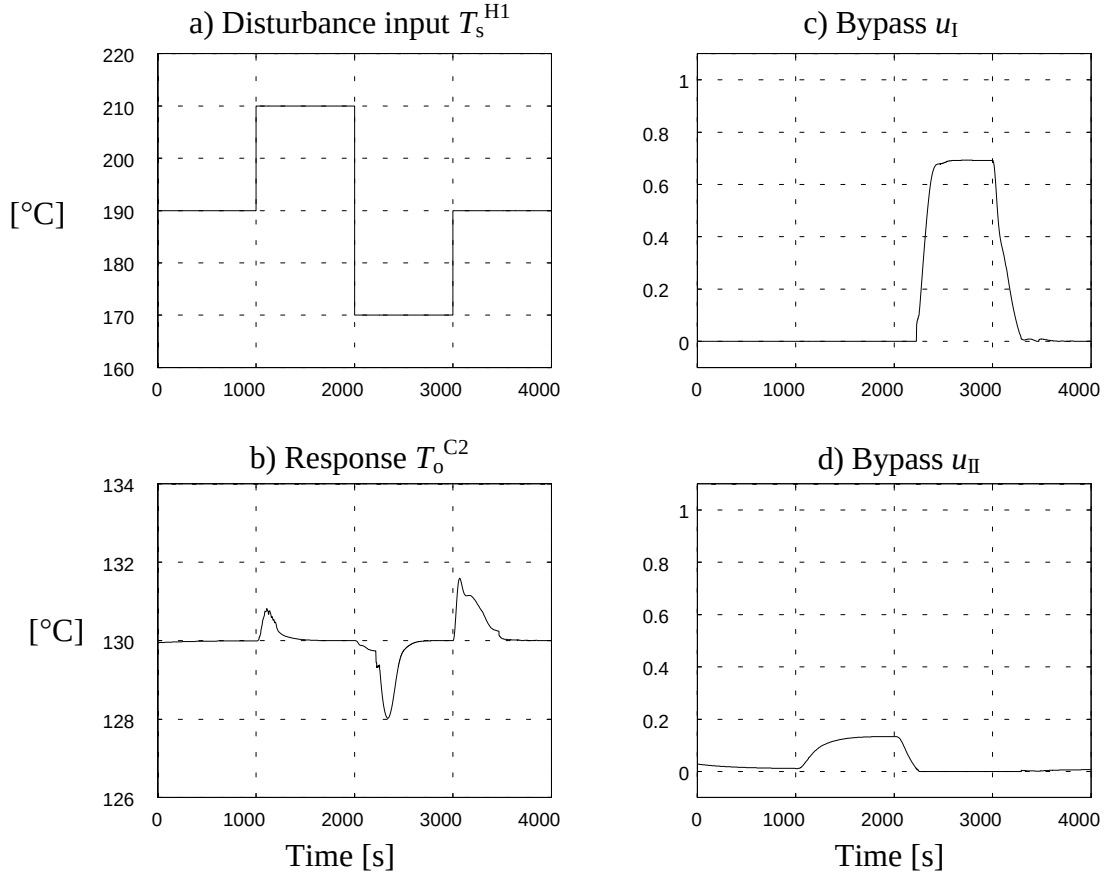

Figure 5.2 Simulation results for motivating example.
(a) Input disturbance T_s^{H1}. (b) Response in T_o^{C2}.
(c) and (d) Bypass fractions u_I and u_{II}.

In this example, a control strategy that minimizes utility consumption has been found from the *structural* properties of the HEN. In the following parts of this chapter, a systematic method to achieve optimal operation using structural information is developed.

To conclude this section, a remark regarding flexibility is given: As the example has shown, the variable control structure yield a controlled HEN with sufficient effective flexibility (recall definition 2.2). A fixed SISO control structure will result in *zero effective flexibility* if the areas are not increased. (Using u_{I} for control can only decrease $T_{\mathrm{o}}^{\mathrm{C2}}$ while u_{II} can only increase $T_{\mathrm{o}}^{\mathrm{C2}}$.) The flexibility can be increased by increasing the area of exchanger II and using u_{II} for control. However, an alternative way of making the controlled HEN more flexible (effective flexibility) is to *reduce* the area of exchanger I (or to bypass it constantly). This corresponds to increasing the utility consumption since the heat transferred in the path from the heater to the cooler is increased. Hence, the effective flexibility may be improved by reducing area.

The variable control strategy used in the example does not only minimize utility consumption, it also maintains the flexibility of the HEN itself, thus no area of process exchangers (compared to the nominal design) need to be added for flexibility.

5.3 Location of optimum

As mentioned in the introduction to this chapter, an important feature of HENs in order to use structual information for operation, is that optimum often is located at the intersection of constraints.

Increasing the bypass fraction of a heat exchanger will monotonically decrease its duty and vice versa. This will give a monotonic increase or decrease of downstream temperatures and hence usually also the outlet temperatures and the utility duties. In a HEN, minimum utility consumption corresponds to maximum heat recovery between the process streams. In a HEN with degrees of freedom, this implies that some bypasses in most cases should be fully closed. These bypasses should only be used if this is the only way to meet the targets. This may happend if bypasses used for regulatory control are saturated. Hence, optimal operation of HENs normally corresponds to saturation of some manipulations.

An obvious exception is when a variable split fraction is used for utility optimization. In such cases, minimum utility consumption is obtained at some intermediate value of the split fraction, thus the optimal solution may not be located at constraints. Other exceptions are when there are independent downstream paths from both hot and cold side of a heat exchanger and to the same outlet temperature/utility exchanger (Mathisen, 1994). The effects from the hot and cold side of a bypassed heat exchanger will always have opposite signs. The net effect (positive or negative) can usually not be deduced from structural information, and optimal operation can not be guaranteed in such cases.

To illustrate the typical situation where optimum is constrained, total utility consumption for the HEN used in the illustrating example is plotted as a function of the two bypass fractions.

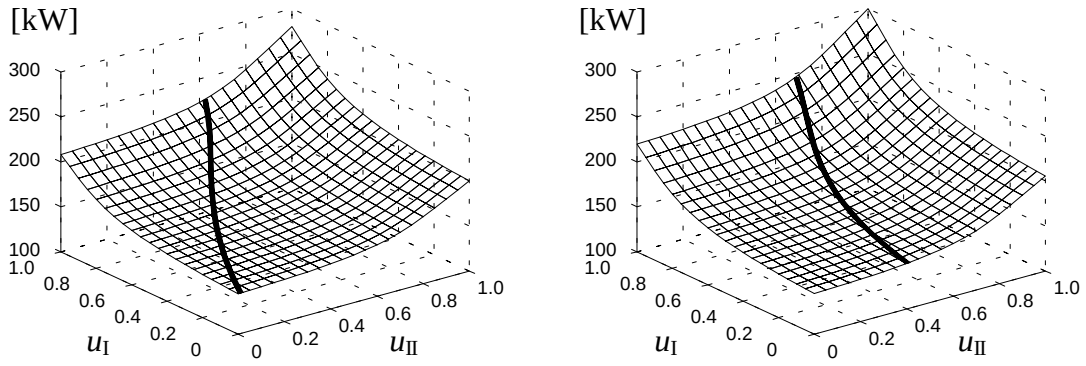

a) T_s^{H1} is nominal (190°C). b) T_s^{H1} is 20°K above nominal value.

Figure 5.3 Utility consumption as a function of u_I and u_{II}. Feasible line is also plotted.

Figure 5.3a (left graph) shows the utility consumption ($Q_c + Q_h$) when no disturbances are present. The line shows the combination of u_I and u_{II} that gives feasible operation, that is, all targets are met. As seen from the figure, feasible (but worst case) operation in the nominal case may be achieved with $u_I = 1$ (fully open bypass) and $u_{II} \approx 0.6$, while *optimal* operation is obtained for $u_I = u_{II} = 0$. The graph in figure 5.3b shows the same when the disturbance, T_s^{H1} has its maximum value. For both cases the optimal solution is constrained. In addition, the results in figure 5.2 are confirmed.

5.4 The sign matrices

The method for optimal operation makes use of "sign matrices". These are used for storage of information that can be exctracted from the structure of the process. In general, a sign matrix is defines as

Definition 5.1 The sign matrix, *sign*(*A*).
Let A be a matrix of real numbers where the precise value of each element $a_{i,j}$ may not be known. The sign matrix *sign*(*A*) is defined as

$$sign(A)_{i,j} = \begin{cases} [+] & \text{if } a_{i,j} > 0 \\ [-] & \text{if } a_{i,j} < 0 \\ [0] & \text{if } a_{i,j} = 0 \\ [\pm] & \text{otherwise} \end{cases} \tag{5.1}$$

■

To avoid confusion with the operators for addition and subtraction, the elements in a sign matrix are enclosed by brackets also when single elements are addressed. Each entry in a sign matrix denote a scalar number, thus e.g. [+] denotes a number that we know is positive, but we may not necessarily know the specific value. In the example in the previous section, we concluded that increasing bypass u_I increases T_o^{C2}. This implies that the corresponding element in the (sign) transfer matrix is [+]. [0] simply denotes the number 0. [±] denotes a

number that may be both positive and negative (and zero) and occurs when there are opposing effects where we cannot conclude that the effects with a certain sign are the dominating.

The arithemic rules for signs (we only need addition and multiplication) follow the normal conventions for scalars. Examples are

$$[+] + [+] = [+]$$
$$[+] + [-] = [\pm]$$
$$[-] + [-] = [-]$$

$$[+] \cdot [+] = [+]$$
$$[+] \cdot [-] = [-]$$
$$[-] \cdot [-] = [+]$$

Further, all operations involving [±], except for multiplication by [0], results in [±].

Now, the relation of the sign matrices and optimal operation will be made. The following two systems for HENs are introduced:

$$y^{BP} = G^{BP}u \tag{5.2}$$
$$y^{U} = G^{U}u \tag{5.3}$$

Here, y^{BP} is a vector containing the bypass controlled output (target) temperatures and G^{BP} is the transfer function matrix from the input vector u (bypasses) to y^{BP}. In equation (5.3), G^{U} is the transfer matrix from u to the output vector y^{U} that contains the utility *consumption* for each of the utility controlled temperatures (assuming that the utility controlled outputs are perfectly controlled).

The procedure makes use of the two sign matrices $sign(G^{BP})$ and $sign(G^{U})$. Note that the definition of the sign matrix in this thesis is different from the sign matrix used by Mathisen *et al.* (1994) where the signs depend on whether a stream is hot or cold. Thereby, that method is useful only for HENs, while the method as presented in this thesis also may be applied to other processes. We will, however, assume a HEN in the presentation of the procedure.

The procedure is based on the following four observations for HENs:

1) A positive (negative) temperature change has a positive (negative) effect on all downstream temperatures.
2) Temperature disturbances are naturally dampened.
3) A flowrate increase of hot (cold) streams has a positive (negative) effect on all downstream temperatures.
4) Bypass increases propagate as a temperature increase from the hot side and temperature decrease from the cold side of the bypassed heat exchanger.

These observations are proven by Mathisen (1994, chapter 5), and they imply the following useful rules when constructing $sign(G^{BP})$:

- sign$(G^{BP})_{k,j}$ = [+] if all downstream paths are from the hot side of bypass *j* to bypass controlled target temperature *k*.
- sign$(G^{BP})_{k,j}$ = [–] if all downstream paths are from the cold side of bypass *j* to bypass controlled target temperature *k*.

Similarly, when constructing *sign*(G^{U}), the following rules may be useful:

- sign$(G^{U})_{i,j}$ = [+] if all downstream paths are from the hot (cold) side of bypass *j* to utility controlled target temperature *i* of a hot (cold) stream.
- sign$(G^{U})_{i,j}$ = [–] if all downstream paths are from the hot (cold) side of bypass *j* to utility controlled target temperature *i* of a cold (hot) stream.

If there are no downstream paths from an input to an output, the corresponding element in the sign transfer matrix is [0]. If there are opposing effects, such as parallel downstream paths from a bypass, the corresponding element in the sign matrix is often [±]. There is, however, an important exception to this as given by the following observation which also is proven by Mathisen (1994, chapter 5):

5) Bypassing a heat exchanger immediately upstream a cooler (heater), increases the cold (hot) utility consumption, irrespective of any opposing effects.

This observation may be used to state that an element may be [+] or [–] even if it consists of opposing effects. In general, it is important to reduce the number of [±]-elements in the sign matrices as much as possible, since these elements do not indicate any specific information about the system.

5.5 The procedure

The procedure aims to combine the elements in *sign*(G^{BP}) and *sign*(G^{U}) in order to find the preferred manipulation for reduction of a control error. A manipulation that decreases the control error and at the same time decreases the utility consumption is desired. If no such manipulation exist (or it is saturated) one may be forced to use a manipulation that increases utility consumption.

As a shorthand notation in the remaining of this chapter, we will not write "*sign*" every time an individual element of a sign matrix is accessed, e.g. $g^{U}_{i,j}$ is the shorthand notation for *sign*$(G^{U})_{i,j}$.

The elements in *sign*(G^{U}) denote the effect of the manipulations (bypasses) on each of the utility exchangers. Instead of adressing each individual utility unit, we want to minimize the total utility consumption. To do this, a sign vector *sign*(g^{U}) is constructed from the *sign*(G^{U}) matrix. Each entry of the row vector *sign*(g^{U}) is simply the sum of the corresponding column of *sign*(G^{U}), i.e.

$$g^{U}_{j} = \sum_{i} g^{U}_{i,j} \tag{5.4}$$

Here, g_j^{U} is an element of the vector $sign(g^{\mathrm{U}})$ while $g_{i,j}^{\mathrm{U}}$ is an element of the matrix $sign(G^{\mathrm{U}})$. Using the conventional arithmetics for adding sign elements, $sign(g^{\mathrm{U}})$ can be found from the following rule:

$$g_j^{\mathrm{U}} = \begin{cases} [+] & \text{if } \left(g_{i,j}^{\mathrm{U}} = [+] \text{ or } g_{i,j}^{\mathrm{U}} = [0]\right) \forall i \quad \text{(at least one } [+]\text{)} \\ [-] & \text{if } \left(g_{i,j}^{\mathrm{U}} = [-] \text{ or } g_{i,j}^{\mathrm{U}} = [0]\right) \forall i \quad \text{(at least one } [-]\text{)} \\ [0] & \text{if } g_{i,j}^{\mathrm{U}} = [0] \quad \forall i \\ [\pm] & \text{otherwise} \end{cases} \tag{5.5}$$

Each element in $sign(g^{\mathrm{U}})$ is easily found from the corresponding column of $sign(G^{\mathrm{U}})$. As an example the following $sign(G^{\mathrm{U}})$ result in the vector $sign(g^{\mathrm{U}})$ written below.

$$sign(G^{\mathrm{U}}) = \begin{bmatrix} + & 0 & 0 & 0 & + & 0 \\ + & + & 0 & 0 & + & 0 \\ 0 & - & - & 0 & \pm & + \\ 0 & 0 & 0 & 0 & 0 & + \end{bmatrix}$$

$$sign(g^{\mathrm{U}}) = \begin{bmatrix} + & \pm & - & 0 & \pm & + \end{bmatrix}$$

The vector $sign(g^{\mathrm{U}})$ denotes the effect from each manipulation on the total utility consumption. Note that there are cases where physical insight may override the arithmetics. Observation 5 in last section is an example where the sum of [+] and [–] may result in [+] *or* [–] since we may conclude that one of the effects always is larger than the other. Another important example is in the calculation of $sign(g^{\mathrm{U}})$ for HENs where all outlet temperatures have targets. To fulfill the total energy balance of the HEN it can be concluded that

$$\begin{aligned} g_j^{\mathrm{U}} = [+] \quad \text{if} \quad & \left(g_{i,j}^{\mathrm{U}} = [+] \text{ or } g_{i,j}^{\mathrm{U}} = [0]\right) \quad \text{for } i \in H \quad \text{(at least one } [+]\text{)} \\ \text{or} \quad & \left(g_{i,j}^{\mathrm{U}} = [+] \text{ or } g_{i,j}^{\mathrm{U}} = [0]\right) \quad \text{for } i \in C \quad \text{(at least one } [+]\text{)} \end{aligned}$$

where H is the set of all hot process streams and C is the set of all cold process streams.

The procedure consists of the following four steps:

Step 1. Initialization.
Initialize bypasses that have increasing or zero effect on utility consumption to zero. Bypasses with decreasing effect on utility consumption is initialized to one.

$$u_j = 0 \text{ if } g_j^{\mathrm{U}} = [+] \text{ or } [0] \tag{5.5a}$$
$$u_j = 1 \text{ if } g_j^{\mathrm{U}} = [-] \tag{5.5b}$$

From step 2, start with the first bypass controlled output ($k = 1$).

Step 2. Give priority to the manipulations j from the sign matrices in the following order:

i. Bypasses that affect bypass controlled output *k* and reduce utility consumption. For each manipulation *j*, priority *i* is given if the following is fulfilled:

$$e_k^{\mathrm{BP}} \cdot g_{k,j}^{\mathrm{BP}} \cdot g_j^{\mathrm{U}} = [+] \tag{5.6}$$

ii. Bypasses that affect bypass controlled output *k* and have zero or mixed influence on utility consumption. That is, priority *ii* are given to bypasses with $g_{k,j}^{\mathrm{BP}} \neq [0]$ which are not included in priorities *i* or *iii*.

iii. Bypasses that affect bypass controlled output *k* and increase utility consumption. For each *j*, priority *iii* is given if the following is fulfilled:

$$e_k^{\mathrm{BP}} \cdot g_{k,j}^{\mathrm{BP}} \cdot g_j^{\mathrm{U}} = [-] \tag{5.7}$$

Step 3. Use heuristics to choose among equal priorities from step 2.

a) Among bypasses with the same priority, choose the one closest to the bypass controlled output.

b) Among bypasses with the same priority, disregard bypasses that may have mixed influence ([±]) on the bypass controlled output *k*.

Step 4. Increase *k* to next bypass controlled output and repeat from step 2.

The priorities given in step 2 are crucial and the result is summarized in a priority table. The following example shows in detail how the procedure is applied to the HEN in the illustration example and how the priority table is generated.

Example 5.1 *Application of the procedure to the illustrating example.*
First we define the input and output vectors of the systems in equations (5.1) and (5.2): $u = [u_{\mathrm{I}} \;\; u_{\mathrm{II}}]^T$, $y^{\mathrm{BP}} = T_{\mathrm{o}}^{\mathrm{C2}}$ and $y^{\mathrm{U}} = [Q_{\mathrm{c}} \;\; Q_{\mathrm{h}}]^T$, where Q_{c} and Q_{h} are the cooler and heater duties when $T_{\mathrm{o}}^{\mathrm{H1}}$ and $T_{\mathrm{o}}^{\mathrm{C1}}$ are perfectly controlled by the cooler and heater, respectively. Using the rules given above to find the two sign matrices for the network structure in figure 5.1 we get

$$sign(G^{\mathrm{BP}}) = [+ \;\; -] \quad \text{and} \quad sign(G^{\mathrm{U}}) = \begin{bmatrix} + & + \\ + & 0 \end{bmatrix}$$

This G^{U} gives $sign(g^{\mathrm{U}}) = [+ \;\; +]$. There is only one bypass controlled output, and the procedure gives:

Step 1. Initialize $u_{\mathrm{I}} = u_{\mathrm{II}} = 0$ since both elements in $sign(g^{\mathrm{U}})$ are [+].

Step 2. Both elements in G^{BP} satisfies $g_{1,j}^{\mathrm{BP}} \neq [0]$ so both bypasses affect the only bypass controlled output. With $k = 1$, priority *i* is given to a manipulation when the conditions in (5.6) are fulfilled and priority *iii* is given when (5.7) is fulfilled. For bypass u_{I} ($j = 1$) we get

$$e_1^{BP} \cdot g_{1,1}^{BP} \cdot g_1^{U} = e_1^{BP} \cdot [+] \cdot [+] \quad \Rightarrow \begin{cases} \text{Priority } i & \text{when } e_1^{BP} > 0 \\ \text{Priority } iii & \text{when } e_1^{BP} < 0 \end{cases}$$

and for bypass u_{II} ($j = 2$) we get

$$e_1^{BP} \cdot g_{1,2}^{BP} \cdot g_2^{U} = e_1^{BP} \cdot [-] \cdot [+] \quad \Rightarrow \begin{cases} \text{Priority } i & \text{when } e_1^{BP} < 0 \\ \text{Priority } iii & \text{when } e_1^{BP} > 0 \end{cases}$$

In this example, there are no cases where priority *ii* are given.

Step 3. No bypasses are given the same priority (for the same value of e_1^{BP}) so no heuristics are needed.

Step 4. There is only one bypass controlled output ($k = 1$), hence no repetitions can be made.

The bypass priorities found by the procedure can be summarized as: When $e_1^{BP} > 0$, use u_I as the primary manipulated input. If u_I is saturated, use u_{II} as secondary input. When $e_1^{BP} < 0$, use u_{II} as the primary input. If u_{II} is saturated, use u_I as secondary input. From the given bypass priorities (*which* bypass to adjust) and the values in $sign(G^{BP})$ (*how* to adjust), we can now construct a priority table for the bypass manipulations:

	Primary manipulation	Secondary manipulation
$e_1^{BP} > 0$	Reduce u_I ($u_I \downarrow$)	Increase u_{II} ($u_{II} \uparrow$)
$e_1^{BP} < 0$	Reduce u_{II} ($u_{II} \downarrow$)	Increase u_I ($u_I \uparrow$)

Table 5.2 Priority table for example.

The control structure suggested by this priority table is identical to the one used in the illustration example. This control strategy will be the same for all networks with this structure, and it will "automatically" find the bypass fractions that give minimum utility consumption together with meeting the target demands at steady state (provided that the HEN is feasible and the SISO-controllers do not give any steady state control error). ■

To construct the sign matrices for networks that include loops, inner matches (process/process heat exchangers with downstream process/process exchangers on both sides) as well as split manipulations, some additional observations for HENs are given in Mathisen *et al.* (1994). These are mainly derived from the four observations given above and may be used to convert some [±] elements in the sign matrices to [+] or [–].

5.6 Parallels to split-range control

The control structure found for the illustrating example in this chapter is very similar to split-range control which is a commonly used control configuration. Figure 5.4 shows a typical

example which is taken from Loe (1993). The process is a utility system with three steam pressure levels. Each level may have several suppliers and consumers (not shown) with varying demands. The objective is to control the pressure of the MP-steam by supplying HP-steam (using u_2) to increase the pressure, or by delivering steam to the LP-level (using u_1). This is obtained using a pressure transmitter (PT) and a pressure controller (PC) for control of the two valves. The signal from the controller is splitted such that both valves are fully closed when the signal is 50%. Valve u_2 opens when the control signal exceeds 50%, and valve u_1 opens when the control signal is leass than 50% (see figure 5.4b which shows the valve positions as a function of the control signal). This is an example of split-range control, and it allows two actuator devices to be controlled by one single controller.

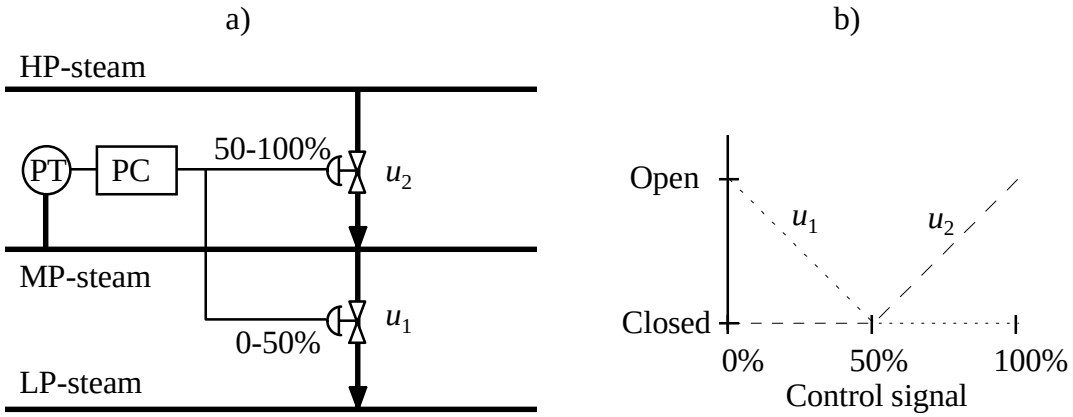

Figure 5.4 Example of split-range control for a steam supply system.

In practice, spilt-range control may be implemented without the use of any swithes: Assume that the physical control signal is electrical current in the range 4 – 20 mA which is supplied to both valves. Scaling valve u_2 to be open at 4 mA and closed at 12 mA, and valve u_1 to be closed at 12 mA and open at 20 mA, the split-range control will work. A perhaps more updated implementation is to perform the scaling in the process control system (software) and to use two separate control signals (individually scaled from 0 – 100 %) in the field.

The control strategy in figure 5.4 is in fact identical to the control strategy in the illustrating example of the HEN in figure 5.1. Instead of implementing the control sceme using two controllers and then switch between them, it is simpler to use only one controller to control the bypasses u_{I} and u_{II} in a split-range configuration as in figure 5.4b. Note that if we in the problem in figure 5.4 want to minimize the (energy) flow from high pressure to low pressure steam, not only the control strategies are similar to each other, in fact, the two problems are completely analogous.

In other applications where split-range is used, the range of each control device may partly or fully overlap. One may question if “split-range” is the correct term when the ranges overlap completely, though.

Using split-range control, the controller parameters when the different valves are active, may be different from each other. Concerning the controller gain, this may be solved by selecting proper settings/scalings for the valves. As an example, assume that for “good” control of the HEN in figure 5.1 it has been found that the gain when using u_{I} is three times the gain when

using u_{II}. Then, if u_{II} is active in the range 0 – 75% and u_I is active from 75 to 100%, there will be no large discontinuities of the process gain when switching between the two bypass valves.

As it has been clear from this section, the method for optimal operation based on structural information often leads to a control strategy that may easily be implemented using split-range control. In fact, one may think of the method as a systematic way to find an optimal split-range control structure. In section 5.8, an example will demonstrate the method and the split-range implementation when a controller may utilize more than two bypasses. In that example, it is not trivial to find the strategy for optimal operation without using a systematic method.

5.7 How to handle multiple bypass controlled outputs

Until now, the method has only been applied to a simple example with only one bypass controlled target. If there are several bypass controlled targets, the following situation will typically occur during operation: Assume that a bypass saturates and thus a new has to be assigned for control of a given outlet temperature. What if the new bypass for this control purpose already is occupied controlling an other outlet temperature? It is clear that a new candidate bypass has to be selected since one bypass cannot control two outlet temperatures independently. However, it is not clear how to select a new bypass, or how the two outlet temperatures and the two bypasses should be paired.

To address this problem when there are several bypass controlled outputs, the following approaches may be considered:

1. All possible pairings may be listed in a prioritized order, and when one bypass is preferred for two different bypass controlled outputs, then find the second best bypass for both outputs (from the priority table), and choose the combination and pairing that gives highest total priority.
2. Minimize switching of pairings. That is, if the selected bypass for one output is occupied, do not change the existing pairing but switch to the next manipulations for the output that needs a new manipulation.
3. When a manipulation saturates, and a new needs to be assigned, the pairing problem is solved simultaneously to find the combination that maximizes the total priority.

Here, it will be focused on the third option – partly because it is expected to give the best results since all manipulations are considered simultaneously and partly because it is very similar to the method proposed in the next chapter. In section 5.5, the following rules were found:

Priority *i*:		$e_k^{BP} \cdot g_{k,j}^{BP} \cdot g_j^U = [+]$
Priority *ii*:	With $g_{k,j}^{BP} \neq [0]$,	$e_k^{BP} \cdot g_{k,j}^{BP} \cdot g_j^U = [0]$ or $[\pm]$
Priority *iii*:		$e_k^{BP} \cdot g_{k,j}^{BP} \cdot g_j^U = [-]$

Recall that k is index for bypass controlled outputs and j is index for the manipulations. All information from these expressions can be stored in a new sign *priority* matrix P given by

$$sign(P)_{i,j} = \begin{cases} e_k^{\mathrm{BP}} \cdot g_{k,j}^{\mathrm{BP}} \cdot g_j^{\mathrm{U}} & \text{if } g_{k,j}^{\mathrm{BP}} \neq 0 \\ [\times] & \text{if } g_{k,j}^{\mathrm{BP}} = 0 \end{cases} \tag{5.8}$$

The new symbol [×] in this sign matrix denotes a forbidden pairing since the corresponding manipulation does not affect the specific bypass controlled output. While sign(G^{BP}) and sign(g^{U}) are constant, the sign of the control error sign(e^{BP}) changes during operation, hence the sign matrix sign(P) will change during operation. When a change in the sign of the control error is detected, sign(P) will change, and new control configurations should be evaluated. This is done automatically by first assigning numerical values to the priority matrix P according to the following rules:

$$\begin{array}{lll} p_{k,j} = -1 & \text{if } \mathrm{sign}(P)_{k,j} = [+] & (\text{priority } i) \\ p_{k,j} = \ \ 0 & \text{if } \mathrm{sign}(P)_{k,j} = [0] \text{ or } [\pm] & (\text{priority } ii) \\ p_{k,j} = \ \ 1 & \text{if } \mathrm{sign}(P)_{k,j} = [-] & (\text{priority } iii) \end{array} \tag{5.9}$$

Now, the task is to select pairings that minimizes the *total* utility consumption, i.e. the objective function to be minimized is $\sum p_{k,j}$ for the selected pairings. Pairings are chosen such that there is one manipulation for each bypass controlled output, and no manipulations control more than one output. In addition, constraints that prevent forbidden pairings and selection of manipulations that are saturated must be included. As an example consider a system with 2 bypass controlled outputs and 3 manipulations, and the priority matrix at one instant during operation is

$$P = \begin{bmatrix} \textcircled{-1} & 0 & \times \\ -1 & \textcircled{-1} & +1 \end{bmatrix}$$

Pairing input 3 with output 1 is forbidden. Assuming that none of the manipulations are saturated, it is preferred to pair input 1 with output 1 and input 2 with output 2, as indicated.

The presentation concerning how multiple bypass controlled outputs can be handled is made very brief in this section. The reason for this is that the method proposed in the next chapter handles multiple bypass controlled outputs in a similar way. In that chapter, the explanations are more thorough and the method may easily be applied to sign matrices as well. For this reason, multiple bypass controlled outputs are not considered any further in this chapter.

5.8 Example

Finally in this chapter, the procedure is applied to an example. The HEN in the example has one bypass controlled outlet temperature.

Consider the stream data in table 5.3 and the design in figure 5.5. From the stream data we see that there are two disturbances; ±20°C in $T_{\mathrm{s}}^{\mathrm{H2}}$, and ±7.5 kW/°C in CP^{C1}. The nominal design in figure 5.5 is based on a design (before retrofit) in Kotjabasakis and Linnhoff (1986),

but modified since T_o^{H2} here is a free outlet temperature. Also, note that the disturbances and the problem statement here are different from the problem discussed by Kotjabasakis and Linnhoff (1986). Assume that the nominal design for control purposes already has been modified by increasing the area of exchanger III and that bypass has been installed across this exchanger so that each of the two disturbances can be rejected completely (one at a time). Added area and bypass on the last heat exchanger is in accordance with common engineering practice, and we will refer to this as case A.

Stream	T_s [°C]	T_t [°C]	CP [kW/°C]
H1	300	80	30
H2	200±20	X	45
C1	40	180	40±7.5
C2	140	240	60

Table 5.3 Stream data for example.

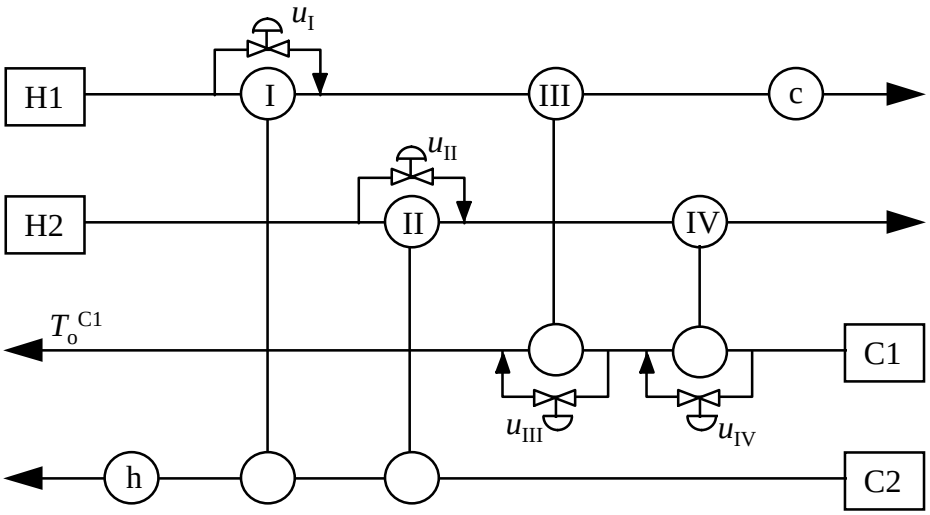

Figure 5.5 Network in example.

We will apply the procedure to this network (including the extra area already installed on exchanger 3) and show that the utility consumption is reduced. This case is denoted B. Remember that bypasses now can be placed across all four process/process heat exchangers. Each bypass is placed on that side of the heat exchanger which is closest to the bypass controlled output. This is to improve controllability, and it will not influence the steady state performance. Defining $u = [u_I\ u_{II}\ u_{III}\ u_{IV}]^T$, $y^{BP} = T_o^{C1}$, $y^U = [Q_c\ \ Q_h]^T$ and $e = T_o^{C1} - T_t^{C1}$ gives the sign matrices:

$$sign(G^{BP}) = \begin{bmatrix} + & \pm & - & - \end{bmatrix} \quad \text{and} \quad sign(G^U) = \begin{bmatrix} + & \pm & + & - \\ + & + & 0 & 0 \end{bmatrix}$$

From $sign(G^U)$, we obtain $sign(g^U) = [+ \ \pm \ + \ -]$, and the procedure yields:

Step 1. From $sign(G^U)$ it is clear that $u_I = u_{III} = 0$ during initialization. Inspecting the network, we assume that the plus in column 2 will dominate the possible negative effect from the $[\pm]$ element so we also set $u_{II} = 0$. u_{IV} reduces the utility consumption and is therefore initialized to one.

Step 2. $e > 0$ gives priority *i* to u_I and u_{IV}, and priority *iii* to u_{III}. $e < 0$ gives priority *i* to u_{III} and priority *iii* to u_I and u_{IV}. Priority ii) is given to u_{II}.

Step 3. To distinguish between u_I and u_{IV}, both have to travel through one exchanger to reach T_o^{C1} but we prefer u_{IV} since it bypasses a larger heat exchanger and therefore probably has larger influence on T_o^{C1}.

Step 4. Not applicable.

When constructing the priority table from the results in step 2 and step 3, the following considerations are made:

- Bypass u_{II} has a mixed influence on T_o^{C1}. Thus, it can not be concluded (from structural information) whether we shall decrease or increase this bypass to counteract a control error. Inspecting the network structure, it is reasonable to assume that u_{II} have little influence on T_o^{C1} since both hot and cold outlet from heat exchanger II traverses two heat exchanger before affecting T_o^{C1}. For simplicity, we totally disregard bypass u_{II} in the control structure.
- With the bypass fractions initialized according to step 1, it is reasonable to assume that T_o^{C1} is too small. The preferred choice for control is to reduce bypass u_{IV}. If u_{IV} should saturate at zero, u_I has to be opened. However, when T_o^{C1} is too high and u_I is opened, we prefer to reset u_I to zero before u_{IV} is used.

The priority table with these considerations is shown in the table below. Note that the "primary", "secondary" and "third" manipulation is not the same as priorities *i*, *ii* and *iii*. Also, preferring u_I before u_{IV} when *e* is positive is not a violation of the priorities given in step 3, but it ensures that u_I returns to zero after it has been opened.

	Primary manipulation	Secondary manipulation	Third manipulation
$e > 0$	$u_I \downarrow$	$u_{IV} \uparrow$	$u_{III} \uparrow$
$e < 0$	$u_{III} \downarrow$	$u_{IV} \downarrow$	$u_I \uparrow$

Table 5.3 Priority table for example.

Figure 5.6 shows the results when simple PI-controllers are used for both case A (traditional engineering approach) and case B ("sign"-method). From figure 5.6c, it is clear that the sign-method results in considerably reduced utility consumption (thick line), compared to the traditional engineering approach (thin line). For nominal disturbances, (4 to 6 hours on the time axis) the utility reduction is close to 0.9 MW at steady state.

Using the sign-method (case B), the controlled HEN has become more flexible (*effective* flexibility has improved) since it is able to compensate for both disturbances occurring at the same time in their worst case combination (8 to 10 hours). In this period, case A has the lowest utility consumption but target temperatures are not met, see figure 5.6b. Thus, the primary goal of optimal operation is not satisfied.

Note that case B does not utilize u_{III} for any of the disturbances in this example. From figure 5.6b, it is clear that the sign-method may result in deteriorated dynamic behavior.

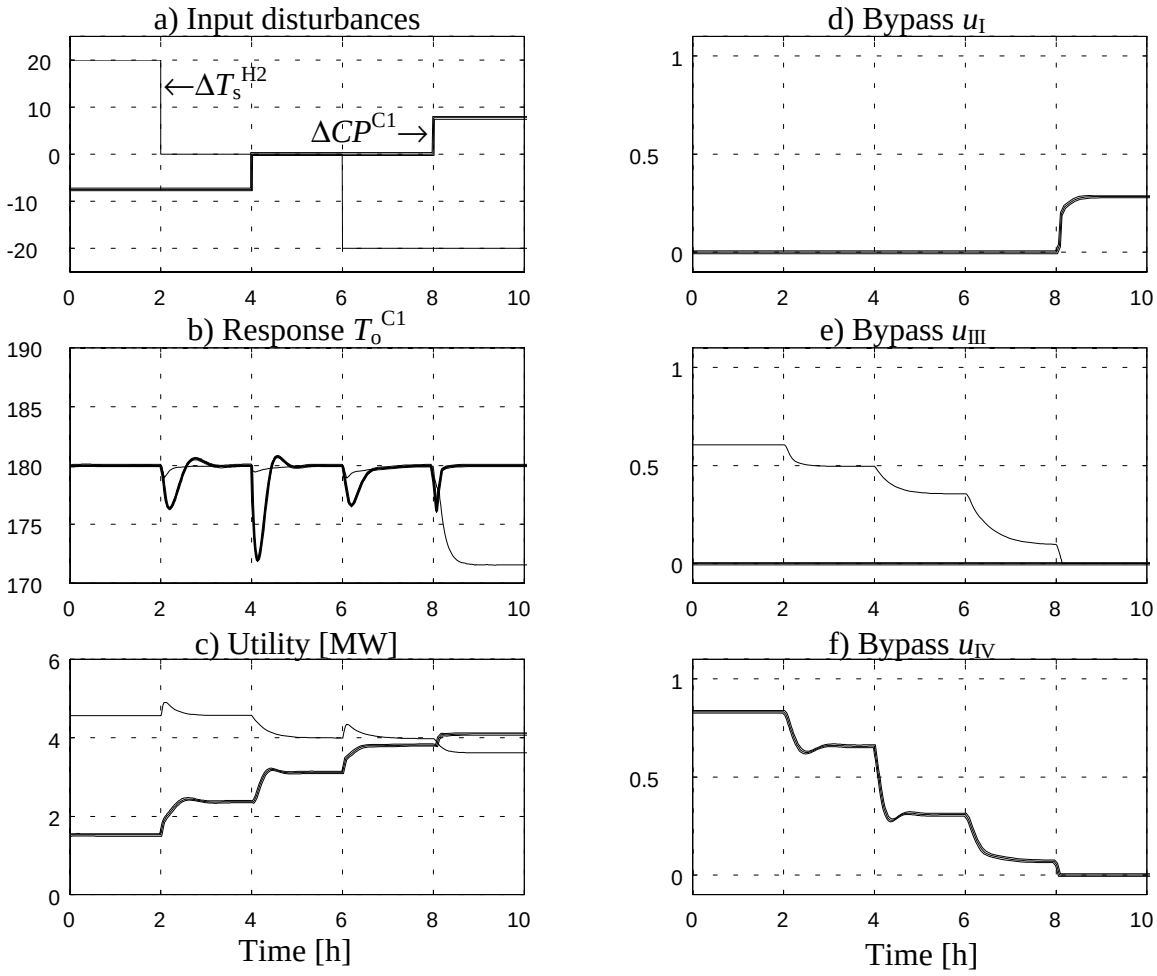

Figure 5.6 Closed loop simulation results. (a) Deviation from nominal disturbance inputs, T_s^{H2} (thin line) and CP^{C1} (thick line). (b) Response in T_o^{C1}, case A (thin) and case B (thick). (c) Utility consumption, case A (thin) and case B (thick). (d), (e) and (f) Bypasses u_I, u_{III} and u_{IV}, case A (thin, (e) only) and cases B (thick).

Finally in this example section, the split-range implementation for this example is discussed. Figure 5.7a shows graphically how the three bypasses open and close in a similar way as in figure 5.4, however, split points are not located correctly.

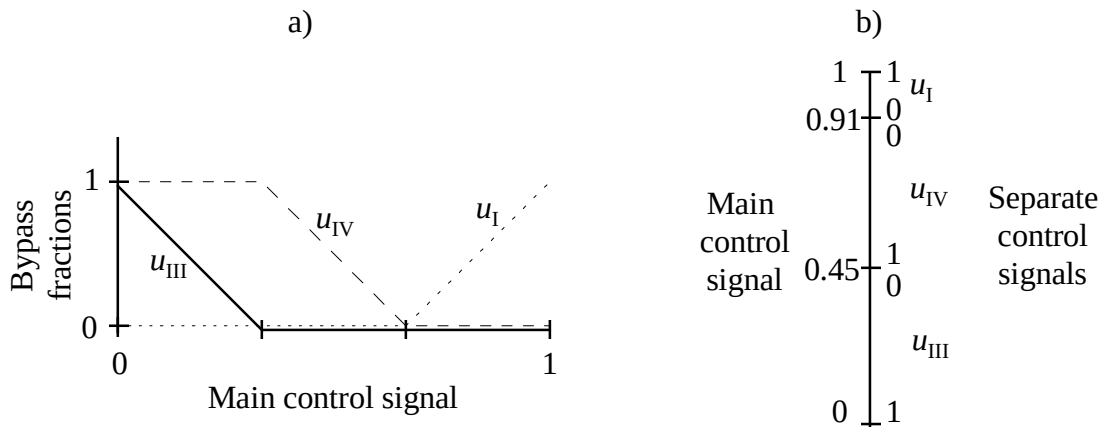

Figure 5.7 Two representations of the split-range implementation.

Figure 5.7b (to the right) shows the same, with the main control signal to the left of the vertical line and the control signal to the separate manipulations to the right. In this figure, the split points (0.45 and 0.91) are shown approximately at their correct positions. The split points were found as follows: First, the parameters of the three separate controllers were found separately such that satisfying results were obtained. Then, the gain of the three controllers were used to compute the split points together with the total gain, such that when using only one controller, the gain is the same as when switching between the separate controllers. The integral time constants were interpolated between the values found for the separate controllers. This interpolation was performed in a range close to each split point, and only on the side with the shortest integral time for the separate controller. The simulations are carried out using only one control algorithm and by splitting the output signal according to figure 5.7b. See also figure 3.6 where the controller (denoted “escreg4d”) is shown in the upper left part.

5.9 Conclusions

In this chapter, a method for optimal operation based on structural information has been discussed. The method has been derived for operation of HENs, but may be applied to other parts of the process as well. Applying the procedure, feasible manipulations for control are given one of three possible priorities:

i. Manipulations that decrease utility consumption while decreasing the control error.

ii. Manipulations with zero or mixed effect on utility consumption.

iii. Manipulations that increase utility consumption while decreasing the control error.

From these three categories, a priority table for the manipulations is constructed and this table dictates the control structure. The control structure may change during operation, however, in many cases it simply corresponds to split-range control.

While it is clear that manipulations with priority *i* is better than manipulations with priority *iii*, no clear conclusions can be drawn for those manipulations priority *ii* with mixed effects [±]. Manipulations with mixed effects may reduce utility consumption more than some manipulations with priority *i*, or they may increase utility consumption more than some

manipulations with priority *ii*. Hence the procedure will not always guarantee that the utility consumption is minimized at steady state. Heuristic rules based on controllability considerations are used to choose among manipulations with the same priority. While these rules may result in selecting a manipulation which is not optimal from a steady state utility consumption point of view, they will usually result in the control structure with best dynamic performance among manipulations of equal priority.

Using structural information only, there may be cases where the available information is not sufficient to distinguish quantitatively between different effects. However, even in cases where the method does not guarantee optimal solution in all situations, it may still result in optimal or near optimal operation. Despite the disadvantage of not guaranteeing globally optimal operation in all cases, the method also has some of nice features:

- The method requires very little information about the process to be operated. In fact, the procedure is easily carried out by hand, and no quantitative information is needed.
- The method results in a decentralized control structure with variable pairing. As it has been shown, the control configuration can usually be implemented as split-range control. The control strategy can be included in today's control systems.
- Optimal operation can often be achieved without any quantitative process model or any numerical optimizations.

Since the method only guarantees optimal operation in a few cases, and since it may result in poor dynamic performance, it is advisable to combine it with dynamic simulations and verify several possible options. Alternatively, the methods proposed in the two next chapters may be evaluated.

Notation

e Control error.
g Element in transfer matrix.
G Transfer matrix.
CP Heat capacity flowrate.
P Priority matrix.
Q Heat load (duty) of heat exchanger.
T Temperature
u Manipulated input (bypass fraction).

Superscripts:
BP Bypass.
U Utility.

Subscripts:
i Index for utility controlled outputs.
j Index for manipulated inputs.
k Index for bypass controlled outputs.
o Actual output or outlet (temperature).
s Supply (temperature).
t Target or reference (temperature).

References

Calandranis, J and G. Stephanopoulos (1988). A Structural Approach to the Design of Control Systems in Heat Exchanger Networks. *Comput. Chem. Eng*., ***12***.

Glemmestad, B., K.W. Mathisen and T. Gundersen (1996). Optimal Operation of Heat Exchanger Networks based on Structural Information. *Comput. Chem Engng.*, **20** Suppl. B, 823-828.

Kotjabasakis, E and B. Linnhoff (1986). Sensitivity Tables or the Design of Flexible Processes. How much Contingency in Heat Exchanger Networks is Cost-Effective. *Chem. Eng. Res*., ***64***, 199-211.

Loe, I (1993). System Structures in the Process Industry. *Lecture Notes* (in Norwegian). Telemark Institute of Technology, Porgsrunn, Norway.

Marselle D.F., M. Morari and D.F. Rudd (1982). Design of Resilient Processing Plants - II. Design and Control of Energy Management Systems. *Chem. Eng. Sci*., ***37***, 259-270.

Mathisen, K.W., S. Skogestad and E.A. Wolff (1992). Bypass Selection for Control of Heat Exchanger Networks. *Paper presented at ESCAPE-1*, Elsinore, Denmark.

Mathisen, K.W. (1994). Integrated Design and Control of Heat Exchanger Networks. *Thesis*. (Trondheim University - NTH, Norway).

Mathisen, K.W., M. Morari and S. Skogestad (1994). Optimal Operation of Heat Exchanger Networks. *Presented at Process Systems Engineering* (PSE'94), Kyongju, Korea.

Papalexandri, K.P. and E.N. Pistikopoulos (1994a). Synthesis and Retrofit Design of Operable Heat Exchanger Networks. 1. Flexibility and Structural Controllability Aspects. *Ind. Eng. Chem. Res*., ***33***, No. 7.

Papalexandri, K.P. and E.N. Pistikopoulos (1994b). Synthesis and Retrofit Design of Operable Heat Exchanger Networks. 2. Dynamics and Control Structure Considerations. *Ind. Eng. Chem. Res*., ***33***, No. 7.

Chapter 6

A PARAMETRIC APPROACH TO OPTIMAL OPERATION OF HENs

The approach for optimal operation of HENs presented in this chapter is heavily inspired by the sign method in the previous chapter. However, instead of using only structural properties, *parametric* information in terms of linear steady state transfer matrices is utilized. The control configuration (pairing of manipulations and measurements) that minimizes utility cost is found from solving an integer programming problem during operation. As for the sign method described in the previous chapter, this parametric approach results in a decentralized control structure that may have variable pairing. The approach actually comprises three methods that differ from each other in the way controllability considerations are handled.

6.1 Introduction

The same problem as in the previous chapter is considered. That is, we want to develop a method for optimal operation of a given HEN. Decentralized control is used and the goal is to find an answer to the question: "*Which pairing reduces control error and minimizes utility cost at the same time?*" At steady state, the solution should give no control error and minimum utility cost. The information about the HEN is given by the transfer matrices G^{BP} and G^{U} introduced in the previous chapter. Recall that y^{BP} are the bypass controlled *temperatures*, while y^{U} are the *duties* of the utility exchangers assuming perfect control of the utility controlled temperatures.

$$y^{BP} = G^{BP}u \tag{6.1}$$

$$y^{U} = G^{U}u \tag{6.2}$$

In the previous chapter, the row vector g^{U} was introduced to denote the effect from each manipulation on the total utility consumption. The corresponding vector introduced in this chapter denotes the effect from each manipulation on the total utility *cost*. It is denoted $g^{\mathrm{U\$}}$ to indicate that it gives the cost rather than energy consumption. $g^{\mathrm{U\$}}$ is given by

$$g^{\mathrm{U\$}} = c^T G^{\mathrm{U}} \tag{6.3}$$

where c is a vector containing the utility cost for each utility exchanger. As opposed to the previous chapter where only sign matrices where utilized, we will in this section use the steady state gains of the transfer matrices to find the optimal control configuration. The method may be regarded as a "quantified" version of the sign method. The motivating example is presented in order to give a brief introduction to the idea.

Motivating example

The example uses the same HEN as in the illustrating example in section 5.2 (figure 5.1). The two following linear systems have been found from small (and positive) perturbations around the nominal operating point $u_{\mathrm{A}} = u_{\mathrm{B}} = 0$.

$$T_{\mathrm{o}}^{\mathrm{C2}} = \underbrace{\begin{bmatrix} 6.57 & -13.7 \end{bmatrix}}_{G^{\mathrm{BP}}} \begin{bmatrix} u_{\mathrm{A}} \\ u_{\mathrm{B}} \end{bmatrix} \tag{6.4}$$

$$\begin{bmatrix} Q_{\mathrm{c}} \\ Q_{\mathrm{h}} \end{bmatrix} = \underbrace{\begin{bmatrix} 4.49 & 6.87 \\ 7.76 & 0 \end{bmatrix}}_{G^{\mathrm{U}}} \begin{bmatrix} u_{\mathrm{A}} \\ u_{\mathrm{B}} \end{bmatrix} \tag{6.5}$$

Here, the bypass fractions are scaled from 0 to 1, the dimension of $T_{\mathrm{o}}^{\mathrm{C2}}$ is °C and the cooler and heater duties are in kW. Given a steam cost of 0.05 \$/kWh and cooling water cost of 0.01 \$/kWh, the cost vector is $c^T = [0.01\ 0.05]$. This yields

$$g^{\mathrm{U\$}} = c^T G^{\mathrm{U}} = \begin{bmatrix} 0.01 & 0.05 \end{bmatrix} \begin{bmatrix} 4.49 & 6.87 \\ 7.76 & 0 \end{bmatrix} = \begin{bmatrix} 0.433 & 0.069 \end{bmatrix} \tag{6.6}$$

That is, increasing u_{A} by one unit increases utility cost by 0.433 \$/h, and increasing u_{B} by one unit increases utility cost by 0.069 \$/h.

Dividing the elements in $g^{\mathrm{U\$}}$ by the elements in G^{BP} yields

$$\frac{g_1^{\mathrm{U\$}}}{g_{1,1}^{\mathrm{BP}}} = \frac{0.433}{6.57} = 0.066 \qquad \text{(Increasing } T_{\mathrm{o}}^{\mathrm{C2}} \text{ by 1°C } \textit{costs} \text{ 0.066 \$/h when } u_{\mathrm{A}} \text{ is used.)}$$

$$\frac{g_2^{\mathrm{U\$}}}{g_{1,2}^{\mathrm{BP}}} = \frac{0.069}{-13.7} = -0.005 \qquad \text{(Increasing } T_{\mathrm{o}}^{\mathrm{C2}} \text{ by 1°C } \textit{saves} \text{ 0.005 \$/h when } u_{\mathrm{B}} \text{ is used.)}$$

However, instead of *increasing* the bypass controlled temperature, the cost to bring it back to its target value is more interesting. Introducing the control error $e = T_{\mathrm{o}}^{\mathrm{C2}} - T_{\mathrm{t}}^{\mathrm{C2}}$, we can define a "priority matrix" P:

$$P = \left[-\frac{g_1^{\mathrm{U\$}}}{g_{1,1}^{\mathrm{BP}}} e \quad -\frac{g_2^{\mathrm{U\$}}}{g_{1,2}^{\mathrm{BP}}} e \right] = \left[-0.066e \quad 0.005e \right]$$

That is, if $e = 1$, it *saves* 0.066 \$/h to reach the target using u_A, while it would *cost* 0.005 \$/h if u_B is used. In general, P consists of as many rows as there are bypass controlled temperatures and as many columns as there are inputs that may be manipulated (here: bypasses). To minimize utility cost, the pairing is chosen such that the sum of the corresponding elements in P becomes as small as possible. In this case, the optimal pairing is easily found by hand. Assuming that $e = 1$, using u_A seem to be optimal choice. However, $g_1^{\mathrm{BP}} e > 0$ and this implies that u_A has to be decreased in order to reduce the control error. If we assume that $u_A = u_B = 0$, it is not possible to reduce e using u_A and we have to pair u_B and T_o^{C2}. The same result is found in the illustrating example in previous chapter (section 5.2). Here, however, the effects have been quantified. ■

Each time a control error changes sign or a new manipulation saturates, the procedure to find optimal pairing should be repeated. Also, the linear transfer matrices may be different in different operating regimes, and there may be a need to update the model in addition to the pairing. There is a need for a general model that enables automation of the procedure to find the pairing that optimizes utility cost.

In the next section, the integer programming formulation to find the pairing that minimizes utility cost is presented (model A). In that model, no dynamic considerations are made, and section 6.3 explains how control aspects may be included in the model. In section 6.4, model A is extended into a hierarchical strategy for operation that includes a simple controllability requirement (model B). Section 6.5 extends the model further into a MILP formulation (model C), which includes a slightly more complex controllability consideration. Before the chapter concludes, some examples to demonstrate the parametric approach are presented.

6.2 A model to find optimal pairing (model A)

The model for obtaining the optimal control configuration is based on the information contained in G^{BP} and G^{U}. These may be found from perturbation of a steady state model of the HEN. The vector $g^{\mathrm{U\$}}$ is obtained from G^{U} and utility cost data according to equation (6.3). Each element in the priority matrix P is given by

$$p_{i,j} = -\frac{g_j^{\mathrm{U\$}}}{g_{i,j}^{\mathrm{BP}}} e_i \tag{6.7}$$

where e_i is the control error of bypass controlled output i. Each entry of the priority matrix denotes the total utility cost (money per time unit) after control error i has been removed using manipulation j. When $g_{i,j}^{\mathrm{BP}}$ is small the corresponding value of $p_{i,j}$ is a large (positive or negative) number. A large negative $p_{i,j}$ may seem to be a good choice, however, this also indicate that the manipulation has a small effect on the output. A value of $p_{i,j}$ of infinity ($\pm\infty$) simply means that $g_{i,j}^{\mathrm{BP}}$ is zero and this pairing can not be used for control at all. To prevent such pairings, an element in P can be denoted [×] to indicate that the corresponding

element in G^{BP} is zero. In the actual implementation given by equation (6.13), the "×-values" in P can be given any numerical value since constraint (6.13f) prevents these pairings from being considered.

Note the similarity and difference from the definitions of P in equation (6.7) and equation (5.8). The definition in chapter 5 is applicable for sign matrices only, thus it does not matter whether we multiply or divide. In order to get the correct numerical value in equation (6.7), *division* by the elements of G^{BP} is required, while for sign matrices, multiplication is sufficient to get the correct sign.

The pairing that results in minimum total utility cost according to P should be selected. The total utility cost is found simply by adding elements in P corresponding to the selected pairing. In order to do this automatically, some variables and constants with logical (binary) elements are introduced. First, the variable matrix X with the same dimension as P is defined as

$$x_{i,j} = \begin{cases} 1 & \text{if } p_{i,j} \text{ is a selected pairing.} \\ 0 & \text{otherwise.} \end{cases} \tag{6.8}$$

A value of X corresponds to a given pairing, and we seek the optimal value of this variable. In addition, the following constant binary vectors/matrices are needed:

$$g^0_{i,j} = \begin{cases} 1 & \text{if } g^{BP}_{i,j} = 0 \\ 0 & \text{otherwise.} \end{cases} \tag{6.9}$$

$$y_{i,j} = \begin{cases} 1 & \text{if } g^{BP}_{i,j} e_i > 0 \text{ (which implies } u_j \downarrow \text{ to reduce } e_i\text{).} \\ 0 & \text{otherwise (which implies } u_j \uparrow \text{ to reduce } e_i\text{).} \end{cases} \tag{6.10}$$

$$z^{lo}_j = \begin{cases} 1 & \text{if } u_j \text{ is saturated at lower bound.} \\ 0 & \text{otherwise.} \end{cases} \tag{6.11}$$

$$z^{up}_j = \begin{cases} 1 & \text{if } u_j \text{ is saturated at upper bound.} \\ 0 & \text{otherwise.} \end{cases} \tag{6.12}$$

The values of these vectors/matrices may change during operation. For example, the values in y are dependent on the sign of the control error which will change. Further, which manipulations that are saturated (z^{lo} and z^{up}) can change. The values of y, z^{lo} and z^{up} are based on information from the DCS (Distributed Control System) in the plant. This information is updated immediately before each optimization to find a new pairing. Even if these vectors/matrices may change during operation, they are not subject to any changes by the optimization procedure. Hence, they are regarded as *constants* in the model to be optimized. The optimal pairing is found from the formulation given by the equations (6.13a) to (6.13f). Note that the model is a pure integer programming problem. The formulation is linear in the variables, thus it is denoted an Integer Linear Programming (ILP) problem.

$$X = \arg\min_{X} \sum_{i} \sum_{j} x_{i,j}\, p_{i,j} \qquad \text{Find pairing } X \text{ that minimizes utility consumption.} \qquad (6.13a)$$

subject to

$$\sum_{j} x_{i,j} = 1 \quad \forall i \qquad \text{One bypass pr. bypass controlled temperature.} \qquad (6.13b)$$

$$\sum_{i} x_{i,j} \le 1 \quad \forall j \qquad \text{Each bypass can not control more than one output.} \qquad (6.13c)$$

$$x_{i,j} + y_{i,j} + z_j^{\text{lo}} \le 2 \quad \forall i,j \qquad \text{Reject pairing that requires } u\downarrow \text{ when } u = 0. \qquad (6.13d)$$

$$x_{i,j} - y_{i,j} + z_j^{\text{up}} \le 1 \quad \forall i,j \qquad \text{Reject pairing that requires } u\uparrow \text{ when } u = 1. \qquad (6.13e)$$

$$x_{i,j} + g_{i,j}^{0} \le 1 \quad \forall i,j \qquad \text{Reject pairing if } g_{i,j}^{\text{BP}} = 0\,. \qquad (6.13f)$$

The objective function (equation 6.13a) is the pairing that minimizes total utility cost, i.e. the sum of $p_{i,j}$ (cost to restore a control error) for the selected pairing ($x_{i,j} = 1$). The purpose of the different constraints are explained in each of the equations (6.13b) to (6.13f). As an example, constraint (6.13d) forbids pairings that require a bypass decrease if it is already zero. If a pairing requires the manipulation to be decreased in order to reduce control error ($y_{i,j} = 1$) *and* that manipulation is saturated at lower bound ($z_j^{\text{lo}} = 1$), then equation (6.13d) forces $x_{i,j}$ to be zero (pairing is forbidden). Otherwise, $x_{i,j}$ is free to take any value (0 or 1). The equations (6.13a) to (6.13f) are referred to as "model A" in the subsequent.

If, for a given operating state, there is no pairing that reduces the control error, model A will not produce any feasible solution. In practice, it is important to know what to do if this should happen. One possibility is to keep the existing pairing and accept the control error, alternatively the plant could be switched into a predefined (and safe) control configuration. In the subsequent it is assumed that model A contains feasible solutions. It is emphasized that in practice, it is important to consider the consequences and remedies if no feasible solution exists.

The complete control algorithm can be summarized by the four following points:

1. Let SISO-controllers regulate bypass controlled output temperatures according to the last pairing that has been found. While this control configuration is active, check steps 2 and 3 continuously (or with frequent time intervals).
2. If the operating point has exceeded some limits or some timer has elapsed, update linear steady state model (G^{BP} and $g^{\text{U\$}}$).
3. Optimize model A to find a new pairing if

   a) a new bypass has saturated, or
   b) a control error has changed sign, or
   c) the model just has been updated.

   An alternative to the points a, b and c is to optimize model A at regular time intervals.
4. Repeat from step 1.

Note that the criterion for selecting pairing according to equation (6.13) is completely different from what is normally done for regulatory control. For regulatory control, the pairing is selected to achieve good dynamic behavior of the closed-loop system (operating cost is not considered), while the method presented above selects a pairing purely for utility cost minimization. Dynamic behavior has not yet been considered. It is clear that neglecting dynamics can result in undesired control configurations, e.g. the closed-loop system (or parts of it) may become unstable if a control loop becomes inactive due to saturation or is switched to manual operating mode. How to implement controllability issues is the topic of the next section. The remaining part of this section will draw some parallels to the sign method in the previous chapter.

In section 5.7, multiple bypass controlled outputs were briefly discussed for the sign method. Numerical values were assigned to the P matrix in equation (4.9), however, for the simple example in equation (5.10), constraints due to saturation (equations 6.13d and 6.13e) were not included. With the numerical values in P of –1, 0 and 1 (priority *i*, *ii* and *iii*), the model in equation (6.13) can be applied for the sign method when there are several bypass controlled temperatures. Hence, the possible pairings are evaluated in a simultaneous manner. The operability heuristics in step three of the sign method were used to distinguish between pairings of equal priority. This can be implemented in the automatic approach by penalizing the objective. The first heuristic rule may be implemented by increasing an element in P by e.g. 0.01 per exchanger the corresponding manipulation traverses before it affects the output. When implementing the sign method in this manner, however, it may not always be possible to use the priority table to find a simple split-range implementation of the control configuration.

6.3 How to implement controllability considerations

Model A (equations 6.13a to 6.13f) only considers operating cost. When the control configuration is selected with no regard to the dynamic properties, the closed-loop dynamic performance may be poor. This section describes how controllability aspects can be included. It is assumed that the only available information about the process is the two transfer matrices G^{BP} and G^{U} (at steady state) together with cost data for the utilities. That is, no explicit dynamic information is available.

The following two controllability requirements will be considered:

1. The plant (HEN) should remain stable when one or more control loops become inactive.
2. Among pairings with similar steady state properties, select the one with the best closed-loop performance

Requirement one is treated first, while the second is treated at the end of the section. A control loop becomes inactive if the input signal saturates. When saturation occurs, model A should be optimized and a new pairing should be found. Until the new pairing is active it is desired that the present closed-loop system is stable. A control loop may also become inactive if the controller is switched to a different operating mode (perhaps deliberately), e.g.

"tracking mode" where the control signal to the actuator is simply given a fixed value. Also, the controller may be switched to manual mode, and then the control loop is inactive if no operator actions are taken. (The loop is of course not inactive when it is operated manually; then the operator is part of the feedback loop). In cases when one or more control loops are inactive, it is highly desirable that the plant remains stable. Otherwise, plant hazard or severe product quality problems may be the result. To ensure stability, we will require that the plant is *decentralized integral controllable* (DIC). Decentralized integral controllability was introduced by Skogestad and Morari (1988), and the following definition is taken from Skogestad and Postlethwaite (1996):

Definition 6.1. *Decentralized integral controllability* (DIC).
The plant $G(s)$ (corresponding to a given pairing) is DIC if there exists a decentralized controller with integral action in each loop, such that the feedback system is stable and such that each individual loop may be detuned (reduced gain) independently by a factor ε_i ($0 \le \varepsilon_i \le 1$) without introducing instability. ■

$\varepsilon_i = 0$ corresponds to an inactive control loop. DIC is a somewhat stronger requirement than requirement 1 above since requirement 1 only concerns a detuning factor of 0 or 1 (not the intermediate values). Plants that are open-loop unstable are not DIC. This follows trivially since with all $\varepsilon_i = 0$, only the uncontrolled (and unstable) plant is left. However, all HENs are open-loop stable, as shown by Mathisen (1994, chapter 3).

No simple conditions (both necessary and sufficient) to test for DIC exists (Skogestad and Morari, 1988). Here, we need necessary conditions for DIC in order to screen pairing alternatives that result in plants that are not DIC. It is desirable with a condition that is easy and efficient to compute so the screening can be automated. Such a simple necessary condition exists and it is based on the steady state RGA. The RGA was introduced by Bristol (1966) as a measure of interactions in multivariable systems. For square systems, the RGA of a transfer matrix G is defined as:

$$RGA(G) = G \times (G^{-1})^T \tag{6.14}$$

The following theorem concerning the steady state RGA and stability was proven by Grosdidier *et al.* (1985).

Theorem 6.1 *Steady state RGA.*
Consider a stable square plant G and a diagonal controller K with integral action in all elements, and assume that the loop transfer function GK is strictly proper (always satisfied for real systems). If a pairing of outputs and manipulated inputs corresponds to a negative steady state relative gain, then the closed-loop system has at least one of the following properties:

1. The overall closed-loop system is unstable.
2. The loop with the negative relative gain is unstable by itself (other loops opened).
3. The closed-loop system is unstable if the loop with the negative relative gain is inactive.

■

This theorem implies the following necessary condition for DIC (Skogestad and Postlethwaite (1996):

A plant $G(s)$ is DIC only if $RGA_{i,j}(G(0)) \geq 0$ for the selected pairings i,j. (6.15)

That is, pairings corresponding to negative steady state RGA elements should be avoided as it will result in a plant which is not DIC. There are other necessary conditions and also sufficient conditions for DIC, see Skogestad and Morari (1988). Note that the condition given by (6.15) is necessary, meaning that even if all selected RGA elements are positive there is no guarantee that the plant is DIC. The steady state RGA, however, is a simple tool since it does not have to be recomputed for each possible pairing. Therefore, we will here only use the simple test given by (6.15) to screen plants that are not DIC. For 2×2-plants, positive steady state RGA-elements are both necessary and sufficient conditions for DIC (Skogestad and Morari, 1988).

The screening method for HENs is based on RGA computed from G^{BP}. This transfer matrix is usually not square as there are more manipulations (bypasses) than outputs (targets). The control configuration being active at any moment, however, is square. Unused manipulations are usually saturated, and each of the active manipulations are paired with one controlled outputs using single loop controllers. Hence, the RGA is computed from G^{BP} with the columns corresponding to unused inputs removed. Since the unused inputs may vary, it is necessary to consider several RGAs, and the following notation is introduced:

RGA^k is the steady state RGA computed from G^{BP} with column k removed. (6.16)

In case of more than one unused inputs, this is indicated with more indices, e.g. $RGA^{k,l}$ the steady state RGA computed from G^{BP} with columns k and l removed. In order to get consistency when addressing individual elements in RGA^k and G^{BP}, columns with only zeros are inserted in RGA^k at the locations of the unused inputs. As an example, we have

$$G^{\mathrm{BP}} = \begin{bmatrix} 1 & 2 & 3 \\ 4 & -5 & 6 \end{bmatrix},\ RGA^2 = \begin{bmatrix} -1 & 0 & 2 \\ 2 & 0 & -1 \end{bmatrix} \text{ since } RGA\left(\begin{bmatrix} 1 & 3 \\ 4 & 6 \end{bmatrix}\right) = \begin{bmatrix} -1 & 2 \\ 2 & -1 \end{bmatrix}. \quad (6.17)$$

Now, the pairing with negative relative gains can be forbidden by adding new constraints to model A. Recall the variable X, where $x_{i,j} = 1$ for selected pairings and $x_{i,j} = 0$ for the remaining elements. To forbid pairing of output 1 with input 1 and output 2 with input 3 for the system given by equation (6.17), we could include the constraints $x_{1,1} = 0$ and $x_{2,3} = 0$. For the remaining 2×2-system (input 2 is unused) it will be sufficient to include only one of these constraints. This method, however, will forbid each of the two pairings in all cases and this is not what we want. If input 1 or 3 is unused, we do *not* want to forbid pairing $x_{1,1}$ or $x_{2,3}$. To forbid both $x_{1,1}$ and $x_{2,3}$ to be 1 at the same time, the following constraint should be included instead:

$$x_{1,1} + x_{2,3} \leq 1 \quad (6.18)$$

With both these pairings selected, the left-hand side of (6.18) is 2 thus the constraint is violated. This constraint, however, allows for selecting e.g. the pairing $x_{1,1} = 1$ and $x_{2,2} = 1$ in the case where input 3 is unused. With 2 controlled outputs the right-hand side of the

constraint is 1 in order to prevent selection of the 2 elements in X with negative relative gains. More general, the sum of each pairing X corresponding to a negative relative gain should be less than or equal to $n_y - 1$ (n_y is the number of controlled outputs). If there are several pairings that have at least one negative relative gain, a constraint similar to equation (6.18) should be included for each of these pairings. Thus, pairings resulting in plants that are not DIC are forbidden. The next section shows how pairings resulting in negative gains (not DIC) are not strictly forbidden, but they are disregarded if there exist any possible pairing with non-negative RGA-elements.

The steady state RGA will also be used for the second controllability requirement given above (best closed-loop performance for pairings with similar steady state properties). We choose to penalize the RGA-number, which for a square plant G with rows and columns ordered such that the pairings are along the diagonal, is:

$$\text{RGA-number} = \left\| RGA(G) - I \right\|_{\text{sum}} \tag{6.19}$$

The sum norm is simply the sum of the absolute values of all elements. The RGA-number is a measure of the diagonal dominance (Skogestad and Postlethwaite, 1996, chapter 10). In our case, the rows and columns of the plant are not ordered, but in model A we have the variable X denoting the selected pairings of G^{BP}. The RGA-number when input k is unused is:

$$\text{RGA-number with input } k \text{ unused} = \left\| RGA^k - X \right\|_{\text{sum}} \tag{6.20}$$

The matrix X with column k removed can be considered as a permutation of I (in 6.19), or as the permutation matrix itself. The matrices in equation (6.20) are not square, however, the elements in the column(s) corresponding to the unused input(s) are zero, both for RGA^k and X. Hence, the unused columns do not contribute to the RGA-number. Penalizing the RGA-number given by (6.20) for the different alternatives of RGA^k, represents a method to include controllability considerations for selection among pairings with similar steady state performance. This method will be used to handle the second controllability requirement.

The next section explains in more detail how model A is extended to include the first controllability requirement presented above, and a hierarchical approach is proposed. Section 6.5 shows how both the first and the second controllability requirement can be included in a more complex hierarchical approach.

6.4 A first hierarchical strategy for operation (model B)

In the previous sections, pairings that have to result in a plant that is not DIC were forbidden by introducing new constraints to model A (equation 6.13). In cases where no DIC plants exist, this approach implies that there are no feasible solution to the pairing problem. This infeasibility is not desired as we still want to operate the plant in the best possible way. This section introduces a hierarchical approach by extending model A to also handle cases where no DIC plants exist. We want to obtain the following strategy for operation:

1. Select the pairing that results in the lowest utility consumption among configurations that are DIC.

2. If no DIC pairing exists, select the pairing that results in the lowest utility consumption (among the plants that are not DIC).

The first point corresponds to the strategy described in the previous sections. The second point cannot be implemented simply by forbidding pairings that results in plants being not DIC. Further, simply penalizing negative values of RGA-elements will not result in the desired strategy since pairings with small negative relative gains (and low utility consumption) may be preferred before plants with only positive relative gains (and high utility consumption). This is not consistent with the two items above. The strategy can be implemented by introducing logical inference in the model. This is explained in the subsequent. Consider the following inequality where α is a logical variable (binary variable, 0-1 variable) and r is a real scalar variable:

$$-M\alpha + r \leq 0 \tag{6.21}$$

M is an upper bound on the real variable r. This constraint connects the real and binary variables in the following way:

$$\text{If } \alpha = 0, \text{ then } r \leq 0. \tag{6.22a}$$
$$\text{If } \alpha = 1, \text{ then } r \text{ is free to take any value (up to } M\text{).} \tag{6.22b}$$

Such constraints are often included e.g. in optimization of process structures using mathematical programming. If r is restricted to a positive real value denoting the size (or cost) of a unit, and $\alpha = 1$ if that unit is present and $\alpha = 0$ otherwise, then constraint (6.21) forces the size (or cost) of the unit to be zero when the unit is not selected (see e.g. Biegler *et al.* (1997). Here, we shall consider r being both positive and negative and also it will be focused on the "complementary" statement of (6.22). That is, instead of using the value of α to draw conclusions about r, we will use the value of r to draw conclusions about α. If a and b are logical propositions, then the following two statements are equivalent:

$$\text{“}a \Rightarrow b\text{” is equivalent to “(not } b) \Rightarrow (\text{not } a)\text{”} \tag{6.23}$$

Using this, constraint (6.21) results in the following relationship between the binary and real variable:

$$\text{If } r > 0, \text{ then } \alpha = 1. \tag{6.24a}$$
$$\text{If } r \leq 0, \text{ then } \alpha \text{ is free to take any value (0 or 1).} \tag{6.24b}$$

In our model, we want $\alpha = 1$ if there exists at least one pairing with no relative gains, and $\alpha = 0$ if no such pairing exists (meaning that all pairings are not DIC). The first step to do this, is to establish the proper relationship between a single variable r (which may be one element of the RGA) and a single binary variable that is denoted β. We want to formulate constraints that are equivalent to the following statements:

$$\text{If } r \geq 0, \text{ then } \beta = 1. \tag{6.25a}$$
$$\text{If } r < 0, \text{ then } \beta = 0. \tag{6.25b}$$

Statement (6.24a) is close to (6.25a) but it should be modified such that the equality part ($r = 0$) forces β to 1. This can be done by changing constraint (6.21) into

$$-RGA_{\max}\beta + (r + \delta) \leq 0 \tag{6.26}$$

$RGA_{\max}$ is the largest absolute value of any element in the RGA thus representing an upper bound on r. The new variable δ is the absolute value of an upper bound (closest to 0) on negative values of r. That is, if the largest negative value r can have is –0.01, then δ must be in the interval $\delta \in (0, 0.01)$ (not including the endpoints).

To satisfy statement (6.25b), the following constraint is introduced:

$$RGA_{\max}(\beta - 1) - (r + \delta) \leq 0 \tag{6.27}$$

Here, $RGA_{\max}$ represents a bound of the largest (in absolute value) negative value of r. With a proper value of δ, constraint (6.27) is equivalent to:

If $r < 0$, then $\beta = 0$. (6.28a)
If $r \geq 0$, then β is free to take any value (0 or 1). (6.28b)

To conclude so far, we have found that the desired statements (6.25a) and (6.25b) can be satisfied by introducing the two constraints (6.26) and (6.27), and the result can be summarized as:

$$\left.\begin{aligned} -RGA_{\max}\beta + (r+\delta) \leq 0 \\ RGA_{\max}(\beta - 1) - (r+\delta) \leq 0 \end{aligned}\right\} \quad \Rightarrow \quad \begin{cases} \text{if } r \geq 0, \text{ then } \beta = 1 \\ \text{if } r < 0, \text{ then } \beta = 0 \end{cases} \tag{6.29}$$

Actually, the correct statements in (6.29) are: If $r > -\delta$, then $\beta = 1$ and if $r \leq -\delta$, then $\beta = 0$. However, with a proper value of δ, this is equivalent to the statements in (6.29). These constraints provide the required connection between one single real number r and the logical variable β. In our case, we want to distinguish whether it can be concluded from negative relative gains that all possible pairings and choice of inputs have to result in plants that are not DIC, or not. This makes the picture somewhat more complicated. β can not just be one single variable; we need one binary value for each element in the RGAs. Using the RGA for selecting pairing is efficient since it does not have to be recomputed for each pairing. It does, however, have to be recomputed for different selections of unused inputs, recall RGA^k introduced in the last section. In the model, β is a set of k logical variables, each with the same dimension as RGA^k. The following constraints provide the necessary relationship between each of the RGAs and the βs:

$$-RGA_{\max}\beta_{i,j}^{k} + \left(RGA_{i,j}^{k} + \delta\right) \leq 0 \quad \forall i, j, k \tag{6.30a}$$

$$RGA_{\max}\left(\beta_{i,j}^{k} - 1\right) - \left(RGA_{i,j}^{k} + \delta\right) \leq 0 \quad \forall i, j, k \tag{6.30b}$$

These constraints ensure that for each unused input k, the elements of β^k are 0 if the corresponding element in RGA^k is negative, and 1 if the corresponding element in RGA^k is zero or positive. As numerical values for the bounds, $RGA_{\max}$ can be set equal to the largest

element (in absolute value) found in any of the RGA^ks and δ can be set equal to the absolute value of the negative number closest to zero found in any RGA^k.

The model including controllability considerations shall reflect the hierarchical strategy given by the two requirements stated first in this section. When extending model A to incorporate this strategy, the following two items are important:

- The model size should be kept small, i.e. if it is possible to carry out some of the computations in advance of the optimization, this should be done.
- No non-linearities should be introduced as this may make the search for the optimal pairing significantly more difficult.

When an optimization is to be performed, the steady state transfer matrix G^{BP} is known. From this matrix, the RGA^ks can be computed in advance. From each RGA^k, also the β^ks may be precomputed. This may be done by implementing the constraints (6.30a) and (6.30b) *separately*, or by means of if-then statements in any conventional computer language. Hence, both the *RGA*s and the βs are computed in advance. This reduces the size of the model, but another advantage concerning the second item above is perhaps more important: With precomputed values of the *RGA*s and the βs, these become *constants* (and not variables) in the optimization procedure. This allows variables to be multiplied by for example β without introducing non-linearities and this is very convenient.

The connection between the set of the βs and the variable α is done by adding 2 new constraints. First, consider the following term:

$$\sum_{i,j}\left(x_{i,j}^k \beta_{i,j}^k\right) \tag{6.31}$$

The multiplication by $x_{i,j}$ within the summation ensures that only the selected pairings are considered (since for pairings that are not selected we have $x_{i,j} = 0$). The constraints in model A (more specifically; constraint 6.13b) ensure that the number of selected pairings is equal to the number of controlled outputs n_y. If all β-elements of the selected pairings are 1 (i.e. relative gains are non-negative) then the term in (6.31) is equal to n_y. If, however, any of the selected relative gains are negative (i.e. $\beta_{i,j} = 0$ for the selected k), then the term in (6.31) is less than n_y and this implies that the plant with this pairing is not DIC. That is, the constraints that connect α and β must be equivalent to the following statement:

For the selected k:

If $\sum_{i,j}\left(x_{i,j}^k \beta_{i,j}^k\right) < n_y$ (one or more negative RGA-elements), then $\alpha = 0$. (6.32a)

If $\sum_{i,j}\left(x_{i,j}^k \beta_{i,j}^k\right) = n_y$ (all RGA-elements are zero or positive), then $\alpha = 1$. (6.32b)

This statement is fulfilled by introducing the following two constraints:

$$n_y\alpha - \sum_{i,j}\left(x_{i,j}\beta_{i,j}^k\right) \le 0 \quad \text{for the selected } k. \tag{6.33a}$$

$$-\alpha + 1 - n_y + \sum_{i,j}\left(x_{i,j}\beta_{i,j}^{k}\right) \le 0 \quad \text{for the selected } k. \tag{6.33b}$$

Constraint (6.33a), forces α to zero if $\Sigma_{i,j}(x_{i,j}\beta_{i,j}^{k}) < n_y$ (otherwise α is free), thus requirement (6.32a) is fulfilled. Likewise, constraint (6.33b) fulfills requirement (6.32b). With the correct value of α, the only remaining task is to prevent pairings resulting in a not DIC plant when there exist DIC pairings that are feasible (fulfills the constrains in model A). This is done simply by adding the term $M_1(1–\alpha)$ to the objective function. M_1 represents an upper bound on the *change* of the objective function from model A (from equation 6.13a). That is, M_1 should be at least as large as the difference between the best and worst case solutions from model A, thus changing α from 0 to 1 will always dominate other changes in the objective function. A suitable value of M_1 can be found from adding the n_y (since n_y is the number of selected elements) largest elements in P and subtracting the n_y smallest elements in P. This should be done when P has been updated prior to an optimization, hence M_1 is a constant in the optimization algorithm.

Now, the necessary extensions to model A have been presented, and the complete extended model B is given by equations (6.34) to (6.36).

$$X = \arg\min_{X}\left(\sum_{i}\sum_{j} x_{i,j}\, p_{i,j} + M_1(1-\alpha)\right) \tag{6.34}$$

subject to

$$\sum_{j} x_{i,j} = 1 \qquad \forall i \tag{6.35a}$$

$$\sum_{i} x_{i,j} \le 1 \qquad \forall j \tag{6.35b}$$

$$x_{i,j} + y_{i,j} + z_j^{\text{lo}} \le 2 \qquad \forall i,j \tag{6.35c}$$

$$x_{i,j} - y_{i,j} + z_j^{\text{up}} \le 1 \qquad \forall i,j \tag{6.35d}$$

$$x_{i,j} + g_{i,j}^{0} \le 1 \qquad \forall i,j \tag{6.35e}$$

$$n_y\alpha - \sum_{i,j}\left(x_{i,j}\beta_{i,j}^{k}\right) \le 0 \quad \text{for the selected } k. \tag{6.36a}$$

$$-\alpha + 1 - n_y + \sum_{i,j}\left(x_{i,j}\beta_{i,j}^{k}\right) \le 0 \quad \text{for the selected } k. \tag{6.36b}$$

As we see, the constraints in (6.35) are the same as the constraints in model A, while the constraints in (6.36) together with the modified objective function handle the controllability requirement. The model works in the following way:

- If none of the pairings have negative RGA-elements ($\alpha = 1$), the model is identical to model A.
- If there are some pairings (that fulfills the constraints in 6.35) where $\alpha = 1$ and others where $\alpha = 0$, then the optimal pairing is that with the smallest operating cost among

those with $\alpha = 1$. That is, even the pairing with the worst case operating cost is preferred before a plant we know is not DIC.

- If all pairings that satisfy the constraints in (6.35) result in a not DIC plant, then the pairing with the smallest operating cost is selected. This last case, however, represents a *potentially* hazardous situation since the plant (or parts of it) will become unstable if one of the selected control loops becomes inactive.

Model B represents an implementation of the two requirements given early in this section, corresponding to a hierarchical strategy for operation. The extension to include the controllability considerations comprises only two additional constraints and a new term in the objective function. The use of this model will be demonstrated in the example section.

6.5 A second hierarchical strategy for operation (model C)

This section presents a hierarchical strategy for operation which is different from that in the previous section. Here, the second controllability consideration (among pairings with similar operating costs, select that with the best controllability properties) is included. The strategy differs from the previous also in the sense that if no DIC plant exists, then utility optimization is sacrificed and focus is exclusively on controllability. We want to apply the following strategy:

1. Select the pairing that results in the lowest utility consumption among configurations that are DIC. Among pairings with similar utility consumption, select that with the best controllability properties.
2. If no DIC pairing exists, give up utility optimization and select the pairing with the best controllability properties.

This strategy is obtained from modifying the objective function of the previous models and extending model B further. The second controllability consideration involves computation of the RGA-number as explained in section 4.3, see equation (6.20). As for the previous model, it is important to keep the model linear. It will become clear that implementing the strategy above, and particularly computation of the RGA-number, represents a major extension of model B.

For the new objective function, we introduce a new variable *OC* (change in operating costs):

$$OC = \sum_{i,j} x_{i,j}\, p_{i,j} \tag{6.37}$$

OC is identical to the objective function in the previous models. To disregard the operating costs when we know the plant is not DIC, it could be tempting to simply include the term αOC in the objective function. However, this is a multiplication of the binary variable α with the continuous variable *OC* and thus it will introduce a non-linearity. A similar term can be implemented without introducing non-linearities by means of logic inference. This is done with the variable OC^* that should have the following properties (identical to the term αOC):

$$\text{If } \alpha = 0, \text{ then } OC^* = 0. \tag{6.38a}$$
$$\text{If } \alpha = 1, \text{ then } OC^* = OC. \tag{6.38b}$$

This is implemented by means of constraints quite similar to constraint (6.21), but four constraints are required. They are explained below.

$$-M_2\alpha - OC^* \le 0 \tag{6.39a}$$
$$-M_2\alpha + OC^* \le 0 \tag{6.39b}$$
$$M_2(\alpha - 1) - OC^* + OC \le 0 \tag{6.39c}$$
$$M_2(\alpha - 1) + OC^* - OC \le 0 \tag{6.39d}$$

M_2 is an upper bound on the operating costs. Constraint (6.39a) is equivalent: If $\alpha = 0$, then $OC^* \ge 0$, otherwise OC^* is free. Likewise, constraint (6.39b) is equivalent: If $\alpha = 0$, then $OC^* \le 0$, otherwise OC^* is free. The intersection of these two constraints (both constraints are fulfilled) corresponds to the equality part of both. That is: If $\alpha = 0$, then $OC^* = 0$, otherwise OC^* is free. Hence, the constraints (6.39a) and (6.39b) together ensure that requirement (6.38a) is satisfied.

The argument is similar for requirement (6.38b). Constraint (6.39c) is equivalent to: If $\alpha = 1$, then $OC^* \ge OC$, otherwise OC^* is free. Likewise, constraint (6.39d) is equivalent to: If $\alpha = 1$, then $OC^* \le OC$, otherwise OC^* is free. The intersection of these two constraints corresponds to the equality part of both. Hence, the constraints (6.39c) and (6.39d) together ensure that also requirement (6.38b) is satisfied.

Note that since model C minimizes OC^*, it is not necessary to provide any upper bounds on this variable. Thus, only constraints (6.39a) and (6.39c) are actually included in the model. This corresponds to replacing the 2 equalities in (6.38) by "greater than or equal"-signs

The objective function in the extended model has the form

$$X = \arg\min_X \left(OC^* + wCM + M_1(1-\alpha)\right) \tag{6.40}$$

The first term, operating cost, is implemented by the constraints (6.37), (6.39a) and (6.39c). The second term involves the variable *CM* (controllability measure) and the weight *w* that scales the controllability relative to OC^* when this is not zero. As controllability measure, we have decided to use the RGA-number, see equation (6.20). This measure is not computed in advance since it is not only a function of the selected RGA^k, but also on the pairing X (that would require computation of the RGA-number for a large number of pairings). To compute the RGA-number, a new variable γ is introduced. This is a binary variable with same dimension as RGA^k (and X). For each element, $\gamma_{i,j} = 1$ if the corresponding element in $(RGA^k - X)$ is positive and $\gamma_{i,j} = 0$ if the corresponding element in $(RGA^k - X)$ is negative. For elements in $(RGA^k - X)$ that are zero, it does not matter which value $\gamma_{i,j}$ takes. For simplicity we choose $\gamma_{i,j} = 0$ in such cases. That is, we want to obtain:

$$\text{If } \left(RGA^k_{i,j} - x_{i,j}\right) > 0, \text{ then } \gamma_{i,j} = 1$$
$$\text{If } \left(RGA^k_{i,j} - x_{i,j}\right) \le 0, \text{ then } \gamma_{i,j} = 0$$

This is achieved by the following constraints:

$$-M_3\gamma_{i,j} + \left(RGA^k_{i,j} - x_{i,j}\right) \le 0 \quad \forall i,j \tag{6.41a}$$

$$M_3\left(\gamma_{i,j} - 1\right) + \left(RGA^k_{i,j} - x_{i,j}\right) \le 0 \quad \forall i,j \tag{6.41b}$$

M_3 is and upper bound on the absolute value of $RGA^k_{i,j} - x_{i,j}$. A simple expression for M_3 is $M_3 = RGA_{\max} + 1$. The next step is to use γ to create a new continuous variable *RGAn* of the same size as γ: The purpose of *RGAn* is that the RGA-number can be found simply from adding all elements in *RGAn*. That is, *RGAn* should have the following definition:

$$\text{If } \gamma_{i,j} = 1, \text{ then } RGAn_{i,j} = \left(RGA^k_{i,j} - x_{i,j}\right)$$

$$\text{If } \gamma_{i,j} = 0, \text{ then } RGAn_{i,j} = -\left(RGA^k_{i,j} - x_{i,j}\right)$$

This is satisfied by introducing the following constraints (similar as 6.39):

$$-M_3\gamma_{i,j} - RGAn_{i,j} + \left(RGA^k_{i,j} - x_{i,j}\right) \le 0 \quad \forall i,j \tag{6.42a}$$

$$-M_3\gamma_{i,j} + RGAn_{i,j} - \left(RGA^k_{i,j} - x_{i,j}\right) \le 0 \quad \forall i,j \tag{6.42b}$$

$$M_3\left(\gamma_{i,j} - 1\right) - RGAn_{i,j} + \left(RGA^k_{i,j} - x_{i,j}\right) \le 0 \quad \forall i,j \tag{6.42c}$$

$$M_3\left(\gamma_{i,j} - 1\right) + RGAn_{i,j} - \left(RGA^k_{i,j} - x_{i,j}\right) \le 0 \quad \forall i,j \tag{6.42d}$$

The intersection (equality parts) of (6.42a) and (6.42b) ensures correct value of *RGAn* when $\gamma_{i,j} = 0$, while constraints (6.42c) and (6.42d) handles the elements where $\gamma_{i,j} = 1$. Apparently, the computation of the controllability measure causes a significant extension of the size of the model. With the values of *RGAn* from constraint (6.42), the RGA-number (*CM*) is simply given by a summation as shown by equation (6.45g) below.

Now, the extensions to include controllability are explained, and the complete extended model is given by equations (6.43) to (6.45). Note that with the introduction of the continuous variables *OC*, OC^* and *CM*, the model has become a MILP-formulation.

$$X = \arg\min_X \left(OC^* + wCM + M_1(1-\alpha)\right) \tag{6.43}$$

subject to

All constraints in model B. That is, equations (6.35) and (6.36).
In addition:

$$OC = \sum_{i,j} x_{i,j}\, p_{i,j} \tag{6.44a}$$

$$-M_2\alpha - OC^* \le 0 \tag{6.44b}$$

$$M_2\,(\alpha - 1) - OC^* + OC \le 0 \tag{6.44c}$$

$$-M_3\gamma_{i,j} + \left(RGA^k_{i,j} - x_{i,j}\right) \le 0 \quad \forall i,j \tag{6.45a}$$

$$M_3\left(\gamma_{i,j}-1\right)+\left(RGA_{i,j}^k-x_{i,j}\right)\le 0 \quad \forall i,j \tag{6.45b}$$

$$-M_3\gamma_{i,j}-RGAn_{i,j}+\left(RGA_{i,j}^k-x_{i,j}\right)\le 0 \quad \forall i,j \tag{6.45c}$$

$$-M_3\gamma_{i,j}+RGAn_{i,j}-\left(RGA_{i,j}^k-x_{i,j}\right)\le 0 \quad \forall i,j \tag{6.45d}$$

$$M_3\left(\gamma_{i,j}-1\right)-RGAn_{i,j}+\left(RGA_{i,j}^k-x_{i,j}\right)\le 0 \quad \forall i,j \tag{6.45e}$$

$$M_3\left(\gamma_{i,j}-1\right)+RGAn_{i,j}-\left(RGA_{i,j}^k-x_{i,j}\right)\le 0 \quad \forall i,j \tag{6.45f}$$

$$CM=\sum_{i,j}RGAn_{i,j} \tag{6.45g}$$

The constraints in (6.44) concern operating costs and except for (6.44a) they concern how to disregard the operating costs when the pairing gives a plant that is not DIC. The constrains in (6.45) concern computation of the RGA-number (second controllability requirement).

Model C represents an implementation of the two requirements given early in this section, corresponding to a more complex hierarchical strategy for operation than model B. As it has become evident, model B had to be extended quite extensively to incorporate the second controllability requirement.

6.6 Examples

This section includes two examples to demonstrate the application of the method described in this chapter. Example 6.1 is a very simple and academic example where model B is demonstrated. Example 6.2 shows how model C may be significantly simplified for a seven stream HEN.

Example 6.1 *Simple demonstration example.*
Consider a plant with 3 manipulable inputs and 2 outputs given by the following transfer function:

$$\begin{bmatrix} y_1 \\ y_2 \end{bmatrix}=\frac{1}{s+1}\underbrace{\begin{bmatrix} 3 & -1 & 3 \\ 4 & -2 & -6 \end{bmatrix}}_{G^{BP}}\begin{bmatrix} u_1 \\ u_2 \\ u_3 \end{bmatrix}+\frac{1}{s+1}\begin{bmatrix} 0 \\ 1 \end{bmatrix}d \tag{6.47}$$

where u_1, u_2, $u_3 \in [0, 1]$ and the objective function is $J = u_1 + u_2 + u_3$ ($G^{U\$} = [1\ \ 1\ \ 1]$). Even if the transfer function in (6.47) may not represent a HEN, we will let superscript U\$ represent operating costs and G^{BP} denotes the steady state transfer function from the manipulated inputs to the controlled outputs. Only the steady state data is known. The transfer function from the disturbance as well as the disturbance d itself is unknown; we can only register the effect on the measurements in terms of control errors.

The problem is to control both outputs to setpoints while minimizing the objective J. The control configuration should result in a DIC plant, and if no DIC plants are possible when the outputs are controlled, then optimization of J is sacrificed and the best control configuration should be selected.

The three RGA^ks computed from G^{BP} (input k unused) are:

$$RGA^1 = \begin{bmatrix} 0 & 0.5 & 0.5 \\ 0 & 0.5 & 0.5 \end{bmatrix}, \quad RGA^2 = \begin{bmatrix} 0.6 & 0 & 0.4 \\ 0.4 & 0 & 0.6 \end{bmatrix} \quad \text{and} \quad RGA^3 = \begin{bmatrix} 3 & -2 & 0 \\ -2 & 3 & 0 \end{bmatrix}$$

For each of the three cases there are two pairings, but only one pairing has negative relative gains. However, it may not always be possible to select the pairing with positive relative gains due to the constraints in the manipulations. The corresponding precomputed values of the βs are:

$$\beta^1 = \begin{bmatrix} 1 & 1 & 1 \\ 1 & 1 & 1 \end{bmatrix}, \quad \beta^2 = \begin{bmatrix} 1 & 1 & 1 \\ 1 & 1 & 1 \end{bmatrix} \quad \text{and} \quad \beta^3 = \begin{bmatrix} 1 & 0 & 1 \\ 0 & 1 & 1 \end{bmatrix}.$$

The initial values are $u_1 = u_2 = u_3 = 0$ and also $d = 0$. The result using model B, showing the time responses for different disturbances when the pairing changes according to the optimal pairing is shown. Initially, we have all $z^{lo} = 1$, i.e. all manipulations are saturated at zero.

At time zero, both setpoints are changed from 0 to 0.5. At the same time, an optimization is done and this results in controlling y_1 using u_3 and controlling y_2 using u_1. The different events in terms of setpoint changes and disturbance are as follows:

At time = 0: Setpoints r_1 and r_2 are changed from 0 to 0.5.
At time = 4: Setpoint r_2 is changed from 0.5 to 0.
At time = 8: Setpoint r_1 is changed from 0.5 to 0.
At time = 14: Disturbance d is changed from 0 to 1.

This is shown in figure 6.1 where the thin solid lines in 6.1a and 6.1b are the setpoints r_1 and r_2, respectively. The disturbance d is shown in figure 6.1c. Optimization to find the control structure (step 3 in the procedure on page 95) is done every fifth minute, regardless of saturation or change of sign for control errors. The resulting pairing matrix X in each period became:

Time: 0-5 min. $\quad X = \begin{bmatrix} 0 & 0 & 1 \\ 1 & 0 & 0 \end{bmatrix}$

Time: 5-10 min. $\quad X = \begin{bmatrix} 0 & 0 & 1 \\ 1 & 0 & 0 \end{bmatrix}$

Time: 10-15 min. $\quad X = \begin{bmatrix} 0 & 1 & 0 \\ 0 & 0 & 1 \end{bmatrix}$

Time: 15-20 min. $\quad X = \begin{bmatrix} 0 & 0 & 1 \\ 0 & 1 & 0 \end{bmatrix}$

The result from dynamic simulations when the system is controlled according to these control structures is shown in figure 6.1. The thick lines in figures 6.1a and 6.1b shows the controlled outputs y_1 and y_2. The manipulations are shown in the 3 figures in the right column. Simple PI-controllers are used for the simulations. In all cases, the controller gain is 1 or –1 (depending on the sign of the transfer function) and the integral time is 1 minute.

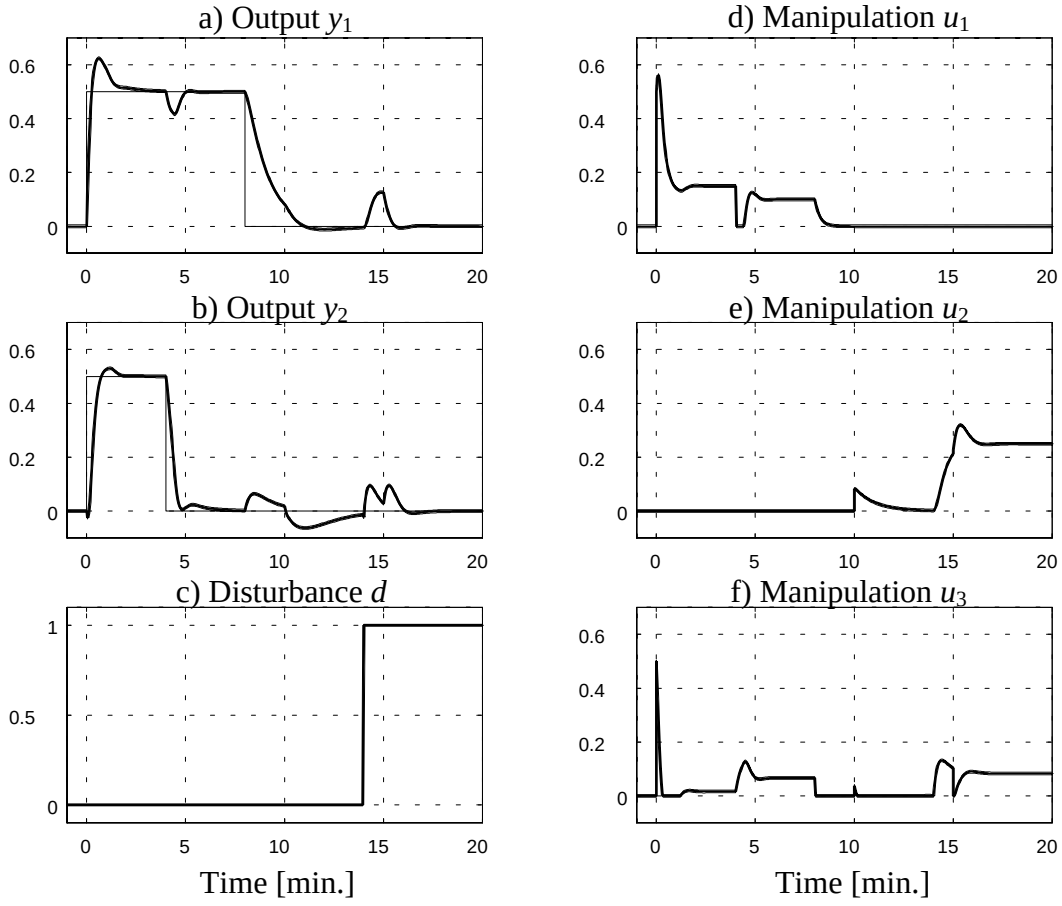

Figure 6.1 Result for example 6.1.

In addition to demonstrate how the method works, this example has also shown that the approach may be applied to other processes than HENs. As long as the process is represented by one steady state transfer function G^{BP} from the manipulations to the controlled outputs, and one transfer function from the manipulations to a scalar objective, the method may be applied. ■

Example 6.2 *Seven-stream HEN example.*
The HEN in this example has the same structure as the largest subnetwork of the aromatics plant studied by Linnhoff *et al.* (1982). The HEN is shown in the figure below.

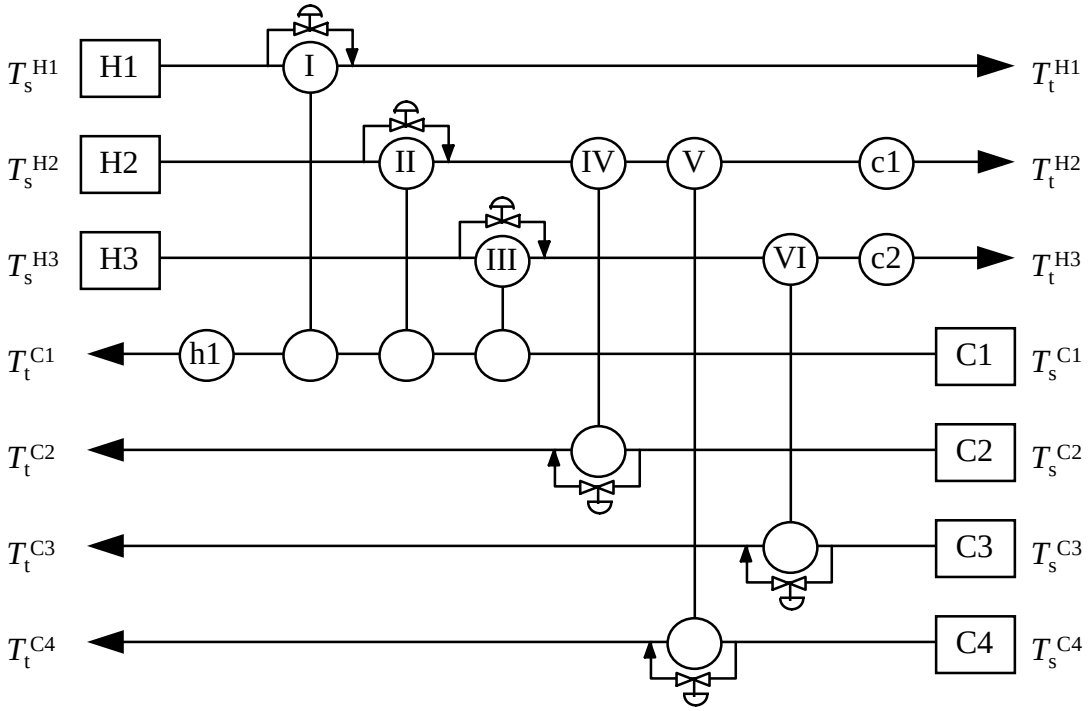

Figure 6.2 HEN in example 6.2.

The stream data has been modified slightly such that the *CP*-values are constant (segments have been removed). As usual, the HEN is decomposed according to rule 2.1 (in section 2.3) and the bypassed controlled temperatures are T_o^{H1}, T_o^{C2}, T_o^{C3} and T_o^{C4}. The transfer functions G^{BP} and G^{U} have been found from small positive perturbations of the nonlinear process model around the operating point $u_I = u_{II} = u_{III} = u_{IV} = u_V = u_{VI} = 0$.

$$\begin{bmatrix} T_o^{H1} \\ T_o^{C2} \\ T_o^{C3} \\ T_o^{C4} \end{bmatrix} = \underbrace{\begin{bmatrix} 58.8 & -13.5 & -1.2 & 0 & 0 & 0 \\ 0 & 14.9 & -2.1 & -3.6 & 0 & 0 \\ 0 & 0 & 12.3 & 0 & 0 & -38.4 \\ 0 & 14.9 & -0.1 & 0.9 & -5.4 & 0 \end{bmatrix}}_{G^{BP}} \begin{bmatrix} u_I \\ u_{II} \\ u_{III} \\ u_{IV} \\ u_V \\ u_{VI} \end{bmatrix} \tag{6.48}$$

$$\begin{bmatrix} Q_{c1} \\ Q_{c2} \\ Q_{h1} \end{bmatrix} = \underbrace{\begin{bmatrix} 0 & 2.9 & -0.40 & 0.17 & 0.50 & 0 \\ 0 & 0 & 0.12 & 0 & 0 & 2.1 \\ 6.8 & 0.88 & 0.08 & 0 & 0 & 0 \end{bmatrix}}_{G^{U}} \begin{bmatrix} u_I \\ u_{II} \\ u_{III} \\ u_{IV} \\ u_V \\ u_{VI} \end{bmatrix} \tag{6.49}$$

The zeros in these transfer functions are given by the structural properties of the HEN. In this example, we simply assume that the cost data are equal to unity ($c^T = [1 \quad 1 \quad 1]$), thus we actually minimize the total utility consumption rather than the utility cost. This gives

$$g^{U\$} = [1\ \ 1\ \ 1]G^{U} = [6.8\ \ 3.78\ \ -0.20\ \ 0.17\ \ 0.50\ \ 2.1] \tag{6.50}$$

Defining $e_1 = T_o^{H1} - T_t^{H1}$, $e_2 = T_o^{C2} - T_t^{C2}$ and so on, the priority matrix ($p_{i,j} = -\frac{g_j^{U\$}}{g_{i,j}^{BP}} e_i$) becomes

$$P = \begin{bmatrix} -0.12e_1 & 0.28e_1 & -0.16e_1 & \times & \times & \times \\ \times & -0.25e_2 & -0.10e_2 & 0.05e_2 & \times & \times \\ \times & \times & 0.02e_3 & \times & \times & 0.05e_3 \\ \times & -0.25e_4 & -2.0e_4 & -0.19e_4 & 0.09e_4 & \times \end{bmatrix} \tag{6.51}$$

For this example, there are 2 excess manipulations thus 2 inputs are unused. This yields 15 combinations of using 4 of the 6 bypasses. The RGAs for these 15 possible candidates are listed below. The columns with the unused inputs are marked with × instead of 0 such that they are easily identified and the zeros in the other columns are not filled in.

$$RGA^{1,2} = \begin{bmatrix} \times & \times & 1 & & \\ \times & \times & & 1 & \\ \times & \times & & & 1 \\ \times & \times & & 1 & \end{bmatrix} \quad RGA^{1,3} = \begin{bmatrix} \times & 1 & \times & & \\ \times & & \times & 1 & \\ \times & & \times & & 1 \\ \times & & \times & 1 & \end{bmatrix} \quad RGA^{1,4} = \begin{bmatrix} \times & 0.6 & 0.4 & \times & \\ \times & 0.4 & 0.6 & \times & \\ \times & & & \times & 1 \\ \times & & & \times & 1 \end{bmatrix}$$

$$RGA^{1,5} = \begin{bmatrix} \times & 0.27 & 0.73 & & \times \\ \times & 0.15 & 0.23 & 0.62 & \times \\ \times & & & & \times\ 1 \\ \times & 0.58 & 0.04 & 0.38 & \times \end{bmatrix} \quad RGA^{1,6} = \begin{bmatrix} \times & 1 & & & \times \\ \times & & & 1 & \times \\ \times & & 1 & & \times \\ \times & & & 1 & \times \end{bmatrix} \quad RGA^{2,3} = \begin{bmatrix} 1 & \times & \times & & \\ & \times & \times & 1 & \\ & \times & \times & & 1 \\ & \times & \times & 1 & \end{bmatrix}$$

$$RGA^{2,4} = \begin{bmatrix} 1 & \times & & \times & \\ & \times & 1 & \times & \\ & \times & & \times & 1 \\ & \times & & \times & 1 \end{bmatrix} \quad RGA^{2,5} = \begin{bmatrix} 1 & \times & & & \times \\ & \times & 0.84 & 0.16 & \times \\ & \times & & & \times\ 1 \\ & \times & 0.16 & 0.84 & \times \end{bmatrix} \quad RGA^{2,6} = \begin{bmatrix} 1 & \times & & & \times \\ & \times & & 1 & \times \\ & \times & 1 & & \times \\ & \times & & 1 & \times \end{bmatrix}$$

$$RGA^{3,4} = \begin{bmatrix} 1 & & \times & \times & \\ & 1 & \times & \times & \\ & & \times & \times & 1 \\ & & \times & \times & 1 \end{bmatrix} \quad RGA^{3,5} = \begin{bmatrix} 1 & & \times & & \times \\ & 0.2 & \times & 0.8 & \times \\ & & \times & & \times\ 1 \\ & 0.8 & \times & 0.2 & \times \end{bmatrix} \quad RGA^{3,6} = \text{Infeasible}$$

$$RGA^{4,5} = \begin{bmatrix} 1 & & & \times & \times \\ & -0.05 & 1.05 & \times & \times \\ & & & \times & \times\ 1 \\ & 1.05 & -0.05 & \times & \times \end{bmatrix} \quad RGA^{4,6} = \begin{bmatrix} 1 & & \times & & \times \\ & 1 & \times & & \times \\ & & 1 & \times & \times \\ & & & \times & 1\ \times \end{bmatrix} \quad RGA^{5,6} = \begin{bmatrix} 1 & & & \times & \times \\ & 0.2 & & 0.8 & \times & \times \\ & & 1 & & \times & \times \\ & 0.8 & & 0.2 & \times & \times \end{bmatrix}$$

The RGAs can be divided into the following three groups:

8 RGAs are equal to a permutation of *I*, i.e. $RGA = X$. (only 1 pairing is possible).
6 RGAs are not equal to *X*, and only 1 of these has negative relative gains.
1 RGA ($RGA^{3,6}$) is infeasible. (With inputs u_{III} and u_{VI} unused, no input affects T_o^{C3}).

For the first group of 8 RGAs equal to *X*, the rows and columns in G^{BP} (disregarding columns that correspond to unused inputs) may be ordered to give a triangular matrix. For each of these 8 possible selections, only one pairing is feasible. Further, these 8 pairings give an RGA-number of zero. That is, the second controllability requirement (minimize RGA-number) is useless to distinguish between these 8 candidates.

Among the 6 in the second group, 5 of these have only 2 possible pairings while 1 RGA ($RGA^{1,5}$) yields 4 possible pairings. This yields a total of 14 possible pairings for this group. Only 1 pairing has negative relative gains and this is the pairing $x_{1,1} = x_{2,2} = x_{4,3} = x_{3,6} = 1$ (see $RGA^{4,5}$). With this information, model C may be significantly simplified:

First, the constraints (6.36) in model B will be replaced by a simpler expression. To force α to zero when the pairing with negative gains is selected, (6.36) can be replaced by

$$\alpha - 4 + (x_{1,1} + x_{2,2} + x_{4,3} + x_{3,6}) \leq 0 \tag{6.52}$$

If another pairing is selected (one or more of the *x*-elements in (6.52) are 0), then α is free. It is not required to force α to 1 if another pairing is selected since the objective function in model C handles this by penalizing $\alpha = 0$.

The other simplification is more significant. For this example with 4 bypass controlled temperatures and 6 manipulations each of the constraints in (6.45a) to (6.45f) actually represents 24 single constraints. In total, the constraint (6.45) includes 145 single constraints. These will now be replaced by a considerably smaller number of constraints.

As mentioned above, all 8 RGAs in the first group have RGA-number = 0. The 14 possible pairings from the second group imply that there are only 14 RGA-numbers different from zero. That is, all RGA-numbers may be computed *in advance* and each RGA-number is associated with the corresponding pairing. No pairing can have RGA-number less than zero, and the following constraint is included:

$$CM \geq 0 \tag{6.53}$$

This constraint handles all 8 pairings in the first group. The infeasibility when inputs 3 and 6 are unused do not need any further consideration as this pairing will violate other constraints in the model (constraints 6.13b and 6.13f in model A). For the 14 possible pairings (in the second group) that have a positive RGA-number, we consider the 2 possible pairings in $RGA^{1,4}$ as an example. The 2 possible pairings are $x_{1,2} = x_{2,3} = x_{3,6} = x_{4,5} = 1$ and $x_{1,3} = x_{2,2} = x_{3,6} = x_{4,5} = 1$. For the first of these pairings we have a RGA-number of 1.6. That is, we want a constraint that fulfills:

$$\text{If } x_{1,2} = x_{2,3} = x_{3,6} = x_{4,5} = 1, \text{ then RGA-number } (CM) \geq 1.6$$

We do not need to have $CM = 1.6$ since CM is penalized in the objective. Thus, the optimal value for CM is the smallest being feasible. The following inequality provides the necessary constraint on CM for this pairing.

$$1.6[(x_{1,2} + x_{2,3} + x_{3,6} + x_{4,5}) - 4] + 1.6 - CM \leq 0 \tag{6.54}$$

If all 4 x-elements are 1, then (5.54) is equivalent to $CM \geq 1.6$. If one or more x-elements are zero, then $CM \geq 1.6$ by at least one of the constraints (6.53) and (6.54). For the second possible pairing in $RGA^{1,4}$ the RGA-number is 2.4. To make this RGA-number active when this pairing ($x_{1,3} = x_{2,2} = x_{3,6} = x_{4,5} = 1$) is selected, the following constraint is added:

$$2.4[(x_{1,3} + x_{2,2} + x_{3,6} + x_{4,5}) - 4] + 2.4 - CM \leq 0 \tag{6.55}$$

Similar constraints are added for all 14 pairings in the second group. That is, the 145 constraints in the general formulation of model C (equation 6.45) can be replaced 15 constraints (constraint 6.53 plus 14 constraints similar to 6.54 and 6.55) for this particular example.

From this example, two points have become evident:

- The second controllability requirement may not always be well suited to distinguish between different pairings because many pairings may have RGA-number =0.
- In a given case, it may be possible to significantly simplify the general formulations of model B and C.

As a conclusion to the example, one should always investigate the characteristics of the particular HEN/plant to be operated instead of applying the general models directly. ■

6.7 Conclusions

The chapter has presented a parametric approach for optimal operation of HENs. The approach may be regarded as a quantified version of the sign method discussed in the previous chapter. The idea may also be utilized to extend the sign method to multiple bypass controlled outlet temperatures.

An ILP (or MILP) problem to find the optimal control configuration (pairing) is solved during operation. This optimization can be carried out periodically, or it may be performed when e.g. a new manipulation has saturated such that a new pairing has to be applied. The optimal control configuration is the pairing that gives the largest reduction (or smallest increase) in operating cost after the present control errors have been canceled. That is, for a given process state with given control errors, the method will find which bypasses should be manipulated in order to move the process towards the optimal state. The actual manipulations of the bypass fractions are done by SISO controllers.

It is emphasized here, that interactions have been disregarded in the formulation of the optimization problem. This may impose limitations in using the presented approach on

MIMO systems (i.e. multiple bypass controlled outlet temperatures for HENs). To what extent the method may fail to find the optimal operating state for MIMO plants should be thoroughly investigated. This investigation, probably together with further improvements, are topics for future research that need to be done before the approach can be recommended for practical use on MIMO plants.

The approach comprises three methods that differ from each other in how controllability considerations are implemented. No controllability considerations are made in model A. In model B, pairings resulting in plants that are not DIC are disregarded when there are alternatives giving DIC plants. Model C optimizes operating cost only when DIC plants exits, and also controllability considerations are used to distinguish between pairings with similar steady state properties. If no DIC plants exist, model C focuses solely on finding the pairing with the best controllability properties. Model C represents a major extension compared to the size of model A and model B. An example has shown that model C may be significantly simplified for a practical HEN.

For processes where the optimal operating state lies at the intersection of constraints, the approach presented in this chapter is an alternative to optimizing control schemes such as MPC (model predictive control) or periodic optimization of a steady state process model to find optimal setpoints. When the optimal operating state is at constraints, other strategies may led to computing an infeasible setpoint due to model errors or unknown disturbances. Alternatively, significant safety margins may be imposed in order to avoid infeasibility and thereby the operating state will be moved away from the optimal one. Of course, other strategies may be combined with on-line identification to improve the process model, but this will increase the complexity of the applied method. Since the optimization problem included in the approach presented here results in a control *configuration*, only errors leading to a different configuration will have any influence. Hence, the approach may be expected to be robust to model errors and unknown disturbances. The robustness to errors is, however, not investigated and a suggestion to further work is to verify this.

A disadvantage with the proposed approach is that the resulting control configuration may have bad control properties, e.g. an output may be controlled by a manipulation with only a small and slow effect. This may happen despite the controllability considerations included in two of the methods. Further, the pairing may vary during operation and this may be confusing for the operators, particularly if it should be necessary to operate the plant (or parts of it) manually.

Two of the proposed methods represent hierarchical strategies for operation. It has been demonstrated that such strategies can be implemented within the framework of mathematical programming. Discrete decisions and logic inference required for the hierarchical strategies are formulated as mathematical inequalities combining continuous and binary (logic) variables.

Notation

c	Vector containing utility costs.
CM	Controllability measure (i.e. value of RGA-number).
CP	Heat capacity flowrate.
d	Disturbance input.
e	Control error.
g	Element in transfer matrix.
G	Transfer matrix.
M	Large number (upper bound on continuous variable).
n	Number of . . . (e.g. n_y is the number of controlled outputs).
OC	Operating cost.
P	Priority matrix.
Q	Heat load (duty) of heat exchanger.
RGA	Relative gain array.
RGAn	Absolute value of each element in ($RGA_{i,j} - x_{i,j}$).
T	Temperature.
u	Manipulated input (bypass fraction).
X	Binary variable ($x_{i,j} = 1$ for selected pairing, $x_{i,j} = 0$ for not selected pairing).
y	Binary constant ($y_{i,j} = 1$ for pairing requiring reduction of u_j, otherwise $y_{i,j} = 0$.
z	Binary constant to denote if *u* is saturated at upper or lower bound.

Greek:

α	Global binary variable to denote whether selected pairing is DIC.
β	Set of binary constants to denote if the corresponding RGA-element is negative.
δ	Upper bound on negative values of RGA-elements.
ε	Detuning factor.
γ	Logical variable for computation of RGA-number.

Superscripts:

BP	Bypass.
k	Index for unused input.
lo	Lower.
up	Upper.
U	Utility (concerns utility consumption in each utility exchanger).
U$	Utility cost (total utility cost in money per time unit).

Subscripts:

max	Maximum.
o	Actual output or outlet (temperature).
s	Supply (temperature).
t	Target or reference (temperature).
y	Controlled outputs.

References

Biegler, L.T., I.E. Grossmann and A.W. Westerberg (1997*). Systematic Methods for Chemical Process Design*. Prentice-Hall Inc. Upper Saddle River, NJ.

Grosdidier, P., M. Morari and B.R. Holt (1985). Closed-loop Properties from Steady state Gain Information. *Ind. Eng. Chem. Fund.*, **24**, 221-235.

Linnhoff, B. *et al*. (1982). *User Guide on Process Integration for the Efficient Use of Energy*. Inst. Chem. Engrs., Rugby, UK.

Mathisen, K.W. (1994). Integrated Design and Control of Heat Exchanger Networks. *Ph.D. Thesis*. University of Trondheim - NTH, Norway.

Skogestad, S. and M. Morari (1988). Variable Selection for Decentralized Control. *AIChE Annual Meeting*, Washington DC. Paper 126f. Reprinted in *Modeling, Identification and Control*, 1992, **13** No. 2, 113

Skogestad, S. and I. Postlethwaite (1996*). Multivariable Feedback Control, Analysis and Design*. John Wiley & Sons, Chichester, UK.

Chapter 7

ON-LINE OPTIMIZATION AND SELECTION OF MEASUREMENTS

This is the last of three chapters that discuss optimal operation of a general heat exchanger network. A method that combines the use of steady state optimization and decentralized feedback control is proposed. A general steady state model is developed, which is easily adapted to any heat exchanger network. Using this model periodically for optimization, the operating conditions that minimize utility cost are found. Setpoints are constant from one optimization to the next, and special attention is paid to the selection of measurements such that the utility cost is minimized in the presence of unknown disturbances and model errors. As opposed to the two preceding chapters, the method in this chapter results in a *fixed* control structure. In addition to heat exchanger networks, the proposed method may also be applied to other types of processes where the optimum lies at the intersection of constraints.

The method is proposed by Glemmestad *et al.* (1997), and much of the content in this chapter is taken from that paper.

7.1 Introduction

The problem being addressed is the same as in the two previous chapters, i.e. optimal operation of a given HEN. The approach in this chapter, however, is different. A fixed control structure for control of the target temperatures is selected, and the optimization is carried out by utilizing the extra manipulations and extra measurements internally in the HEN. The method uses steady state optimization which is carried out on-line with regular time intervals. The result of this optimization is then implemented by specifying the optimal value (setpoint) of some variables ("optimization variables"). It will be shown that the

selection of which optimization variables that are controlled affect the performance of the HEN when unknown disturbances are present. A procedure for optimal selection of these variables is presented.

In the following, it is assumed that the stream data (heat capacity flowrates and supply/target temperatures), network structure and heat exchanger areas are given and that the HEN is sufficiently flexible. To manipulate the network it is assumed that utility duties can be adjusted and that a variable bypass is placed across each process-to-process heat exchanger. In case of stream splits, we may also assume that split fractions can be varied.

The remaining part of the chapter is organized as follows: First, the complete method is outlined in section 7.2 and it is demonstrated that the selection of which variables that are kept at setpoints influences the performance. In section 7.3, the procedure for selection of optimization variables will be described in detail, and the term robust optimum will be introduced in section 7.4. The steady state optimization model is presented in section 7.5, then the complete method is applied to an example in section 7.6 and finally some conclusions are drawn.

7.2 Outline of method

In order to perform a meaningful on-line optimization, it is required that there is at least one extra degree of freedom during operation. As shown in chapter 4, most HENs have this feature.

Figure 7.1a shows a schematic block diagram of the method that will be described. The optimizer contains a scalar objective function (criterion) J which indicates how well the HEN is operated, and a steady state model of the HEN. As the objective function we will use total utility cost of the HEN. The model is optimized regularly and reference values for the optimization variables are passed to the controller K_2. The reference values (setpoints) are constant in the period between each optimization.

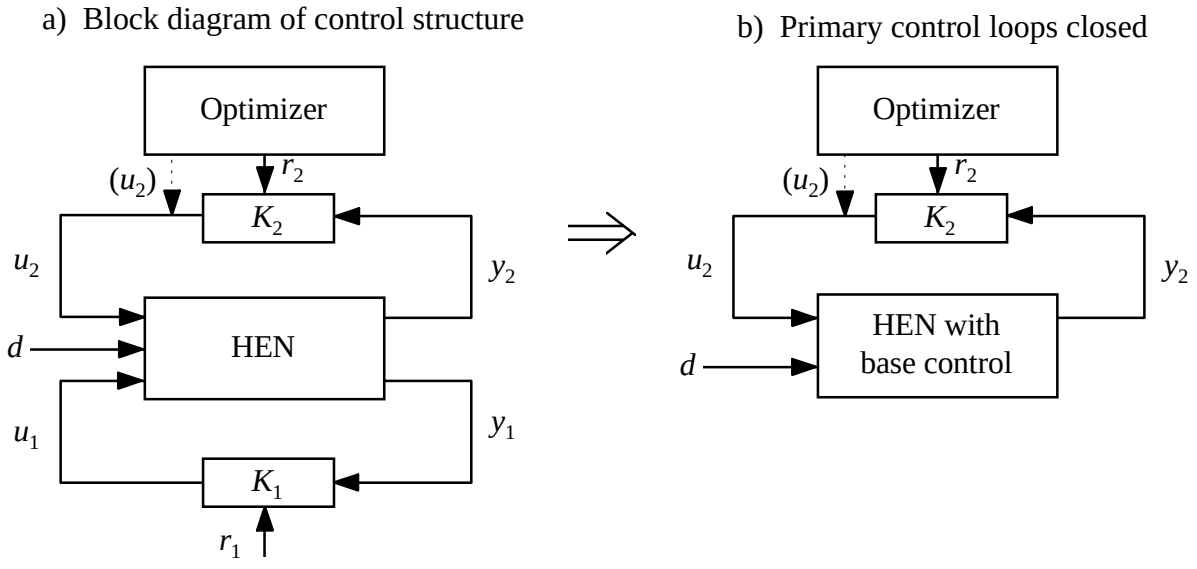

Figure 7.1 General optimizing control structure.

All inputs (manipulations) u and outputs (measurements) y are separated into $u = [u_1 \quad u_2]^T$ and $y = [y_1 \quad y_2]^T$, respectively. y_1 are those outputs which have given target (reference) values and u_1 are those manipulations dedicated to keep y_1 at their target values. Satisfying the targets for y_1 is simply the primary goal of optimal operation (definition 2.1). Now, we close the control loops for the primary outputs with controller K_1 ("base control") and assume integral action in the loops (no steady state control error). This leads to figure 7.1b where focus is on the remaining part of the system, i.e. the secondary variables (u_2, y_2 and setpoints r_2) and the optimizer. It is simply assumed that the base control is implemented and that it works.

We want to focus on the secondary goal of optimal operation; utility cost minimization (variables associated with this goal have index 2). u_2 is the "excess" manipulation(s) which represent the degree(s) of freedom that we will use to minimize utility cost. Of course, one could compute optimal values for u_2 and apply these directly (open-loop implementation) as indicated by the dashed line in figure 7.1a and 7.1b. Alternatively, the optimizer could pass reference values for some "extra" measurements y_2 (closed-loop implementation). If the disturbance d was perfectly known (and constant), it would not matter (at steady state) which variables were chosen. However, from the explanation below it will be clear that the selection of *which* variables that are passed from the optimizer down to the control level affects how close to optimum the HEN can be operated.

The variables (setpoints) r_2 that are passed from the optimizer to the control level will be denoted *optimization variables*.

Let the disturbance d be partitioned into the following two contributions:

$$d = d_0 + d_u \tag{7.1}$$

where d_0 is the information that the optimizer has about the disturbances when it performs an optimization, and d_u (unknown disturbances) are all deviations from d_0 and the real disturbance until a new optimization is carried out. That is, d_u consists of for example unknown disturbances and model errors in addition to changes of the disturbances in the period between two optimizations (optimization interval). Measurement/estimation errors will not be handled explicitly in this chapter, but these errors may be included in d_u and treated as any other deviation.

Since the optimizer has no specific information about d_u, the optimization is based on $d = d_0$. In practice, however, d_u may vary within some known (or selected) bounds. The effect of $d_u \neq 0$ should be taken care of in the optimizer in order to avoid that the HEN becomes infeasible (primary goal can not be satisfied) for some disturbances. Figure 7.2 shows a typical situation for a general plant with one degree of freedom (one extra manipulation) and an objective function J that should be minimized. The plant has one disturbance input and two candidate measurements A and B ($y_2 = [y_{2,A} \quad y_{2,B}]^T$) that can be controlled to a desired value using the extra manipulation u_2. (Since subscripts 1 and 2 are used to distinguish between the primary and secondary sets of inputs and outputs, we uses letters A, B etc. to denote individual elements of u and y). Also, remember that base control to keep primary outputs at fixed setpoints is already implemented.

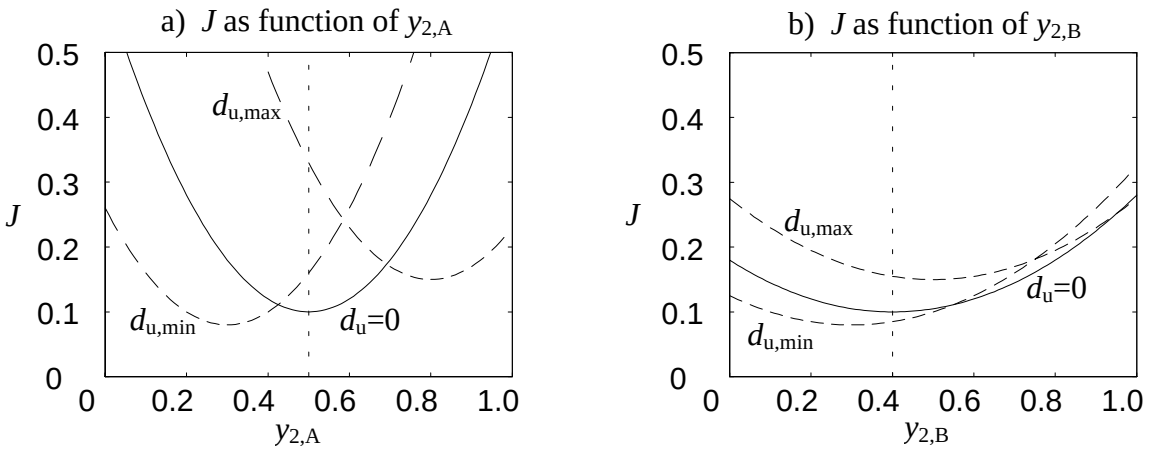

Figure 7.2 Unconstrained process.

Figure 7.2a shows J as a function of $y_{2,A}$ with the disturbance as a parameter. The solid line is for $d_u = 0$, and the two dashed lines represent the extremes for d_u. Figure 7.2b shows similar curves as a function of $y_{2,B}$. Since we have to base our optimal values on $d_u = 0$, we can choose to keep either $y_{2,A} \approx 0.5$ or $y_{2,B} \approx 0.4$ using feedback control. From the figure, however, we see that when keeping $y_{2,B}$ constant, J is *less sensitive to both variations in* y_2 (control error) *and to unknown disturbances*, than when keeping $y_{2,A}$ constant. Therefore we prefer to keep $y_{2,B}$ constant between the optimizations. This simple example illustrates how the choice of optimization variables affects the objective function for an unconstrained process. Figure 7.3 shows similar curves as in figure 7.2 for a process where the optimum is *constrained*, which is typical for most HENs. (Minimum utility consumption corresponds to maximum utilization of process-to-process exchangers which again means that some bypasses are closed).

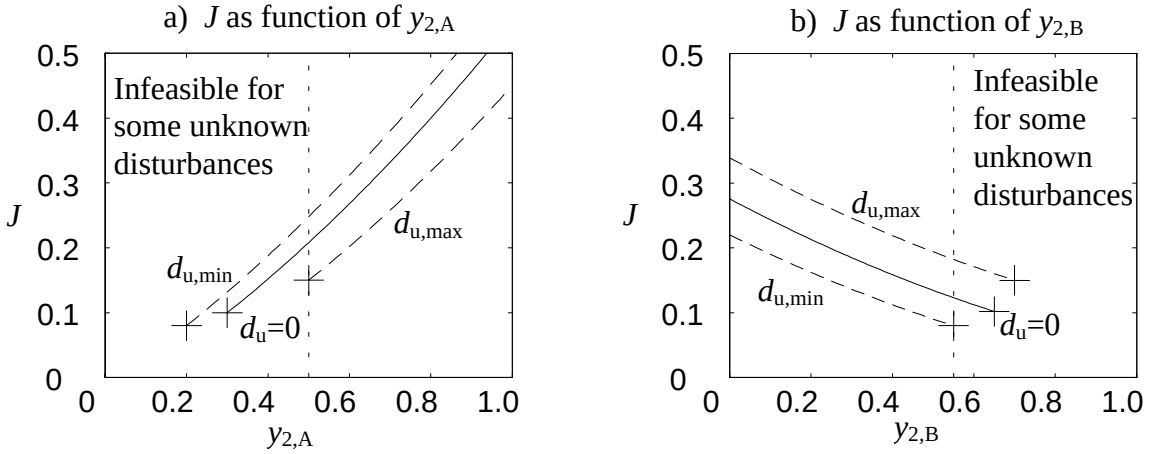

Figure 7.3 Constrained process (typical for HENs).

In figure 7.3a the process is infeasible when $y_{2,A}$ becomes too small (marked with "+"). In a HEN this typically happens when a bypass saturates such that a target temperature no longer can be met. When $y_{2,B}$ is kept at a given value (figure 7.3b) the process is infeasible when the value becomes too *large*. More interesting in the constrained case, however, is that the *nominal* optimum ($d_u = 0$) is *infeasible* for some unknown disturbances. That is, we have to "back off" from the nominal optimum and find the optimal values that are feasible for all

unknown disturbances. These values are indicated with the vertical dashed lines in figure 7.3a and 7.3b. Again we see that it is preferred to keep $y_{2,B}$ (rather than $y_{2,A}$) constant. However, a new obstacle has occurred; we need a remedy in the optimizer to find the values that are optimal also in the presence of the unknown disturbances. We do not want to compute optimum for all possible disturbances during operation since this may be too time consuming. This problem can be solved by computing proper constraints ("safety margins") on u_1 that are implemented in the optimizer. The optimal value of these safety margins is strongly correlated to the choice of optimization variables.

The following steps summarize the main parts of the complete procedure for on-line optimization of HENs:

1. Determine which manipulations (u_1) that should be used to control the primary outputs y_1 and design a control configuration and controllers for the primary goal (base control).
2. For each excess manipulation u_2 choose a measurement y_2 (among all candidates) such that the operation is insensitive to disturbances (see more details in next section). The additional constraints (safety margins) on u_1 are also found. Design decentralized controllers to control y_2.
3. Implement the steady state model including the constraints found in step 2 in the optimizer.

During operation, the optimizer computes setpoints for the optimization variables and apply these to the controller K_2 at regular intervals.

7.3 Selection of measurements

This section describes a procedure for selection of optimization variables (step 2 in the complete method given above). The selection of outputs for optimizing control is discussed in Morud (1995, chapter 8) and in Skogestad and Postlethwaite (1996, chapter 10). In the latter, a method that is based on choosing outputs that maximize $\underline{\sigma}(G_{22})$ (smallest singular value) for a properly scaled system is proposed. In this chapter a more direct method is applied (which is also mentioned in Skogestad and Postlethwaite, 1996). Before the procedure is presented, the following notation is introduced:

$y_{2,\text{cand}}$ is a vector containing all candidates to y_2.

y_{opt} is the optimal value of $y_{2,\text{cand}}$ for a given d_u.

y_{opt}^s is a fixed value of $y_{2,\text{cand}}$ such that the objective function is minimized while the network is feasible for all d_u.

J^s is $J(y_{\text{opt}}^s)$ for a given value of d_u.

Δu_1 is the constraint imposed on u_1 such that an optimization problem based on $d_u = 0$ gives feasibility for all d_u within prespecified bounds.

The steps in the procedure are listed below and some of the points will be further explained. For simplicity, we will assume there is only one degree of freedom (one optimization variable).

a) Select (i) minimum and maximum values for d_u, (ii) the objective function J, (iii) the entries of $y_{2,cand}$, (iv) the values for d_u that should be included in the computations and (v) define the type of J_{mean} that will be used for choosing optimization variable.

b) Compute y_{opt} and J_{opt} for "all" cases of d_u (i.e. the values from step (iv) in the previous point), see table 7.1. This table may also include row(s) for $u_{2,opt}$ (open-loop implementation). Note that $d_{u,j}$ is *case j* of d_u while $y_{opt,i}$ denotes *element i* in y_{opt}.

	$d_{u,1}$	$d_{u,2}$	$d_{u,j}$
$y_{opt,\,A}$	$y_{opt,\,A}(d_{u,1})$	$y_{opt,\,A}(d_{u,2})$	$y_{opt,\,A}(d_{u,j})$
$y_{opt,\,B}$	$y_{opt,\,B}(d_{u,1})$	$y_{opt,\,B}(d_{u,2})$	$y_{opt,\,B}(d_{u,j})$
$y_{opt,\,i}$	$y_{opt,\,i}(d_{u,1})$	$y_{opt,\,i}(d_{u,2})$	$y_{opt,\,i}(d_{u,j})$
J_{opt}	$J_{opt}(d_{u,1})$	$J_{opt}(d_{u,2})$	$J_{opt}(d_{u,j})$

Table 7.1 y_{opt} and J_{opt} for all cases of d_u.

c) Keep $y_{2,cand,i} = y^s_{opt,i}$ for each output candidate, and evaluate $J_i^s(d_{u,j})$ and the resulting J_{mean}. In general, the setpoint $y^s_{opt,i}$ should be optimized in order to minimize J_{mean}, but for constrained processes it will be some extreme value from table 7.1 (to ensure feasibility for all d_u).

	$d_{u,1}$	$d_{u,2}$	$d_{u,j}$	J_{mean}
J^s_A	$J^s_A\,(d_{u,1})$	$J^s_A\,(d_{u,2})$	$J^s_A\,(d_{u,j})$	$J_{mean,\,A}$
J^s_B	$J^s_B\,(d_{u,1})$	$J^s_B\,(d_{u,2})$	$J^s_B\,(d_{u,j})$	$J_{mean,\,B}$
J^s_i	$J^s_i\,(d_{u,1})$	$J^s_i\,(d_{u,2})$	$J^s_i\,(d_{u,j})$	$J_{mean,\,i}$

Table 7.2 J^s for all cases of d_u.

d) Choose the variable that gives the smallest J_{mean} from the last column in table 7.2 as optimization variable, i.e. this measurement should be controlled to a setpoint which is updated periodically by the optimizer.

We have now found the best optimization variables. To simplify the on-line optimization we may want to use only the nominal disturbance set, $d_u = 0$. To ensure that we find the correct value of y^s_{opt} (which ensures feasibility for all disturbances), we may impose some constraint ("safety margin") for the optimizer, e.g. $u_1 \geq \Delta u_1$. This will be explained in more detail for a simple example in section 7.6. (See also remark 7.1 at the end of this section). The "safety margin" on u_1 should of course not be implemented in the regulatory control level.

Until now we have only considered one degree of freedom. If there were 2 degrees of freedom, 2 elements of $y_{2,cand}$ would have to be fixed at a time. Table 7.2 would need as many rows as there are possibilities to pick two variables out of the total number of candidate

measurements. For example, if there are 6 candidate measurements and 2 degrees of freedom, the number of possibilities is $\frac{6!}{2!4!} = 15$.

REMARK 7.1. It is clear that the value of Δu_1 may depend on d_0. We assume that this change is small and that the value can be used for all d_0. In practice, one should carry out the procedure for selection of optimization variables for different d_0, to verify that Δu_1 does not change too much. The worst case value should be chosen if it is not acceptable to violate the primary goal, while a mean value can be used if a small violation to the targets is tolerable.

7.4 Robust optimum

This section introduces the term *robust optimum*. It will be clear that, when we have made a selection of variable(s) for y_2, we seek the value of this variable that corresponds to the robust optimum. The robust optimal value is the optimal value when unknown disturbances and model errors are encountered. The robust optimum will often be different from the nominal optimum, where no disturbances (only nominal disturbance values) or model errors are considered.

For the unconstrained and smooth objective function in figure 7.2, the value of y_2 resulting in robust optimum is approximately equal to the value resulting in nominal optimum. For the constrained objective function in figure 7.3, the situation is different. We require that the process is feasible for the unknown disturbances. When $y_{2,A}$ is selected, the *nominal* optimal value is $y_{2,A} = 0.30$ whereas the value resulting in *robust* optimum is $y_{2,A} = 0.50$. When $y_{2,B}$ is selected, the *nominal* optimal value is $y_{2,B} = 0.65$ whereas *robust* optimum is achieved for $y_{2,A} = 0.55$. It is clear that the nominal optimal value cannot be applied since this will result in infeasiblity for some unknown disturbances.

Mathematically, if we have an objective function $J(x, d)$ where the value of the variable (argument) x can be selected/manipulated and d represent the disturbances, we can write

$$\text{Nominal optimum:} \quad J_{\text{nopt}} = \text{opt}(J(x, d = d_0))$$

$$\text{Robust optimum:} \quad J_{\text{ropt}} = \text{opt}(J(x, d \in D))$$

In operation, we are not interested in the objective value directly, however, the argument (e.g. manipulations or setpoints) that minimize the objective is more relevant:

$$\text{Nominally optimal argument:} \quad x_{\text{nopt}} = \arg \operatorname*{opt}_x (f(x, d = d_0))$$

$$\text{Robust optimal argument:} \quad x_{\text{ropt}} = \arg \operatorname*{opt}_x (f(x, d \in D))$$

The set D represent the possible values of the unknown disturbances. D may also represent a *probability distribution* of the unknown disturbances. The disturbances may for instance be assumed to be normally distributed with a given mean (nominal) value and a given standard deviation. If the probability distribution is not bounded, we cannot require the process to be feasible for *all* possible disturbances. Instead, we could require feasibility with a specified probability, such as requiring feasibility in 99% of the operating time. We shall, however, use a different approach where the disturbances are specified by probability distributions:

When a HEN is announced infeasible during operation, this normally does not imply that the HEN cannot be operated. Typically, the reason for infeasibility is that it is impossible to reach the targets for the primary measurements (outlet temperatures). Instead of requiring that the targets are satisfied, we choose to penalize the deviation (control error in primary control loop). In this way, the constrained problem is transformed into an unconstrained problem, however, the new objective function will often be *asymmetric*. This implies that the robust optimum is different from the nominal optimum.

In the search for the robust optimum, we simply use Monte Carlo simulations. That is, random disturbances are generated from the given probability distribution. For each set of random disturbances the objective J is computed as a function of the selected secondary variable. This is repeated for a large set of randomly generated disturbances, and the robust optimum is the optimum of the mean value of J for the set of disturbances.

An example is shown in figure 7.4. below. There are 2 different disturbances and they are both normally distributed. The thin solid line shows the objective J as a function of the selected secondary measurement y_2 for the nominal disturbances. Starting from a high value of y_2, the objective decreases when y_2 decreases until the nominal optimum where $y_2 = 150$. Decreasing y_2 further, the primary outputs can no longer be kept at target. This is penalized in the objective function resulting in a steep increase of the objective.

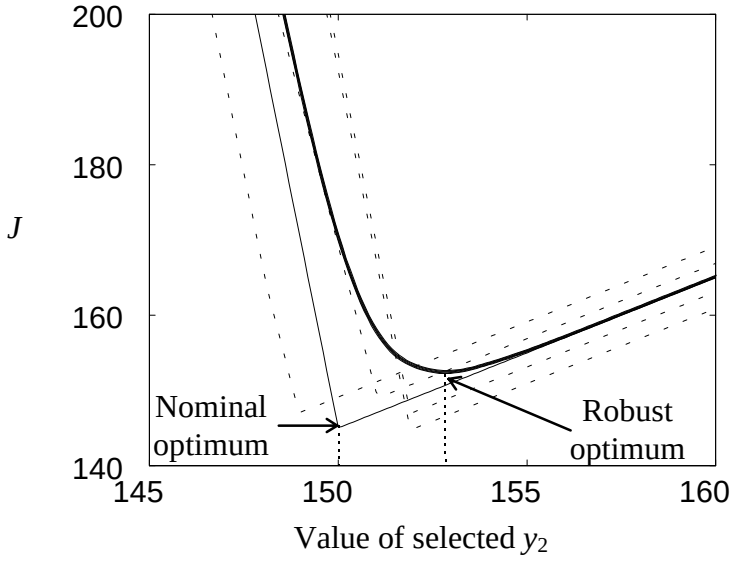

Figure 7.4 Robust optimum

The 4 dashed lines show the objective for 4 different sets of the disturbances. The location where the primary targets are violated and objective increases steeply, depends on the value of the disturbances. The most interesting curve in figure 7.4, however, is the thick solid curve. This curve is the average of 1000 randomly generated sets of disturbances. While each fixed disturbance result in a sharp break of the corresponding curve, the average curve is smooth. To reach the robust optimum, a setpoint of $y_2 \approx 153$ should be applied. The robust optimum is slightly above 150, which is higher than the nominal optimum of $J = 145$. However, applying the nominally optimal values of $y_2 = 150$, the *expected* value of the objective is roughly $J \approx 170$. Since we do not know the exact value of the disturbances, only

the probability distribution, the optimal setpoint for y_2 is the value corresponding to the robust optimum ($y_2 \approx 153$).

The curves in figure 7.4 are actually based on the results for the HEN in the example in section 7.6, when the disturbances are normally distributed. The supply temperature of stream H1 has a mean value of 190°C and a standard deviation of 3°C, while CP_{C2} has a mean value of 0.50kW/°C and a standard deviation of 0.01kW/°C. The variable selected for y_2 is the setpoint for temperature T_1 (in figure 7.6) and the objective function is:

$$J = \text{utility consumption [kw]} + 25\left|T_{C2}^{o} - T_{C2}^{t}\right| + 25\left|y_2 - r_2\right|$$

That is, a deviation of 1°C in the bypass controlled temperature or in T_1 is assumed to "cost" the same as 25kW.

If the Monte Carlo method is not used and one requires the process to be feasible (primary targets met) for all possible unknown disturbances, a number of difficulties may be encountered in practice:

1. The worst case may not be at the corner points for the disturbances, thus finding the worst case disturbances may be a difficult task itself.
2. Even a corner point check may be time consuming and even prohibitive when there are many independent disturbances.
3. If there are more than just a few disturbances, the probability that all have the worst case values at the same time is very small.

Taking these 3 points into account, it is assumed that Monte Carlo simululations will give reasonable results for most practical cases. Using the Monte Carlo approach, it is also straightforward to include dependencies between different disturbances when such information is available. Despite this preference for the Monte Carlo approach, in the example in section 7.6 it is required that the HEN is feasible at the corner points for the 2 disturbances.

A disadvantage with the Monte Carlo method is that a large number of disturbance sets may have to be generated in order to get good results, and it is difficult to say in advance how many disturbance sets that are necessary. However, as it is explained in the previous section, the robust optimum is only determined once (or for a few cases) and this is done off-line. The difference in the nominal and robust optimal values are used to find a constraint on the primary manipulations u_1. With this constraint, the (approximate) robust optimum is found periodically from the measured and inaccurate values of the disturbances.

7.5 Steady state optimization model

This section presents a steady state model that can be adapted to any HEN. It is developed primarily for implementation in the optimizer, however, it may also be used in the procedure for selection of optimization variables (to generate tables 7.1 and 7.2).

Before we present the general model, consider the two alternatives (equations (7.2) and (7.3), respectively) to model a single heat exchanger with bypass, see figure 7.5.

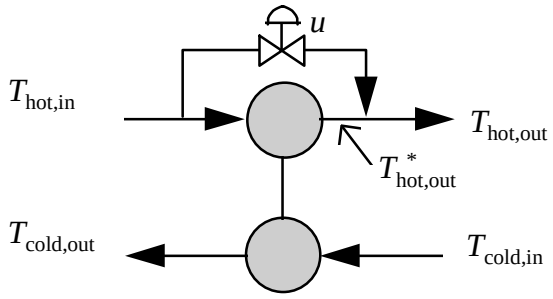

Figure 7.5 Single heat exchanger with bypass.

At steady state it is of no consequence whether the bypass is placed across the hot side or cold side, and the choice in the figure is arbitrary. The temperature driving force $\Delta T_m(\cdot)$ may be the logarithmic mean or some approximation to it. Note particularly the difference between equations (7.2a) and (7.3) regarding the arguments of $\Delta T_m(\cdot)$.

$$Q = UA\Delta T_m(T_{hot,\,in}, T_{cold,\,in}, T^*_{hot,\,out}, T_{cold,\,out}) \tag{7.2a}$$

$$T_{hot,\,out} = uT_{hot,\,in} + (1-u)T^*_{hot,\,out} \tag{7.2b}$$

$$Q \le UA\Delta T_m(T_{hot,\,in}, T_{cold,\,in}, T_{hot,\,out}, T_{cold,\,out}) \tag{7.3}$$

Equation (7.2) includes the hot exit temperature before it is mixed with the bypass stream and this results in bilinearities in (7.2b). The inequality in (7.3) expresses a constraint on Q when the boundary is placed *outside* the bypass splitter and mixer. The bypass fraction u does not even occur in (7.3), but the equality part of (7.3) corresponds to $u = 0$. In the optimization model, we choose the second alternative for each heat exchanger since this eliminates the bilinearities in the bypass mixer. If u is needed, it can be found after the optimization of the network by solving one nonlinear equation for each bypass fraction. This equation can be found from solving (7.2b) for $T^*_{hot,\,out}$ and inserting this expression into (7.2a), which is solved for u through iteration. (Solving one unknown in one nonlinear equation n times is much simpler than solving n unknowns in n nonlinear equations simultaneously). As it will be shown, the value of u is often *not* required explicitly as it normally is the manipulated input in a feedback control loop.

The steady state model for a general HEN uses the following sets of heat exchangers:

PHX : Set of all Process-to-process Heat eXchangers.

HBT : Subset of PHX with Hot side outlet directly entering a Bypass controlled Target.

CBT : Subset of PHX with Cold side outlet directly entering a Bypass controlled Target.

HUT : Subset of PHX with Hot side outlet entering a Utility controlled Target (through a cooler).

CUT : Subset of PHX with Cold side outlet entering a Utility controlled Target (through a heater).

HS : Subset of PHX with Hot side inlet directly entering from a (hot) Supply.

CS : Subset of PHX with Cold side inlet directly entering from a (cold) Supply.

The general HEN model shown below (equations 7.4 to 7.12b) is an NLP problem. The variable *c* in equation (7.4) denotes the cost (pr. energy unit) for the utilities.

$$\min\left(\sum_{i\in\mathrm{HUT}} c_i^{\mathrm{coolers}} Q_i^{\mathrm{coolers}} + \sum_{j\in\mathrm{CUT}} c_j^{\mathrm{heaters}} Q_j^{\mathrm{heaters}}\right) \tag{7.4}$$

subject to

Equalities, (7.5) to (7.9)

$$Q_i = CP_i^{\mathrm{hot}}\left(T_i^{\mathrm{hot,in}} - T_i^{\mathrm{hot,out}}\right) \qquad i \in \mathrm{PHX} \tag{7.5a}$$

$$Q_i = CP_i^{\mathrm{hot}}\left(T_i^{\mathrm{hot,in}} - T_i^{\mathrm{hot,out}}\right) \qquad i \in \mathrm{PHX} \tag{7.5b}$$

$$Q_i^{\mathrm{coolers}} = CP_i^{\mathrm{hot}}\left(T_i^{\mathrm{hot,out}} - T_i^{t}\right) \qquad i \in \mathrm{HUT} \tag{7.6a}$$

$$Q_i^{\mathrm{heaters}} = CP_i^{\mathrm{cold}}\left(T_i^{\mathrm{t}} - T_i^{\mathrm{cold,out}}\right) \qquad i \in \mathrm{CUT} \tag{7.6b}$$

$$T_i^{\mathrm{hot,out}} = T_i^{\mathrm{t}} \qquad i \in \mathrm{HBT} \tag{7.7a}$$

$$T_i^{\mathrm{cold,out}} = T_i^{\mathrm{t}} \qquad i \in \mathrm{CBT} \tag{7.7b}$$

$$T_i^{\mathrm{hot,in}} = T_i^{\mathrm{s}} \qquad i \in \mathrm{HS} \tag{7.8a}$$

$$T_i^{\mathrm{cold,in}} = T_i^{\mathrm{s}} \qquad i \in \mathrm{CS} \tag{7.8b}$$

Interconnection equations (problem specific) (7.9)

Inequalities, (7.10) to (7.12b)

$$Q_i \le \alpha_i U_i A_i \Delta T_{\mathrm{m}\,i} \qquad i \in \mathrm{PHX} \tag{7.10}$$

$$Q_i \ge 0 \qquad i \in \mathrm{PHX} \tag{7.11}$$

$$Q_i^{\mathrm{coolers}} \ge 0 \qquad i \in \mathrm{HUT} \tag{7.12a}$$

$$Q_i^{\mathrm{heaters}} \ge 0 \qquad i \in \mathrm{CUT} \tag{7.12b}$$

Note that the index denotes heat exchangers and *not* streams (which is common in many other models), and that ΔT_{m} denotes the temperature driving force *outside* the bypass stream as in equation (7.3). As an example, the network in figure 7.6 will lead to the following sets: PHX = {A,B}, HUT = {B}, CUT = {A}, HBT = ∅, CBT = {B}, HS = {A} and CS = {A,B}, and the only interconnection equation (7.9) is $T_{\mathrm{A}}^{\mathrm{hot,out}} = T_{\mathrm{B}}^{\mathrm{hot,in}}$.

During each optimization, T^{t}, T^{s}, *CP* and *UA* for each heat exchanger are treated as constants. The model is valid without modifications for networks with fixed stream split fractions since *CP* denotes heat flow capacity in each heat exchanger. For networks with variable stream splits, *CP* in the split streams can be regarded as variables, and equations that

preserve the mass balance in the splitter(s) and energy balance in the mixer(s) must be included. During operation, variable stream splits can be used as manipulated inputs.

The constant α in equation (7.10) is a factor that may limit the duty of a heat exchanger somewhat below its theoretical maximum. This is simply the way that the constraint on u_1 is implemented. Instead of implementing $u_1 \geq \Delta u_1$ directly (which is impossible since the model does not include u_1), the corresponding value for α has to be computed. This is done separately for each heat exchanger that controls a primary output. The example below explaines how this can be done. For heat exchangers associated with u_2, we have $\alpha = 1$.

The model does not include any upper constraints on the duty of the utility exchangers, and this implies the assumption that these are designed to handle the required duty. If this is not the case, additional constraints have to be added to the model, e.g. an upper limit on the duty.

The only possible source of nonlinearities in the model (for networks without variable splits) is the term ΔT_m in equation (7.10). In other words, if arithmetic mean (as opposed to logarithmic mean) is used as the temperature driving force, the model can be solved as an LP problem. The following procedure for solving the model has proven to be reliable: First, use arithmetic mean in (7.10) for all exchangers and solve the corresponding LP problem. Second, replace arithmetic mean with logarithmic mean (or e.g. Paterson or Chen approximations) and solve the NLP problem using the LP solution as the initial value.

7.6 Example

The HEN used in the example is shown in figure 7.6. The primary outputs are the outlet temperatures of each stream which should be controlled to their target values of 30, 160 and 130°C for streams H1, C1 and C2, respectively. That is, we have

$$y_1 = \begin{bmatrix} T_{H1}^{o} & T_{C1}^{o} & T_{C2}^{o} \end{bmatrix}^T$$

where superscript ^{o} denotes outlet temperature. There is a total of four manipulations (two bypasses and two variable utility duties) which gives

$$u = \begin{bmatrix} u_A & u_B & q_c & q_h \end{bmatrix}^T$$

There are two disturbances; ±10°C in the supply temperature of stream H1 and ±0.05 kW/°C in the *CP* of stream C2. These values represent the maximum variations d that may be present. The smaller variations/errors (d_u) that may occur within the optimization interval is defined in step 2a) of the procedure. *UA* for heat exchangers A and B are 0.523 and 1.322 kW/°C, respectively. For simplicity, it is assumed that the utility exchangers are able to deliver sufficient duty for all possible cases. With this assumption and the given *UA*-values, all target temperatures can be reached for all combinations of disturbances mentioned above.

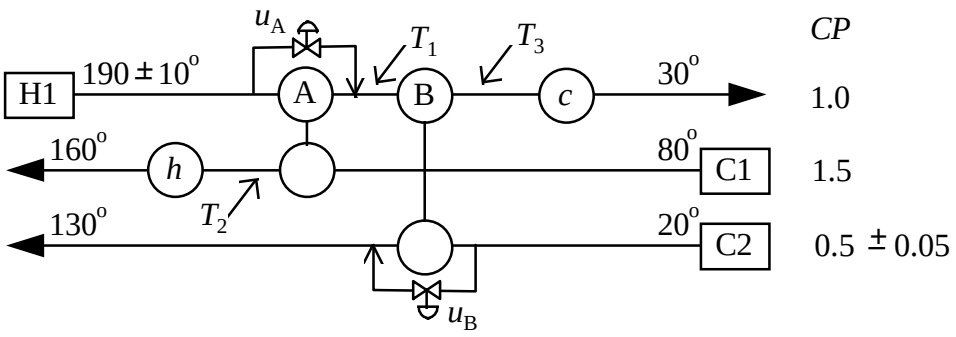

Figure 7.6 Heat exchanger network used in example.

Applying the procedure step by step yields:

Step 1. Assign primary manipulations.
We use the main rule for selection of manipulations in HENs which is to choose the manipulation closest to the measurement (e.g. Mathisen, 1994, chapter 4). This implies that the primary manipulations u_1 become q_c, q_h and u_B and these control the outlet temperatures of streams H1, C1 and C2, respectively.

Step 2. Selection of optimization variable.
There is one excess manipulation, $u_2 = u_A$, and the steps a) to d) below illustrate the selection of optimization variable.

2a) We assume:

(i) $d_u = [\pm 3°C, \pm 0.01 kW/°C]^T$ (maximum variations/errors of the disturbances within the optimization interval).

(ii) The objective function is $J = q_c + q_h$ (utility consumption)

(iii) Possible candidates to y_2 are $y_{2,cand} = [T_1 \ T_2 \ T_3 \ u_A]^T$ (see figure 7.6). Note that the open-loop implementation (u_A) is an alternative.

(iv) The computations are done for the four "corner points" of d_u in addition to $d_u = 0$. J_{mean} is the arithmetic mean of these five cases. (We require that target temperatures have to be reached for the five cases).

2b) y_{opt} and J_{opt} for different d_u are shown in table 7.3. The table is generated for $d_0 = [0 \ 0]^T$, i.e. for nominal values of the disturbances (190°C and 0.5kW/°C). Also a row for $u_{B,opt}$ is included for extra information.

2c) Table 7.4 shows J for optimal fixed values of $y_{2,cand}$. Note that in this example, the values for $y_{2,cand}$ can be found without optimization, but simply from table 7.3 and physical insight (see remark 7.2 at the end of this section). If there is a possibility that the optimum is not constrained one would have to resort to conventional optimization.

2d) From the last column of table 7.4 it is clear that keeping T_1 constant is preferred.

Step 3. Implementation of optimizer.
The model (including the sets and connection equations) was described in the previous section. The constraint ("safety margin") that should be included in the optimizer is

$u_B \geq 0.025$. We will explain how this value is obtained, but first we explain the details in the implementation of this constraint. To implement the constraint, we first find $q_B = 55$kW for $d_u = 0$ (55kW is the deficit heat of stream C2). Then we find $\alpha_B = 0.946$ from $q_B = \alpha_B UA_B \Delta T_{m,B}$, where the last term is the logarithmic mean for heat exchanger B for $d_u = 0$ and $T_1 = 151.9°C$. Implementing $\alpha_B = 0.946$ (and $\alpha_A = 1.0$) in equations (7.10) will ensure the required safety margin on u_B when unknown disturbances d_u are present.

	Case 1 $d_{u,1} = \begin{bmatrix} 0 \\ 0 \end{bmatrix}$	Case 2 $d_{u,2} = \begin{bmatrix} -3 \\ -0.01 \end{bmatrix}$	Case 3 $d_{u,3} = \begin{bmatrix} -3 \\ +0.01 \end{bmatrix}$	Case 4 $d_{u,4} = \begin{bmatrix} +3 \\ -0.01 \end{bmatrix}$	Case 5 $d_{u,5} = \begin{bmatrix} +3 \\ +0.01 \end{bmatrix}$
$T_{1,\,opt}$	150.0	149.0	151.0	151.9	151.9
$T_{2,\,opt}$	106.7	105.4	104.0	107.4	107.4
$T_{3,\,opt}$	95.0	95.1	94.9	98.0	95.8
$u_{A,\,opt}$	0.000	0.105	0.292	0.000	0.000
$u_{B,\,opt}$	0.000	0.000	0.000	0.038	0.011
J_{opt}	145.0	147.0	149.0	146.9	144.7

Table 7.3 Values for y_{opt} and J_{opt} for all cases of d_u in the example. Case 1 is the nominal disturbance.

	Case 1	Case 2	Case 3	Case 4	Case 5	J_{mean}
$J(T_1^s = 151.9)$	148.9	153.0	150.8	147.0	144.8	148.9
$J(T_2^s = 104.0)$	153.0	151.2	149.0	159.2	155.0	153.0
$J(T_3^s = 98.0)$	151.0	152.9	155.1	146.9	149.1	151.0
$J(u_A^s = 0.292)$	151.1	151.2	149.0	153.2	151.0	151.1

Table 7.4 J^s for the possible choices of measurement and for all cases of d_u in the example.

Note that all values for u_B (and the constraint Δu_B) differ from the values given in Glemmestad *et al.* (1997) for the same example. The values in that paper actually refer to the bypass fractions on the hot side of heat exchanger B (which is inconsistent with figure 7.6), while the correct values for the bypass fractions on the cold side are given here.

The actual value for the safety margin ($\Delta u_B = 0.025$) is obtained as follows: The values of u_A and u_B for the five cases in table 7.4 corresponding to $T_1 = 151.9°C$ are given in table 7.5. For cases 4 and 5, u_A saturates at zero which implies that it is no longer possible for u_A to maintain $T_1 = 151.9°C$. The optimizer uses d_0 (case 1) where u_B takes the value of 0.025. Thus, in order to handle cases 4 and 5, a safety margin of $\Delta u_B = 0.025$ has to be used by the optimizer. Note that if we accepted that T_1 deviated from its setpoint (due to saturation in u_A) it would be possible to further reduce utility consumption somewhat. Then the setpoint for T_1 could be reduced slightly below 151.9°C until u_B saturated for some disturbance. In this example we require that setpoints for secondary measurements have to be satisfied.

The reason for implementing the "safety margin" on u_B as an *inequality* constraint is that other values of d_0 may give $u_{B,opt} > 0.025$. Requiring $u_B = 0.025$ in such cases will result in infeasibility.

	Case 1	Case 2	Case 3	Case 4	Case 5
u_A	0.207	0.354	0.354	0	0
u_B	0.025	0.038	0.012	0.038	0.012

Table 7.5 Values of u_A and u_B when T_1 = 151.9°C.

The value for J_{mean} of 148.9 kW in table 7.4 should be compared to the mean value of J_{opt} from table 7.3 which is 146.5 kW. That is, it costs 1.6% of the utility consumption to guarantee feasibility for the worst case unknown disturbance.

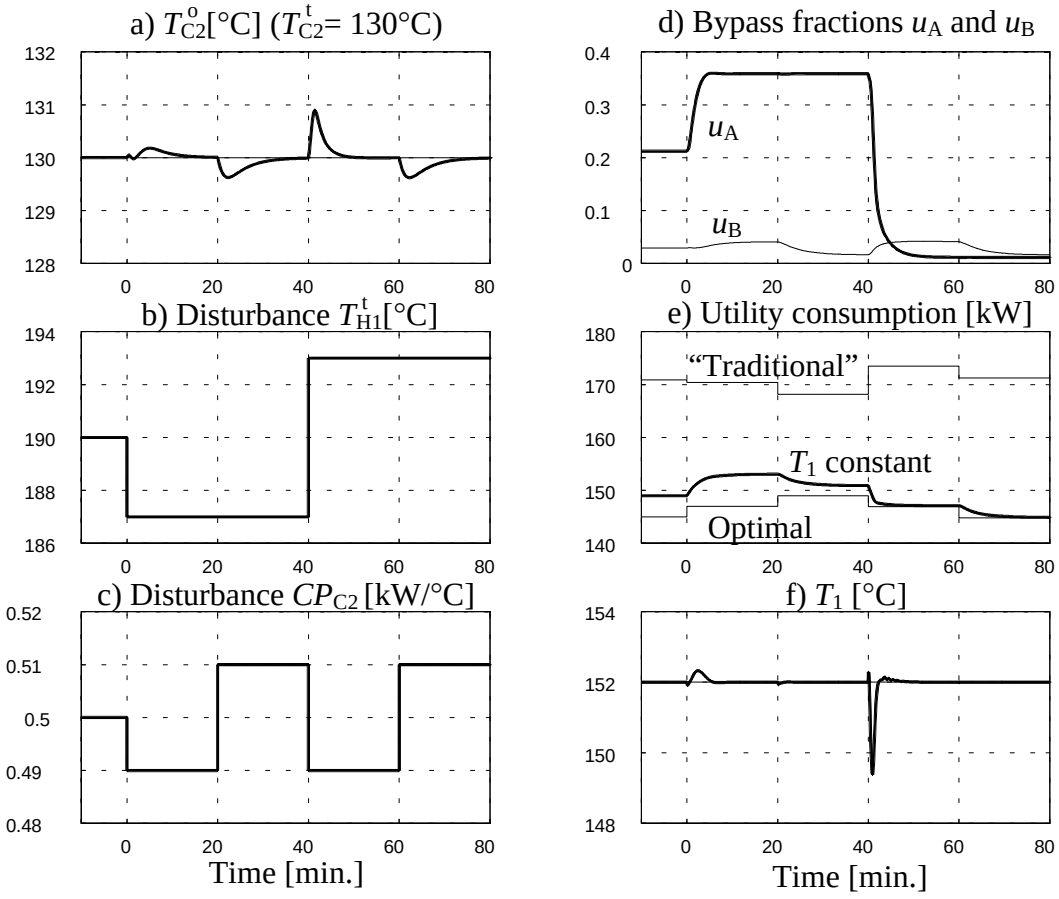

Figure 7.7 Results for example 7.1. (a) Controlled output T_{C2}^o with setpoint 130°C. (b) Disturbance T_{H1}^s. (c) Disturbance CP_{C2}. (d) Bypass u_A (thick line) and bypass u_B (thin line). (e) Utility consumption. (f) Temperature T_1 (secondary measurement), thick line shows actual value while thin line shows setpoint.

Figure 7.7 shows the results for the example when T_1 is selected as secondary measurement (optimization variable). Figure 7.7a shows that T_{C2}^o can be controlled to its setpoint for all unknown disturbances around the nominal operating point $d_0 = [0\ \ 0]^T$. Note from figure 7.7b and 7.7c, that the time up to zero corresponds to case 1 of d_u, from 0 to 20 minutes corresponds to case 2, from 20 to 40 minutes is case 3 and so on. Bypass fractions are shown in figure 7.7d, and u_A drops to close to zero after 40 minutes (case 4 and 5). The perhaps most important curves are shown in figure 7.7e. The steady state values for the utility consumption corresponds to the values in table 7.4 (upper row). The optimal values (when d_u is perfectly known) from the lower row of table 7.3 is also plotted for comparison. The utility

consumption should be compared with the "traditional" scheme *without* optimization also shown in figure 7.7e. The latter is implemented by fixing u_A at a value such that the network is just feasible for *all* possible disturbances, i.e. $d = [\pm 10, \pm 0.05]^T$, using u_B only. (This requirement gives $u_A = 0.680$). From the results given in figure 7.7 and table 7.4, it is clear that the main reduction in utility consumption compared to the traditional case is due to the periodic optimization (about 13% nominally), whereas the selection of optimization variable squeezes another 2.75% (between best and worst case).

Figure 7.7 has shown results around the nominal operating point corresponding to the cases 1 to 5 in tables 7.3 and 7.4. Only one optimization is done prior to the simulations, and the optimal setpoint for T_1 found here is maintained during the simulation (see figure 7.7f). Figure 7.8 shows similar results, but for a larger part of the operating region and with optimizations updating the setpoint for T_1 at 0, 20 and 40 minutes.

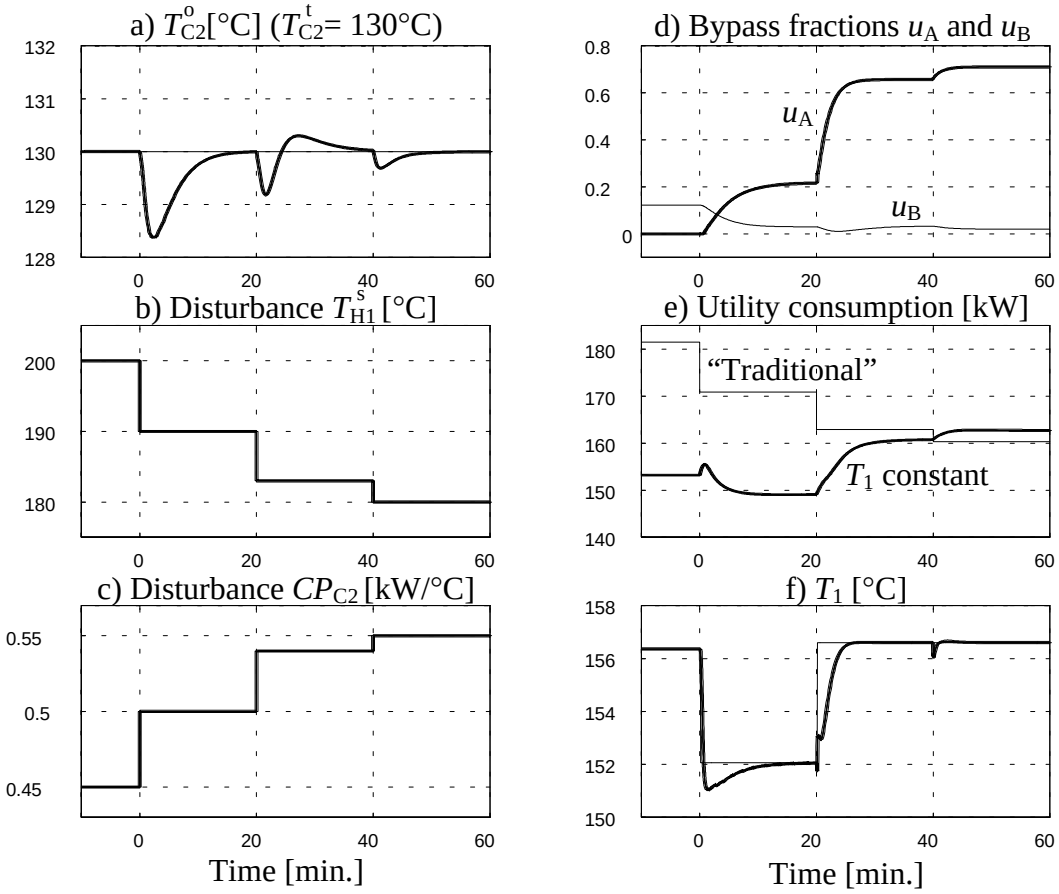

Figure 7.8 Results for example 7.1. The different curves show the same as figure 7.7 but for a larger part of the operating region, and with steady state optimization done at 0, 20 and 40 minutes.

At $t < 0$, we have $T^s_{H1} = 200$°C and $CP_{C2} = 0.45$kW/°C (i.e. $d = [10 \ -0.05]^T$). For this operating state, u_A is saturated at zero. For the steady state optimization carried out before the simulations started, the constraint on u_B was not active. From figure 7.8d we see that u_B cannot saturate if unknown disturbances (within the prespecified bound of $d_u \leq [\pm 3 \ \pm 0.01]^T$) occur. At time equal to zero, nominal operating conditions are encountered and an

optimization is performed immediately after. Figure 7.8f shows how T_1 is controlled to its new setpoint (which now has the same value as in figure 7.7). At $t = 20$, the (known) disturbance $d = [-7 \;\; 0.04]^T$ is applied and a new optimization is done. At $t = 40$, an *unknown* disturbance of $d_u = [-3 \;\; 0.01]^T$ is applied which brings the operating state to the opposite corner of where we started. Since the new disturbance is unknown, the optimizer now returns the same setpoint for T_1 as it computed at $t = 20$. The steady state value for u_B at this corner point is close to zero.

Note that the utility consumption at the last part of the simulation is similar for the "traditional" approach (u_A is fixed at 0.680) and the proposed method. This is because this corner point is limiting u_A for the traditional approach, thus this approach is optimal for this corner of the operating region. After 40 minutes (the extreme corner point) the traditional approach actually has lower utility consumption than the proposed method. This can be explained from the requirement we have made in this example that also the setpoint for T_1 should be satisfied when unknown disturbances are present. As mentioned above, relaxing this requirement could reduce the utility consumption somewhat further for this example.

REMARK 7.2. From figure 7.6, it is clear that decreasing T_1, T_3 (by decreasing u_A) or u_A will reduce utility consumption (J). I.e. optimal values for these variables in table 7.3 are minimum values (smaller values will violate the primary goal). Therefore, the case with the *largest* value has to be chosen as this is the smallest value feasible for all d_u. For T_2, a similar (but opposite) argument leads to choosing the *smallest* value in table 7.3.

7.7 Conclusions

A method for optimal operation of heat exchanger networks based on periodic steady state optimization is proposed. Compared to the methods in the two previous chapters, the method here focuses more on the control task. This is accomplished by the first step of the method where a fixed control structure for the outlet temperatures (primary measurements) is selected. Thus, all outlet temperatures are usually controlled by the heat exchanger located immediately upstream, and a fast response is obtained. The periodic steady state optimization concerns the setpoints for measurements *internally* in the HEN, which are controlled by the remaining manipulations. An important issue is the selection of which measurements that are kept at constant setpoints (using feedback control) between each optimization. The objective functions used during operation and for selection of optimization variables are identical. Optimal operating conditions for heat exchanger networks are normally located at the intersection of constraints, and additional constraints ("safety margins") have to be implemented in the optimizer in order to maintain the target temperatures when unknown disturbances are present.

Notation

c	Cost data
CP	Heat capacity flowrate
d	Disturbance
e	Control error
g	Element in transfer function/matrix

G	Process transfer function
K	Transfer function for controller
Q	Heat load (duty) of heat exchanger.
r	Reference (setpoint)
T	Temperature
t	Time
u	Manipulated input (bypass fraction)
y	Output (measurement)

Superscripts:

BP	Bypass
U	Utility
o	Actual output or outlet (temperature)
s	Supply (temperature)
t	Target or reference (temperature)

Subscripts:

0	Nominal
1	Primary
2	Secondary
C*i*	Cold stream *i*
H*j*	Hot stream *j*
m	Mean value
nopt	Nominal optimum
ropt	Robust optimum
u	Unknown

References

Glemmestad, B., S. Skogestad and T. Gundersen (1997). On-line Optimization and Choice of Optimization Variables for Control of Heat Exchanger Networks. *Comput. Chem. Engng.*, **21** Suppl., 379-384.

Mathisen, K.W. (1994). Integrated Design and Control of Heat Exchanger Networks. *Thesis*. (University of Trondheim - NTH, Norway).

Morud, J. (1995). Studies on the Dynamics and Operation of Integrated Plants. *Ph.D. Thesis.* University of Trondheim - NTH, Norway.

Skogestad, S. and I. Postlethwaite (1996*). Multivariable Feedback Control, Analysis and Design*. John Wiley & Sons, Chichester, UK.

Chapter 8

DISCUSSION AND CONCLUSIONS

In this concluding chapter, the first section provides a short discussion focusing on the compliance with industrial HEN operation problems. The second section summarizes the conclusions and contributions of the thesis. In the third and last section, some suggestions for future work within the area of operation of HENs are given.

8.1 Short discussion

This section provides a short discussion of some of the main topics covered in the previous chapters. The emphasis is on compliance with industrial problems.

In this thesis, the HEN operation problem has been treated to be completely decomposed from other parts of the process. This is in accordance with most other academic work within this area. In section 2.1 it was argued that "good" control of the HEN is desired as it gives "small" interactions and "small" effects of unwanted feedback in the overall plant. Thus, good control of the HEN (treated as a separate system) is important for the overall plant behavior. For the *industrial* HEN operation problem, a number of deviations from common assumptions may be faced. Examples are:

1. Heat capacity flowrates are often assumed to be constant, or changes in heat capacity flowrates are treated as *disturbances*. In practice, there are cases where flowrates actually are *manipulations*.
2. For an industrial HEN operation problem, temperatures *internally* in the HEN may have (soft) targets. As an example, consider a steam generation plant where an economizer is placed before the boiler. The outlet temperature from the economizer will have an upper limit to prevent boiling in this unit.

3. In this thesis, it is assumed that utility exchangers (where present) always are located as the last unit on the stream. For the industrial HEN operation problem, there may exist internal utility exchangers, for example when multiple utilities such as various steam levels are present.
4. In operability and flexibility analyses, it is often assumed that *all* heat exchanger duties can be manipulated through a bypass. This is only rarely the case for industrial HENs.

Now, some short comments to these 4 points related to the previous chapters are given. The three different methods for operation of HENs presented in the preceding chapters can deal with the first point (flowrates as manipulations) without any particular difficulties. The four observations in chapter 5 give the necessary information for putting up sign matrices when flowrates are used as manipulations. For the methods in the chapters 6 and 7, a flowrate manipulation is treated as any other manipulation. When using flowrates for manipulations, one should keep in mind the non-convexity problem that may be encountered. Chapter 4 concerning degrees of freedom during operation does not, however, consider using flowrates as manipulations.

The second point concerning internal temperature targets has not been treated explicitly in the thesis. If there is a target temperature between two heat exchangers in a HEN, one option is simply do redraw the HEN such the stream with internal target temperature is defined as two separate streams. This does not apply for targets within a bypass line. While internal targets are not explicitly considered, an internal measurement does not differ from any other measurement/output. Internal targets are discussed in Mathisen (1994, p.115). Regarding DOF during operation, an internal target represents an additional constraint in the inner HEN. When computing $N_{\mathrm{DOF,\,U}}$, this *may* reduce the rank of the inner HEN and thus reduce the number of DOF.

The third point concerns internal utility exchangers. If the duty of an internal utility exchanger is used for control of the temperature immediately downstream, then one should definitely consider redrawing the HEN such that the stream with an internal utility exchanger is treated like two separate streams. If the duty of an internal utility exchanger cannot be manipulated, it will not pose any difficulties. For a internal utility exchanger controlling some other temperature than immediately downstream, that manipulation can in principle be considered as any other manipulation. Computing DOF during operation, an inner utility exchanger is part of the inner HEN. Thus, the inner utility exchanger may affect the rank of the inner HEN. Further, inner utility exchangers are not considered for the general structure of HENs described in section 2.3 (page 21).

The fourth and last item above points out that a common assumption for flexibility and operability analyses (at least in academia) is that *each* heat exchanger has a bypass. While this assumption may have been used for illustration purposes early in the chapters concerning operation (chapters 5, 6 and 7), all of the methods described handle heat exchangers without bypasses. Chapter 4 concerning DOFs in operation also covers heat exchangers without bypasses. In chapter 2, the *effective* flexibility is introduced in order to point out that it is the flexibility of the *controlled* HEN that matters during operation

In addition to these 4 points, one may face other and more problem specific challenges for the industrial HEN operation problem. These may be related to fouling, interaction between heat and material balances, thermal energy versus mechanical/electrical energy etc.

The industry has for a long time been concerned about energy consumption and how to operate the plants in order to maximize heat recovery. While there exists fairly general and simple methods for *design* of energy efficient plants (e.g. the pinch design method), strategies for *operation* of HENs have often been developed in a much more *ad hoc* manner. For instance, the strategy for operation may be based on experience from similar plants, or from simulations of one or a few selected control strategies. In many cases, such approaches will result in good control strategies for the particular plant. The purpose of the work presented in this thesis, is to equip personnel involved in operation of plants (or design of control strategies) with *systematic* methods that result in equally good (or better) control strategies in a faster and more reliable way.

One may ask why not use some general optimizing control scheme such as Model Predictive Control (MPC) for operation of HENs. MPC has experienced a growing popularity in industry during the last years and the number of implementations is increasing (Morari and Lee, 1997). In industry, MPC is usually implemented on top of the regulatory control system. One reason for not using MPC for the control of HENs is, as it has been shown in the thesis, that many HENs can be operated optimally using traditional decentralized control. Simple physical insight and using e.g. the sign method in chapter 5, will in many cases lead to which bypasses that should be opened and which should be closed in order to achieve optimal operation. This is a much simpler method than MPC, and should therefore be preferred. MPC requires a dynamic model of the process to be operated, while the 3 methods presented in the thesis all have less requirements concerning the process model.

An important difference between the 3 presented methods is the amount of information needed. For the sign method in chapter 5, only the *structure* of the HEN is used to deduce how it should be operated. In cases where structural information alone is not sufficient, the parametric method described in chapter 6 may be an alternative. This method is very similar to the sign method, except that the signs are replaced by numbers. However, no information about the disturbances is required. Chapter 7 describes the third method for operation of HENs, and this method differs significantly from the other two. Among the 3 methods, this last method requires most information about the HEN. It uses a complete steady state model and in addition information about disturbances is utilized. Which method to use may depend on the available information.

Finally in this section, it is emphasized that there are cases where the HEN can be designed to operate optimally with zero degrees of freedom. As an example, consider a HEN with 1 DOF when all process exchangers have bypass. If it is found (e.g. from simulations) that one of the bypasses should always be closed (i.e. keeping this bypass closed minimizes utility cost for all operating regions), then this bypass should not be installed. In such cases, the HEN is always operated optimally in a trivial manner. This thesis has focused on cases where there is at least 1 DOF, and where there is a need for a strategy during operation in order to minimize the energy consumption.

8.2 Conclusions

This section summarizes the main conclusions and contributions in this thesis.

In chapter 2, it is argued that the HEN can be considered as a separate part of the process, with its own properties regarding heat recovery level and dynamic behavior. The most important aspect of operation of HENs is to maximize heat recovery, however, good dynamic properties also reduce the influence of undesired feedback in the overall process introduced by heat integration. While it is rather obvious that the process structure affects the operability, chapter 2 also points out that the opposite sometimes may be the case. If e.g. the control system applies a bypass fraction of 1, this corresponds to removing the bypassed unit.

Chapter 3 concerns dynamic simulation of HENs. While this chapter does not contribute significantly, it gives some recommendations regarding how to model HENs to obtain simple dynamic simulations. The chapter concludes that modeling each side (hot and cold) of a heat exchanger as a series of tanks and using arithmetic mean as the temperature driving force (AMTD), in most cases gives good agreement with steady state properties combined with fair dynamic behavior. This result is found through two different approaches (modifying the pure mixing tank concept, and discretizing one-dimensional partial differential equations).

The perhaps most important contribution in this thesis is chapter 4. This chapter shows that all degrees of freedom (after control of targets is implemented) may *not* be utilized for energy optimization. The number of DOFs that *can* be utilized for optimization of utility cost ($N_{\mathrm{DOF,\,U}}$) is defined, and a novel quantitative expression for $N_{\mathrm{DOF,\,U}}$ is derived. An important step in developing this expression is to divide the HEN in one inner and one outer network. A bottleneck to $N_{\mathrm{DOF,\,U}}$ is often the number of process streams entering the outer HEN, thus increasing the number of manipulations (bypasses) in the inner HEN may not always increase $N_{\mathrm{DOF,\,U}}$.

Relaxing one target temperature to become a free outlet temperature increases $N_{\mathrm{DOF,\,U}}$ by one. A surprising result in chapter 4 is that relaxing another target temperature does not increase $N_{\mathrm{DOF,\,U}}$ any further. In addition to the quantitative expression for $N_{\mathrm{DOF,\,U}}$, a simple rule to determine whether optimization may be possible or not is presented. It is also shown that the quantitative expression may be simplified considerably by assuming that the rank of the inner HEN is only limited by the number of process streams and the energy balance.

In chapter 5 it is shown that how to operate a HEN optimally may often be deduced from structural information only. This “sign” method for optimal operation of HENs has been presented earlier by Mathisen (1994, chapter 5). However, chapter 5 in this thesis includes some further development of the method. First, the definition of the signs has been redefined to fit a general process and not only HENs (previously, the definition of the signs depended on whether the corresponding stream was hot or cold). This improvement makes the method applicable to all types of processes with at least one extra DOF for optimization and where information about the signs is available. It is emphasized, however, that the sign method does not always guarantee optimality. Second, the presentation of the procedure is simplified with the introduction of the vector g^{U} denoting the effect of each manipulation on the *total* utility consumption. This does not change the method itself, but is included to make the procedure simpler to understand and to make it more similar to the parametric method. The sign

method results in a priority table denoting the preferred manipulation, and which manipulation to switch to if the preferred manipulation is saturated. Chapter 5 shows that this variable control structure in some cases simply is identical to split-range control.

The parametric method in chapter 6 is very similar to the sign method. In fact, replacing the signs in the sign matrices with real numbers is the most important difference. The control structure that optimizes the utility consumption is found by solving an integer programming problem. Note that if there is only one bypass controlled temperature, this optimization is reduced to selecting the smallest number from a vector (similar to the priority table of the sign method). For HENs with multiple bypass controlled temperatures, the method does not guarantee that the optimal solution is found. The basic optimization model does not include any controllability considerations and the basic model is extended to include controllability in two different ways. Controllability is included by additional constraints which in both cases represent a hierarchical control strategy. It is shown that these hierarchical strategies can be implemented by logical propositions formulated as additional mathematical constraints involving binary variables. In this way, logic inference is embedded into the optimization model. It is not external logic in terms of "if-then" statements etc. added on top of the basic formulation.

Chapter 7 presents a different approach to optimal operation of HENs. This method combines periodic steady state optimization and optimal selection of secondary measurements. While periodic steady state optimization does not represent much new, a general model designed for optimization of HENs is presented. The basis of the method for selection of measurements is also presented earlier (Skogestad and Postlethwaite, 1996, chapter 10). The contribution in the thesis is to adapt and apply the method for processes where optimum lies at the intersection of constraints. This is often the situation also for other parts of a process than the HEN. The problem in such cases is that the nominal optimum may be infeasible when unknown disturbances or model errors are present. Therefore, the selection of measurements have to be based on values that are optimal when unknown disturbances and model errors are considered. A second, but related problem is to find the optimal value of the selected measurements considering unknown disturbances and model errors (robust optimum) during operation. In order to avoid computing optimal values for all possible disturbances periodically, it is proposed to use an additional constraint (safety margin) that represents the difference between the nominal and the robust optimum. This constraint is computed once and by adding this constraint to the model, estimates for the robust optimal values will be found directly, i.e. without considering all possible unknown disturbances and model errors. It is shown that the robust optimal values are different from the nominal optimal values also for systems with asymmetric objective functions. An asymmetric objective may occur when deviations in the primary variable are penalized rather than considered infeasible. Also in such cases, a safety margin can be used to find robust optimum directly.

8.3 Suggestions for future work

This thesis is devoted to operation of integrated processes, and in particular to operation of HENs. Even though this may seem to be a well defined and perhaps also a narrow research area, there is definitely room for further work. This section suggests some directions for

future work related to the main parts of the thesis. The topics are not prioritized, and they appear in the same order as they do in the thesis.

Simple dynamic simulation of HENs can be performed using the models described in chapter 3. One possibility is to further investigate the limitations imposed by the use of AMTD, and to find conditions at which the use of AMTD leads to crossover at steady state. Also, for more accurate dynamic predictions, more detailed models are required. This may include modeling of heat exchangers where the fluids are compressible and heat exchangers where phase transitions take place. Further, models that more explicitly include the mechanical construction of the unit may be needed.

Even if degrees of freedom for optimization during operation of HENs are given a fairly thorough treatment, future work could be to include the use of flowrates as manipulations. It may be argued that this is implicitly included in chapter 4 since it will affect the rank of the inner HEN. With flowrates as manipulations, it may be expected that the energy balance is not constraining the rank of the inner HEN. A consequence of this may be that relaxing a target to a free outlet temperature will not increase $N_{\mathrm{DUF,\,U}}$. Such issues should be addressed in future work.

Regarding the sign method for optimal operation of HENs, more work can be done in order to find classes of HENs for which optimal operation is guaranteed. Also, more work is needed for HENs with more than one bypass controlled target. A method to handle multiple bypass controlled targets is presented in the thesis, however, this method should be verified on larger examples, and alternative solutions should also be assessed.

The sign method as it is presented in chapter 5 is not restricted only to HENs. The method can be regarded as a general framework for utilization of structural information in operation. Future work should include application of the method on other types of processes. The method is, however, not assumed to be well suited for processes where optimum is unconstrained.

The parametric method in chapter 6 is basically the presentation of an idea, and further work is needed to develop it into a method that can be recommended in practice. This will have to include investigating under what conditions the method may fail to reach the optimal operating state. How to incorporate controllability considerations could also be further developed in addition to the 2 methods proposed in chapter 6. The way logical constraints are used to obtain hierarchical control strategies, could perhaps be utilized in other optimizing control schemes such as MPC. In section 6.7 it is argued that the method has a potential of being robust to model errors and this should be further investigated. As for the sign method, examples from other processes than HENs should be studied in order to verify and further develop the parametric method.

The method combining steady state optimization and selection of secondary measurements in chapter 7 is at a level where it can be applied in practice. Of course, a practical implementation has to handle problems like, “what if the optimizer does not return a feasible solution?” or “how much should setpoints be allowed to change from one optimization to another?” etc. Future work on this method should include larger examples (more than one secondary manipulations) and the effect of having a constant value for the safety margin should also be investigated.

References

Mathisen, K.W. (1994). Integrated Design and Control of Heat Exchanger Networks. *Thesis*. University of Trondheim - NTH, Norway.

Morari, M. and J.H. Lee (1997). Model Predictive Control: Past, Present and Future. *Presented at PSE'97-ESCAPE-7*, 25-29 May, Trondheim, Norway.

Skogestad, S. and I. Postlethwaite (1996*). Multivariable Feedback Control, Analysis and Design*. John Wiley & Sons, Chichester, UK.